Petrologie sedimentárních hornin

G421P13, ZS 2/1, 3-4.roč.

3. Karbonáty II. diageneze, dolomitizace

Karel Martínek

Ústav geologie a paleontologie

diageneze zrn – mikrobiální mikritizace, vrtby, rekrystalizace argonit (A), high-Mg kalcit (HMC) → low-Mg kalcit (LMC) kalcit

tmelení – pórová fluida přesycená $CaCO_3$, mineralogie tmelů závisí na PCO_2, poměru Mg/Ca

neomorfismus – rekrystalizace – změna minerál.sl. a/nebo struktury

rozpouštění – krasovění, tlakové rozpouštění, stylolity

kompakce

dolomitizace, dedolomitizace

diagenetická prostředí – meteorické vadózní, meteorické freatické, mořské freatické , pohřbení

diagenetická prostředí

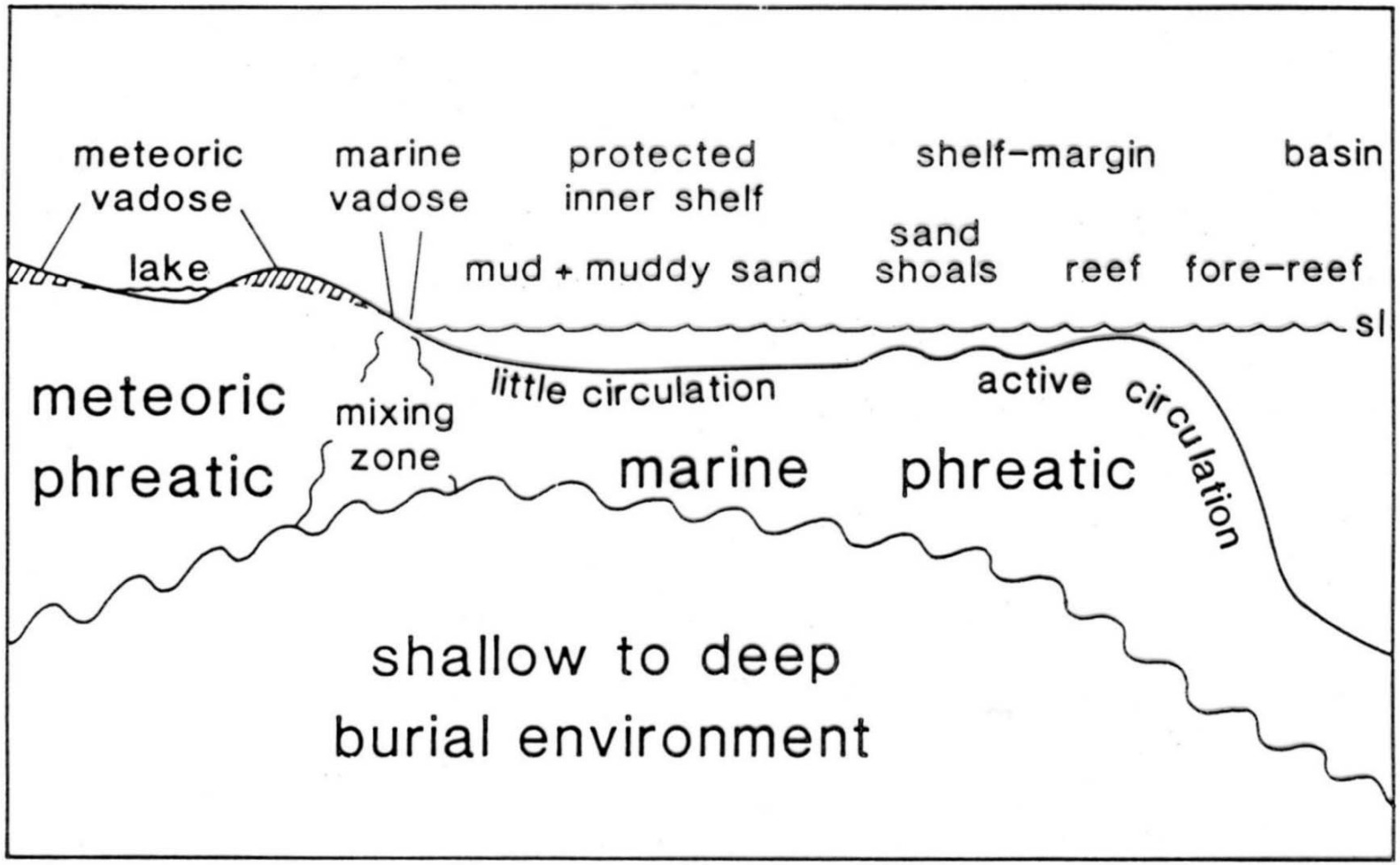

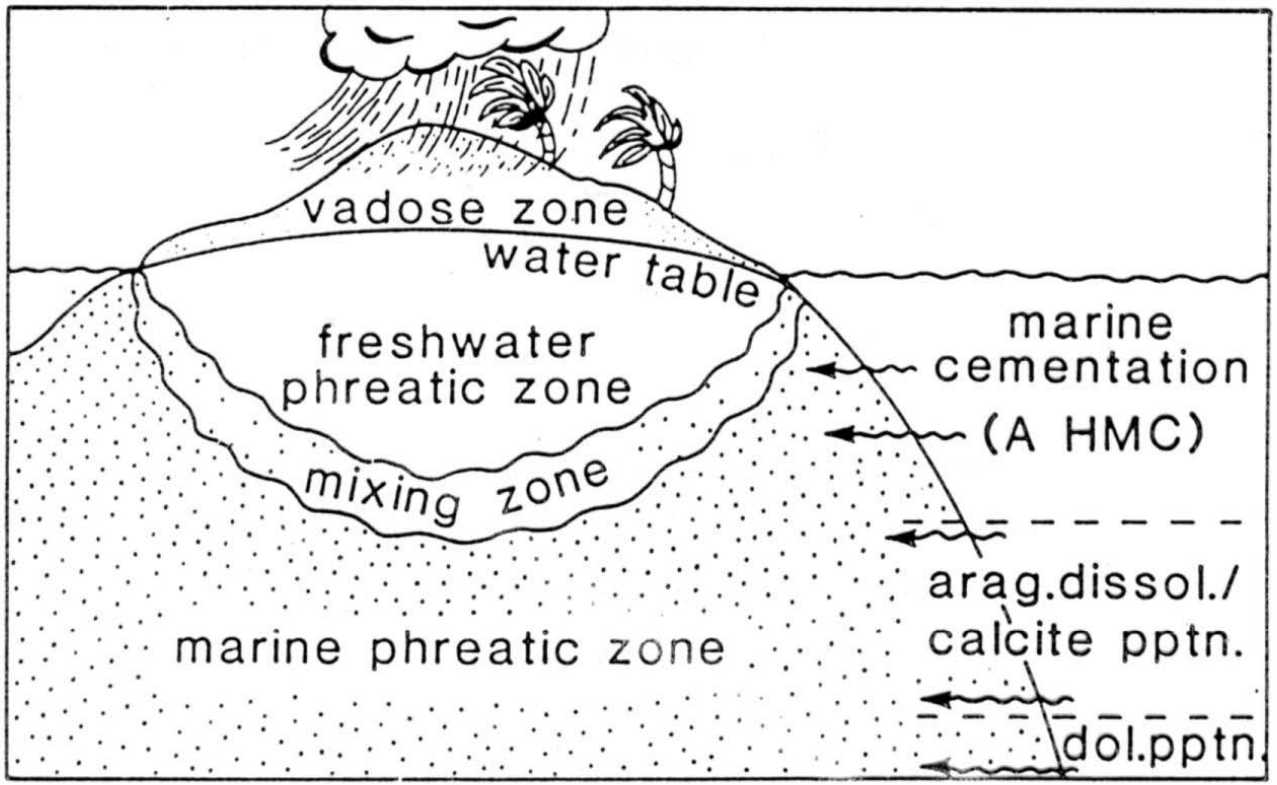

Fig. 7.2 *Diagenetic environments fo · an isolated platform, atoll or shelf margin, where an island is present with a freshwater lens. With increasing depth, seawater will become less saturated with respect to* $CaCO_3$ *so that aragonite may be dissolved and calcite precipitated, and eventually dolomite may be precipitated. This part of the model could apply to any platform or shelf margin. Depths will depend on the saturation state of seawater at the time.*

mořská diageneze

recentní tmely

recentní intertidál-subtidál – beachrock; A, HMC tmely – **jehlicovité lemy** kolem zrn, kolmo na povrch zrn; freatické – **isopachové**; HMC tmavé mikritové povlaky zrn, výplně pórů; mikritizace zrn; zdroje tmelu: a) fyz.-chem. srážení během evaporace na tidál.plošině, b) biochem. mikrobiální srážení (fotosynt.řas, bakteriální kalcifikace, rozklad org.hmoty)

rec. mělký subtidál – laguny – **mikrobiální mikritizace**; vyšší energie – tmelení, **hardgroundy**; tmely: **jehlicovitý A**, **mikritický HMC** – **povlaky zrn, peloidní struktury**, povrchové krusty; útesy – značná variabilita typů tmelů

rec. hlubokovodní tmelení – až do 3,5 km hloubky, impregnace fosfáty a Fe,Mg oxidy; Bahamy - tmely: mikritický LMC, ve větších hloubkách nodularizace; teplé spodní proudy: tenké krusty, nodule litifikovaného pelag. materiálu, jehlicovitý A a mikritický A tmel; tmely – tam kde je pomalá sedimentace, interakce voda-sediment (né pórové vody)

rec.mořské rozpouštění – ve vyšších zem.š. nízké nasycení vody $CaCO_3$ – rozpouštění bioklastů už v prvních 100 m hl.

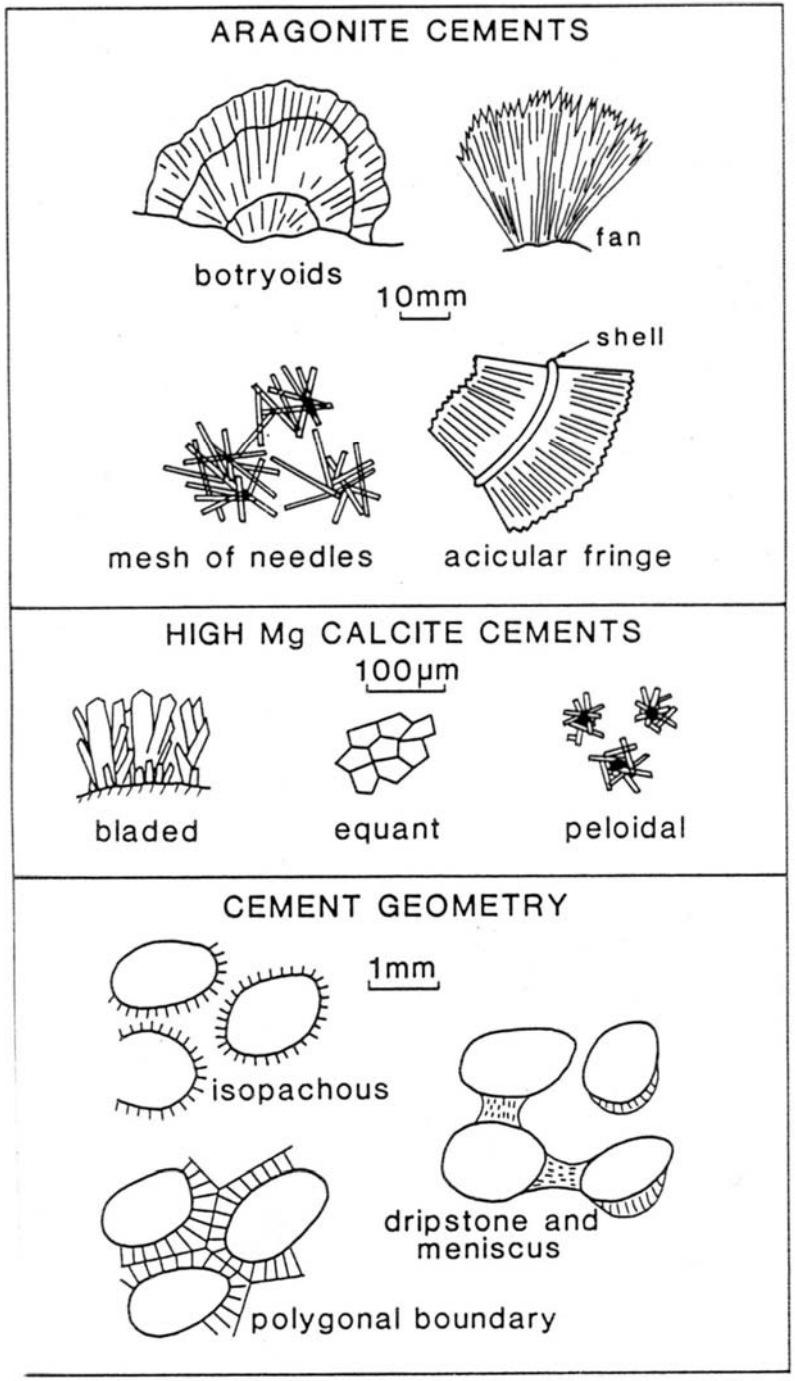

morfologie recentních mořských tmelů

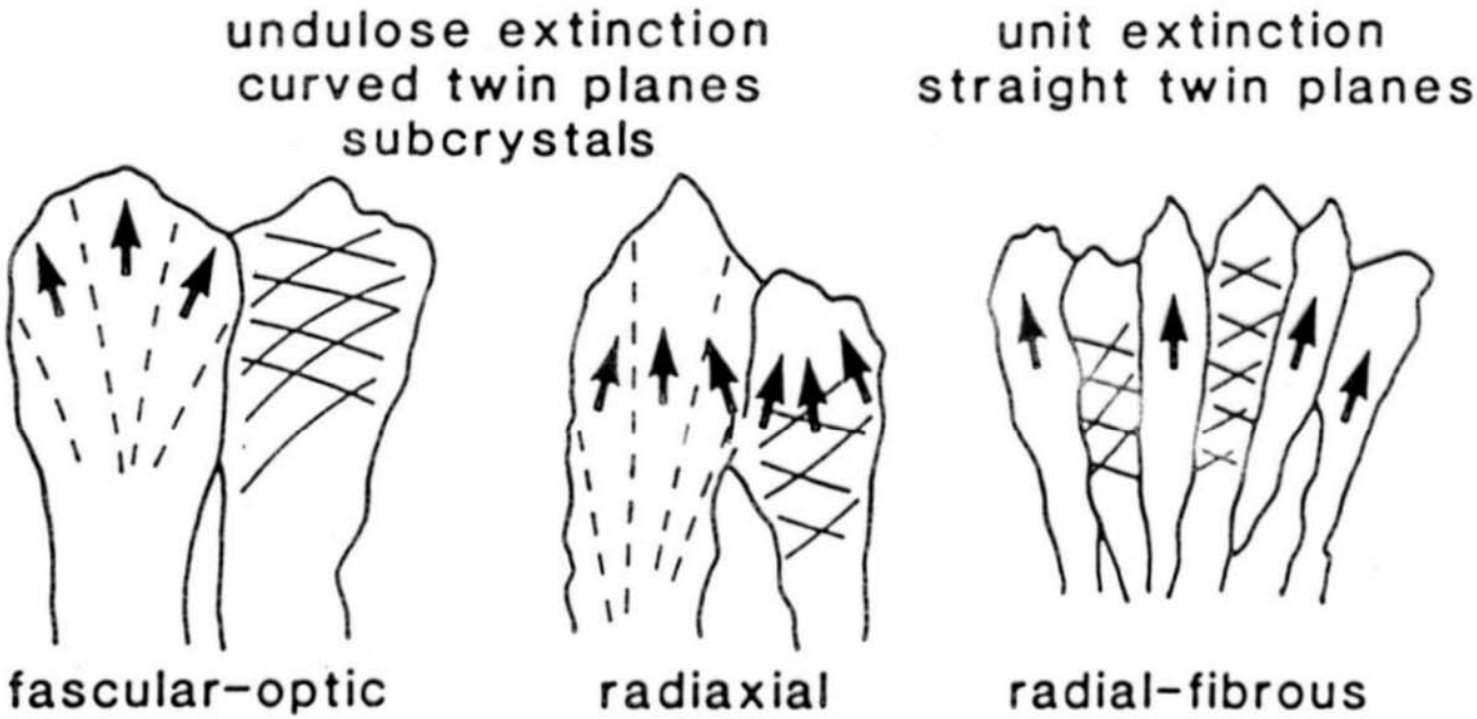

Fig. 4.50 Common types of fibrous calcite. After Kendall (1985).

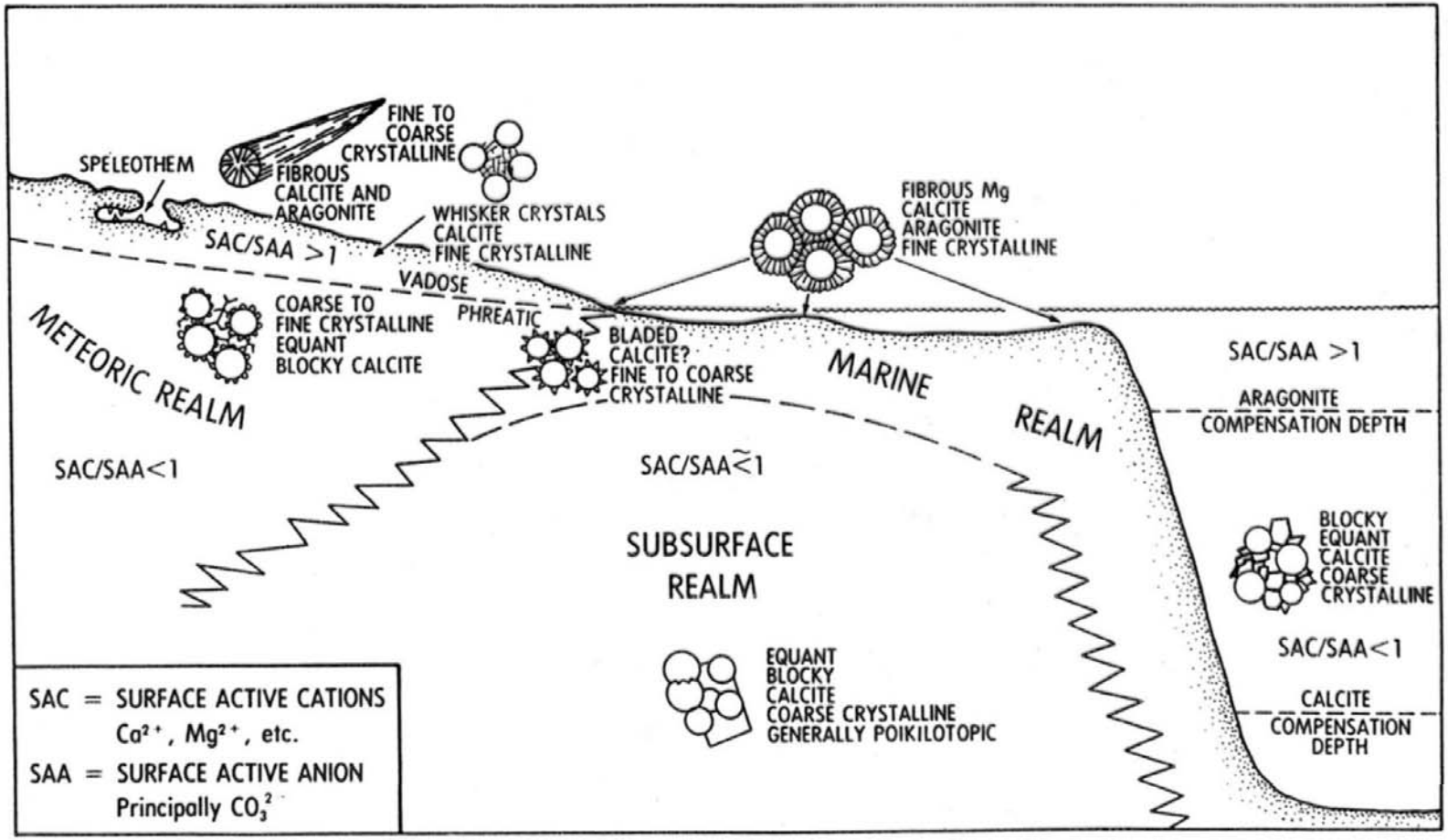

Fig. 3.5 Schematic diagram showing anticipated growth habits of pore-fill calcite cement in the principal diagenetic environments. as controlled by the ratio of surface active cations (SAC) to surface active anions (SAA).

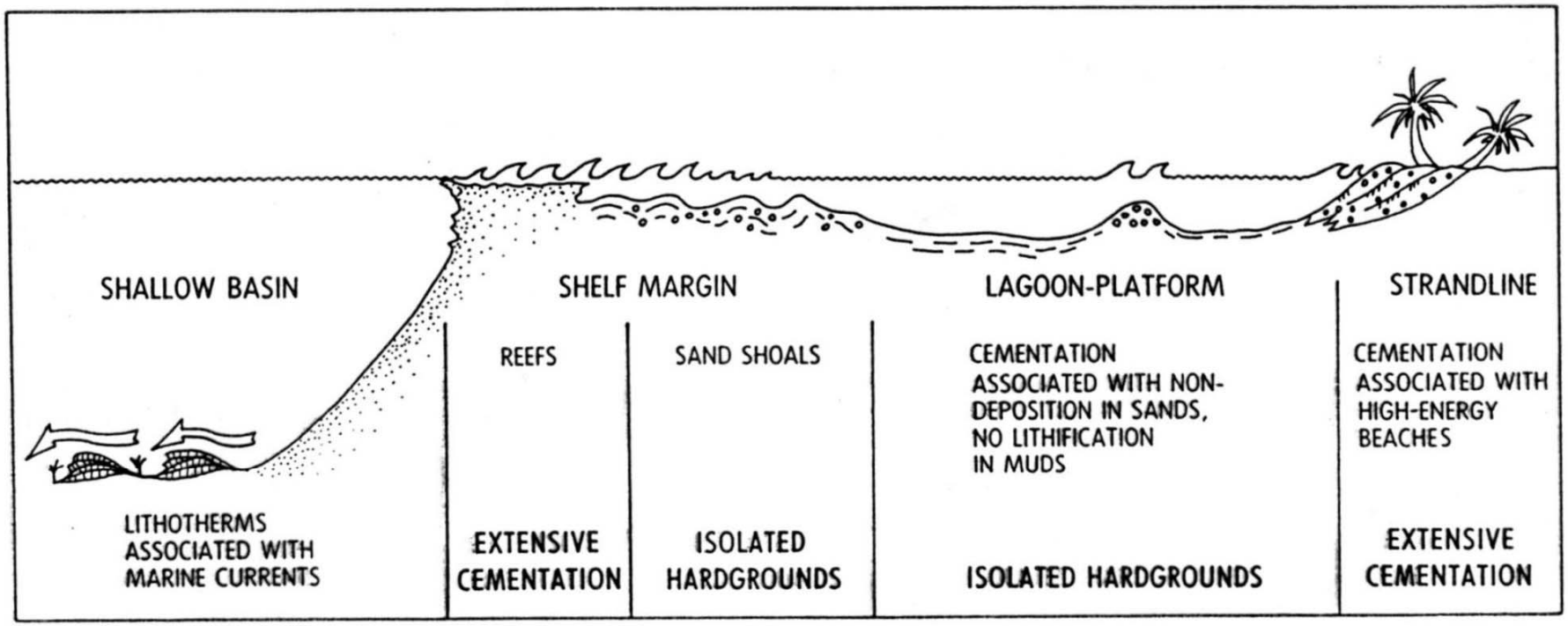

Fig. 4.5. Diagenetic processes associated with shallow marine depositional environments.

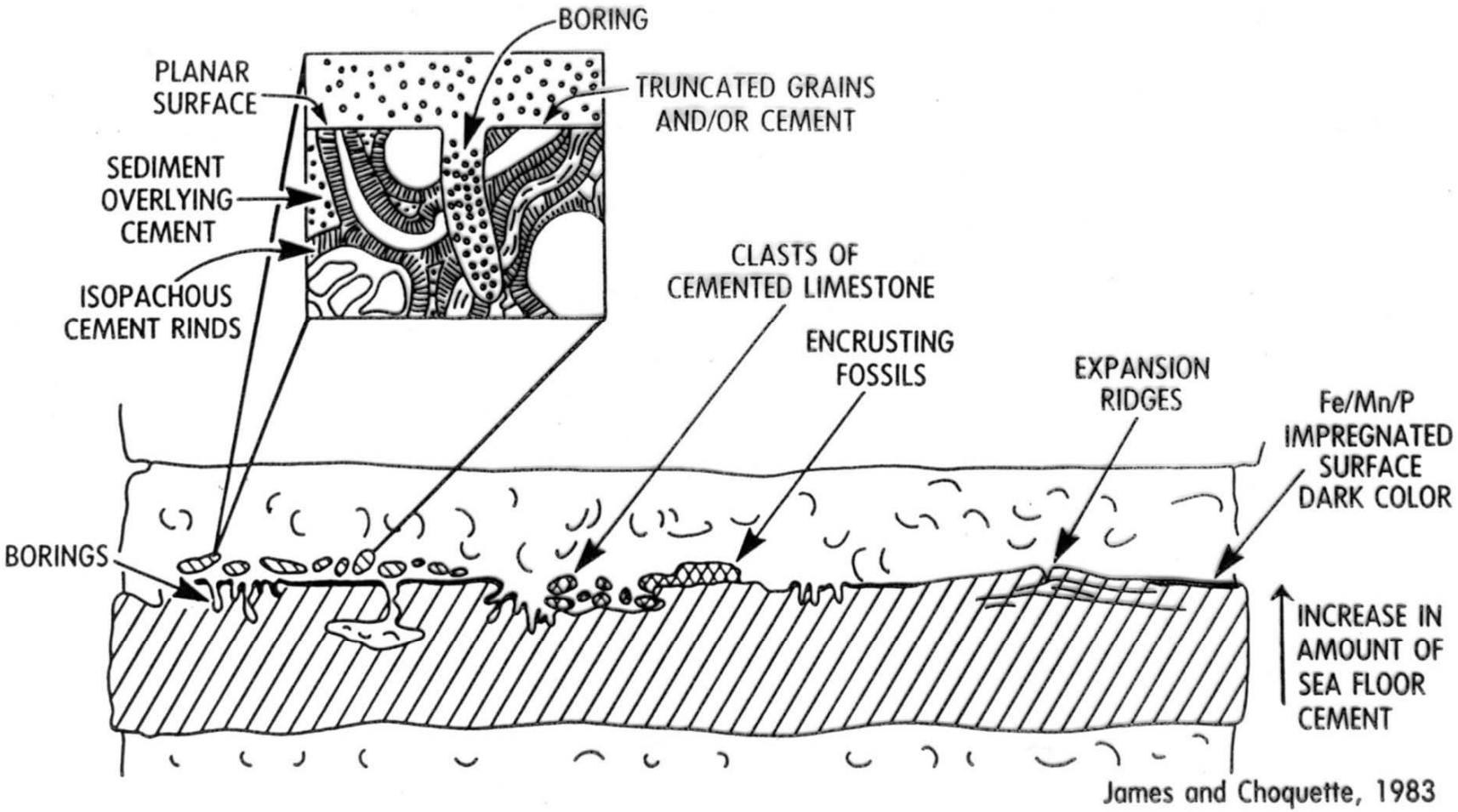

Fig. 4.10. Criteria for the recognition of marine hardgrounds. Reprinted with permission of the Geological Association of Canada.

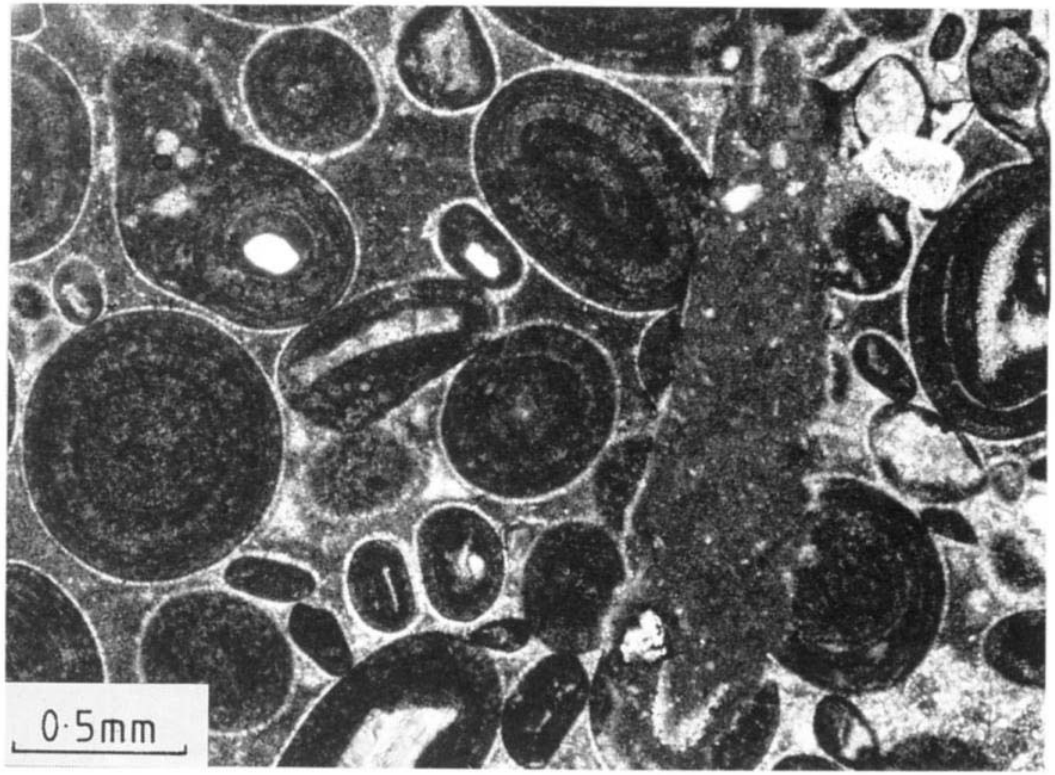

Fig. 7.9 *Oolitic sand cemented in the submarine environment to form a hardground which was then bored. Photomicrograph shows thin isopachous fringe of fibrous calcite around ooids and then micrite partly filling the intergranular porosity. The micrite may be an internal sediment or in part a cement. The ooids, micrite and fibrous calcite are cut by a boring which is itself filled with micrite. The early cementation prevented any compaction of this oolite which has grains in point contact. Middle Jurassic, Cotswolds, UK.*

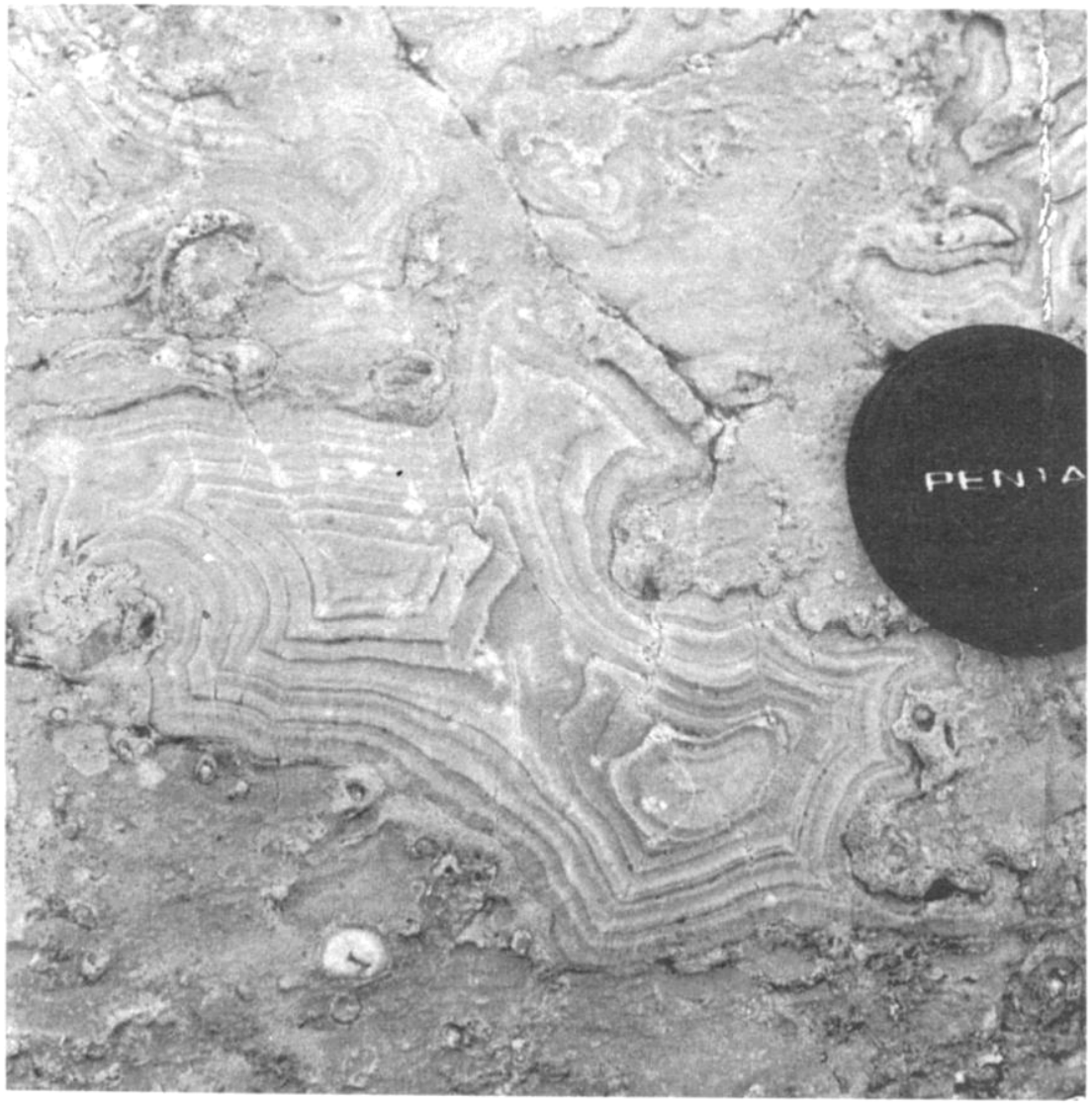

Fig. 7.8 *Marine cement in a Triassic reef, Hafelekar, Austria. Isopachous layers of fibrous calcite cementing fore-reef debris and known locally as 'Grossoolith'. Lens cap 6 cm diameter.*

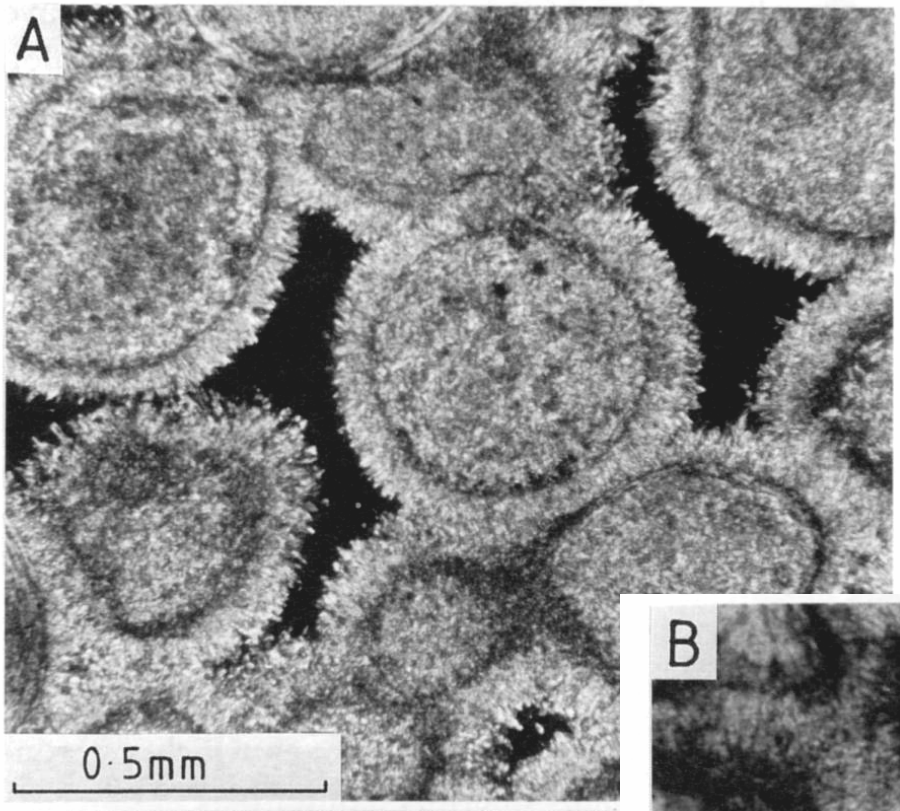
A
0·5mm

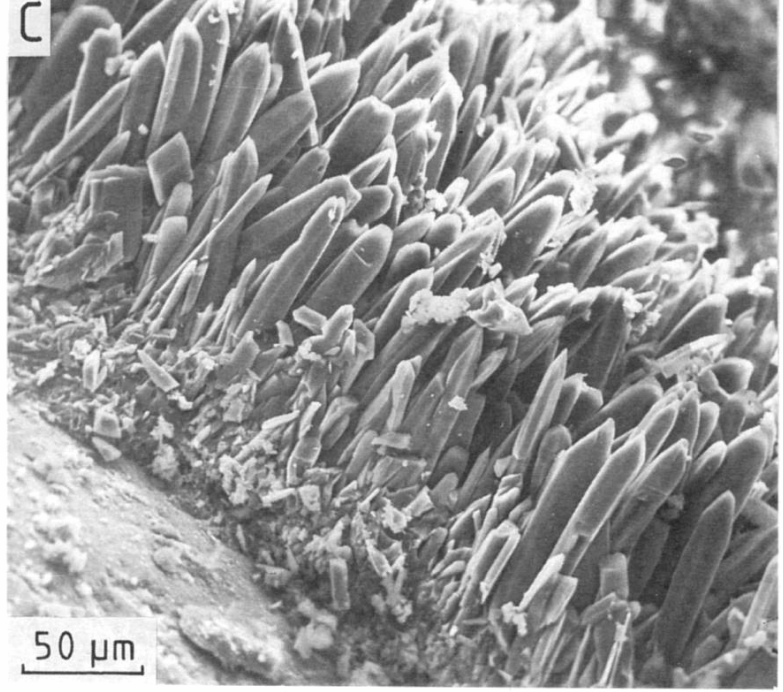
C
50 µm

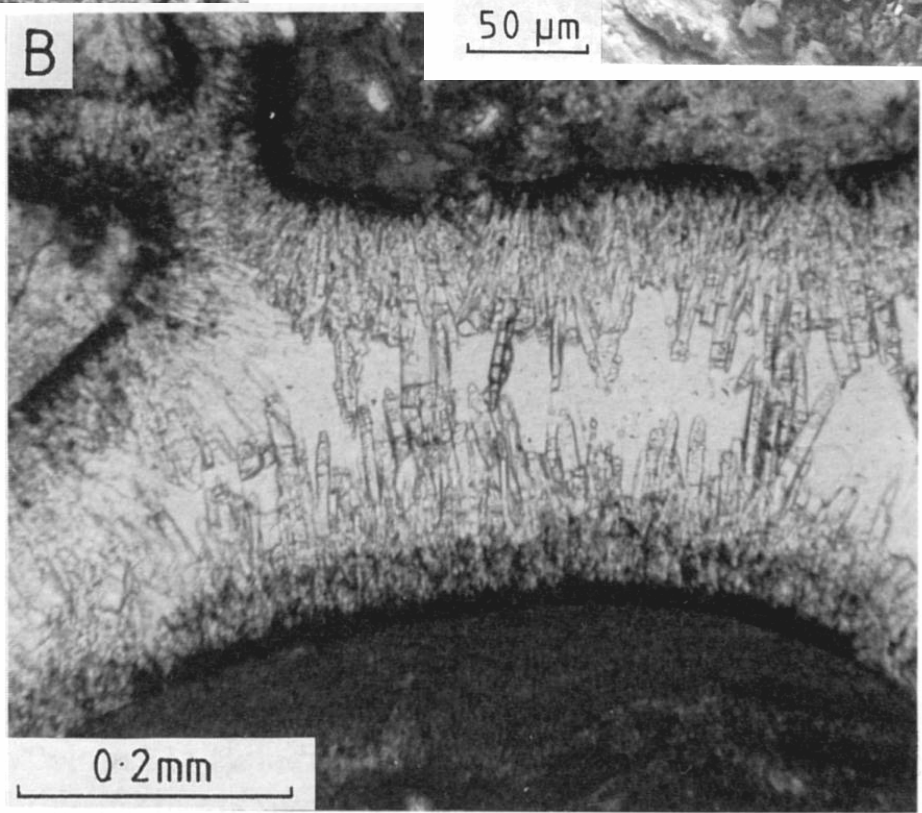
B
0·2mm

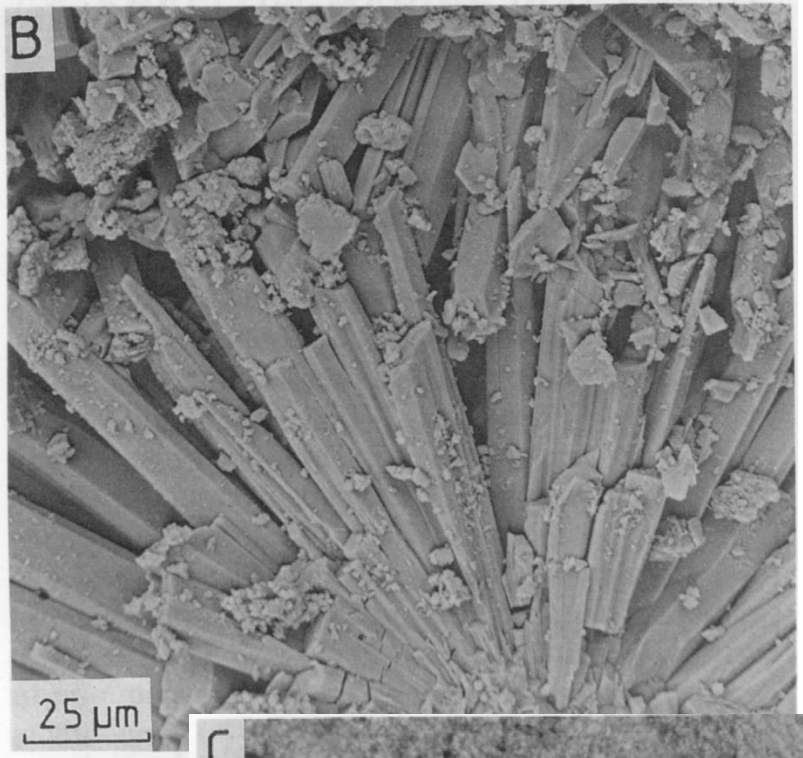
B
25 µm

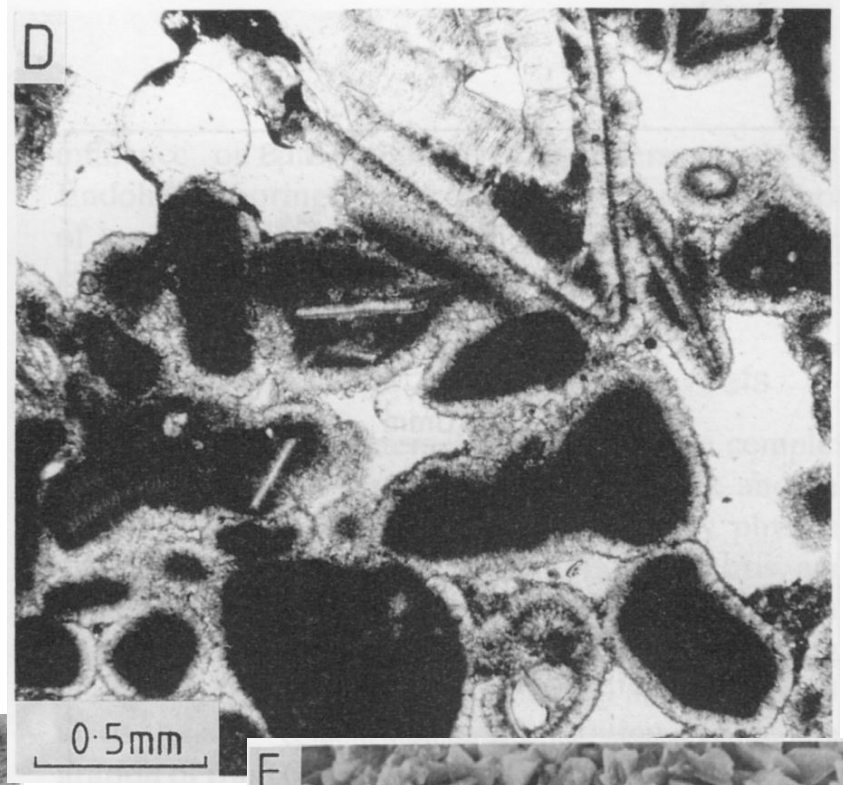
D
0·5mm

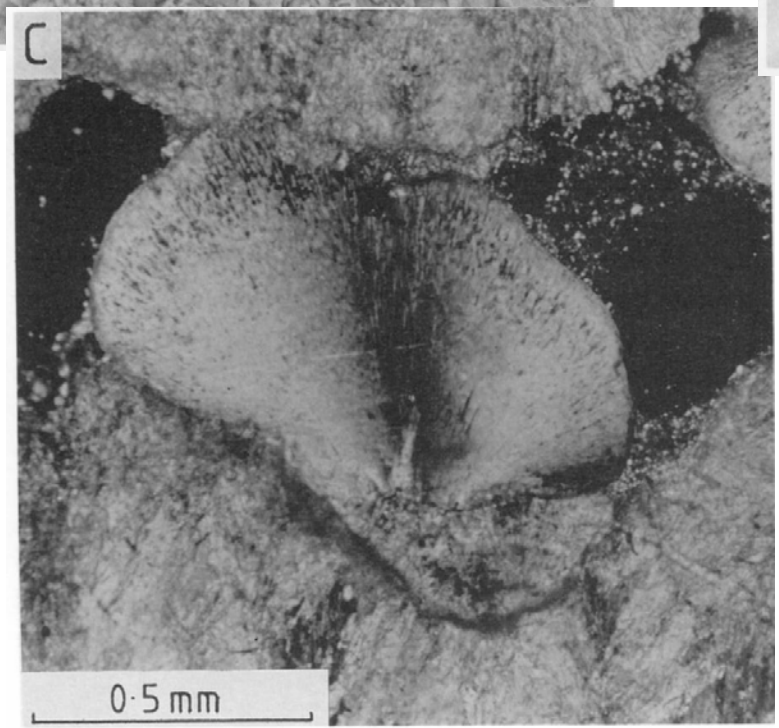
C
0·5 mm

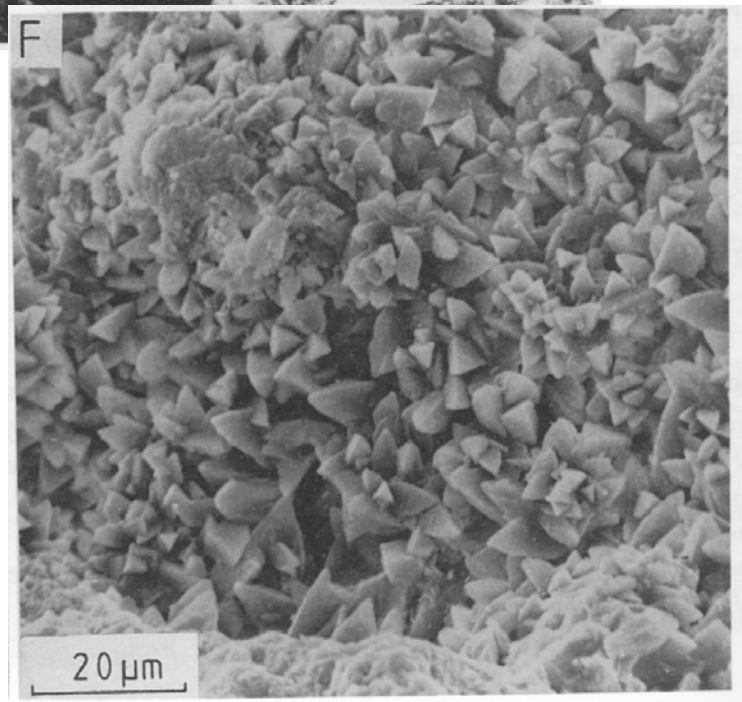
F
20 µm

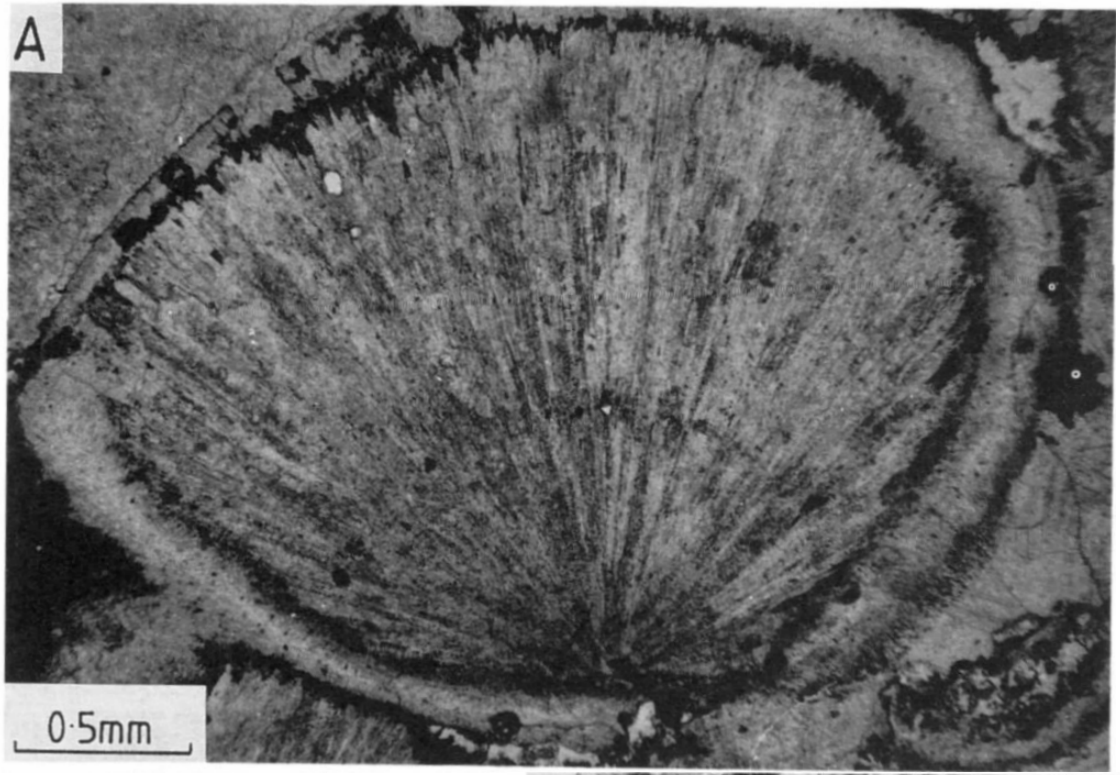
A
0·5mm

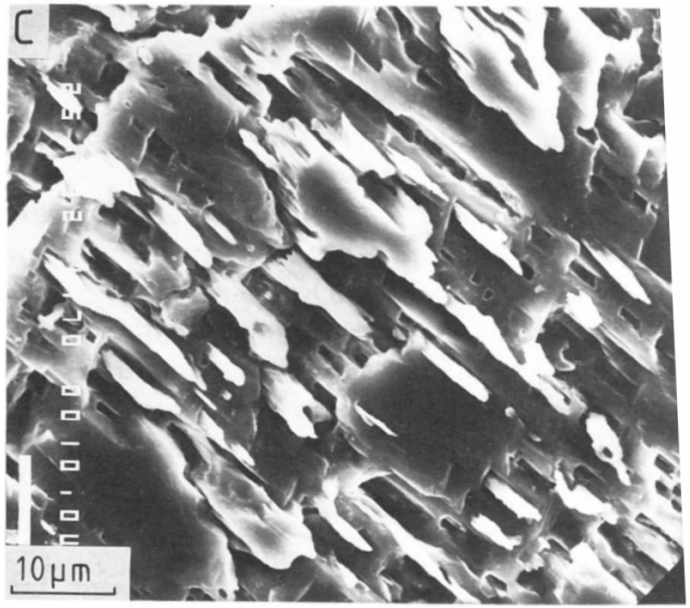
C
10μm

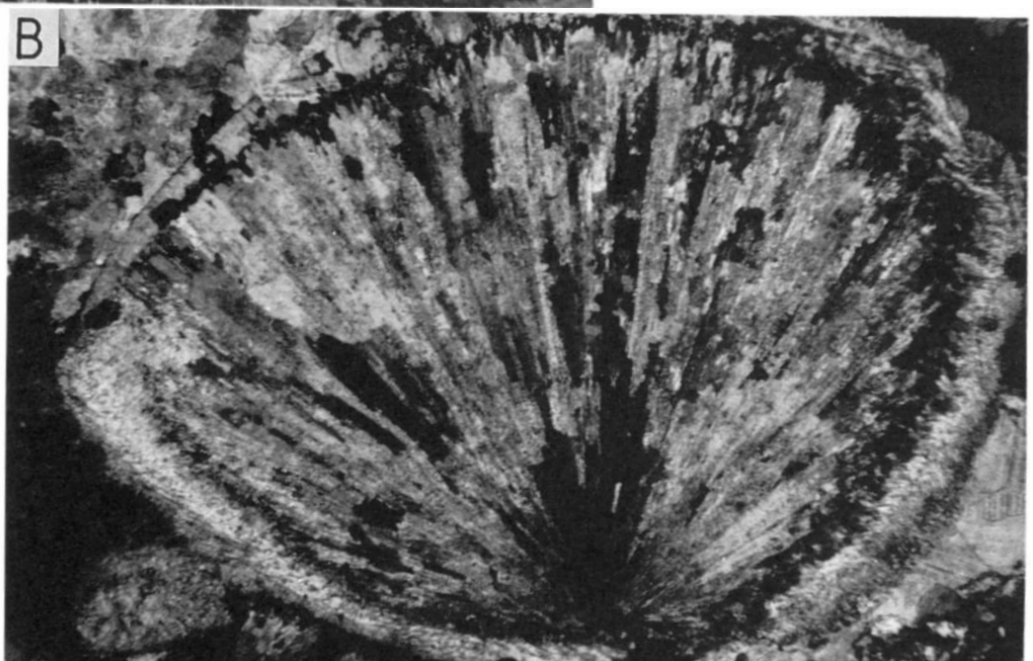
B

mineralogie tmelů

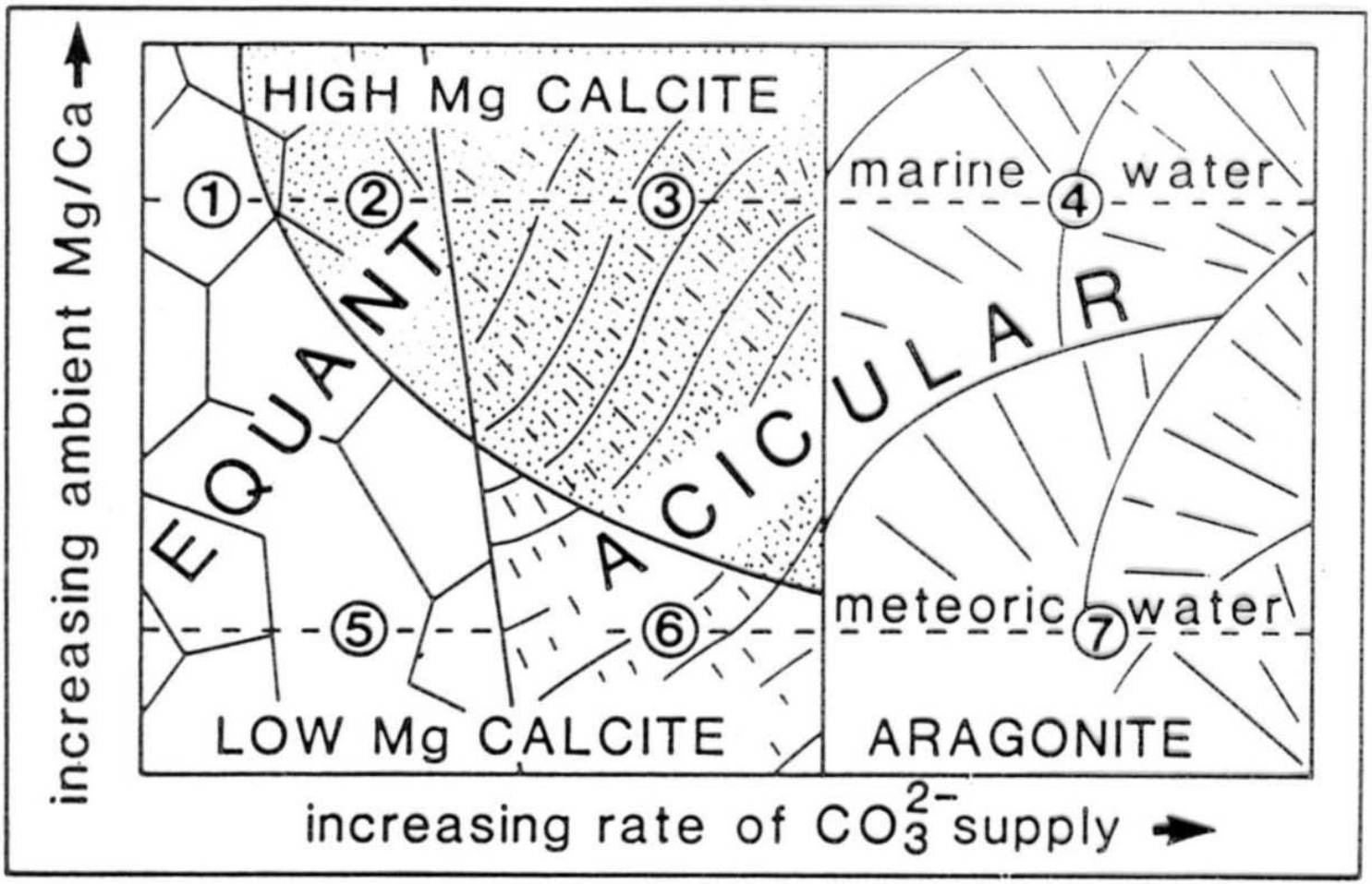

rozpouštění

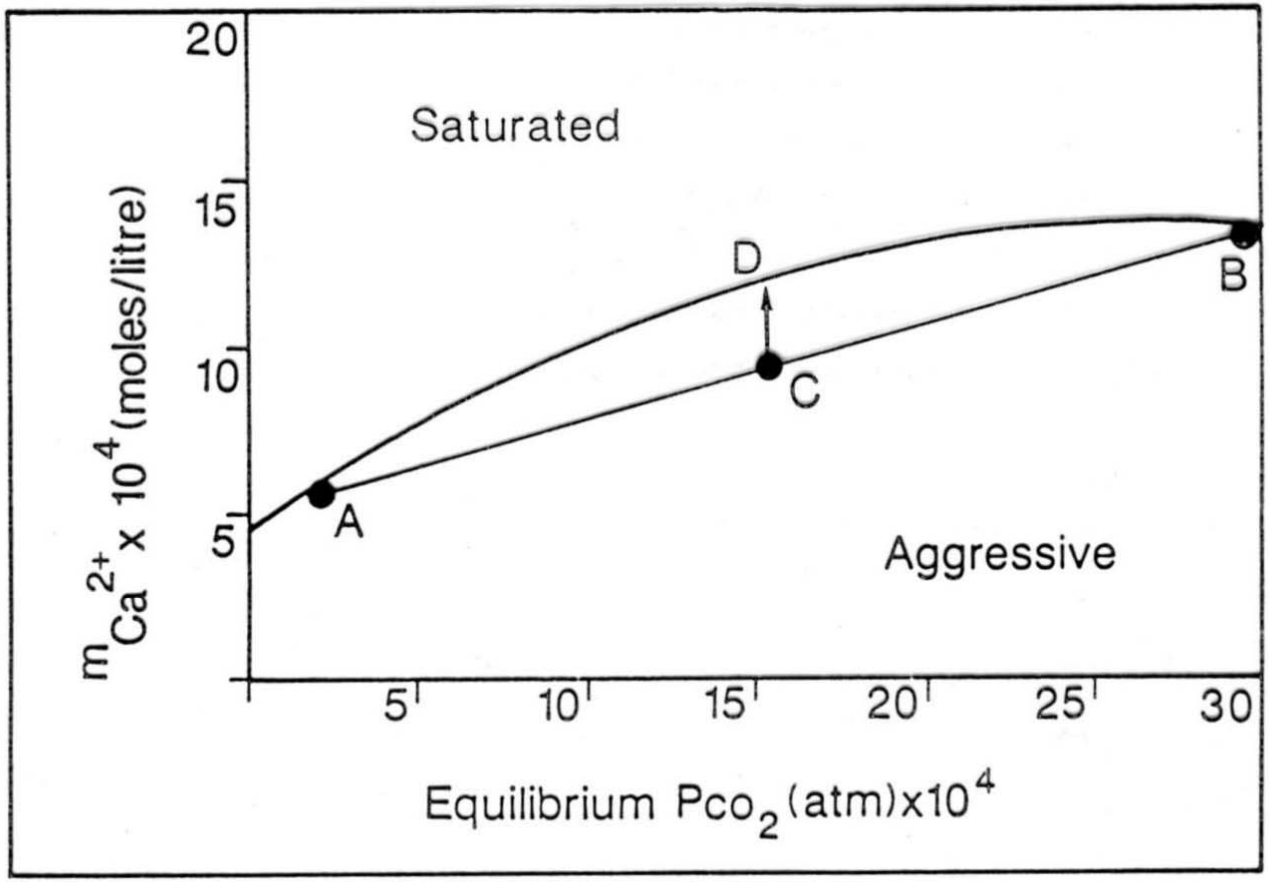

Fig. 7.20 *Mixing corrosion effect. The solid curve shows the solubility of $CaCO_3$ with respect to the total CO_2 in solution. If two liquids, A and B are mixed, an undersaturated solution results, C. It evolves by dissolution of calcite to equilibrium at D. From various sources.*

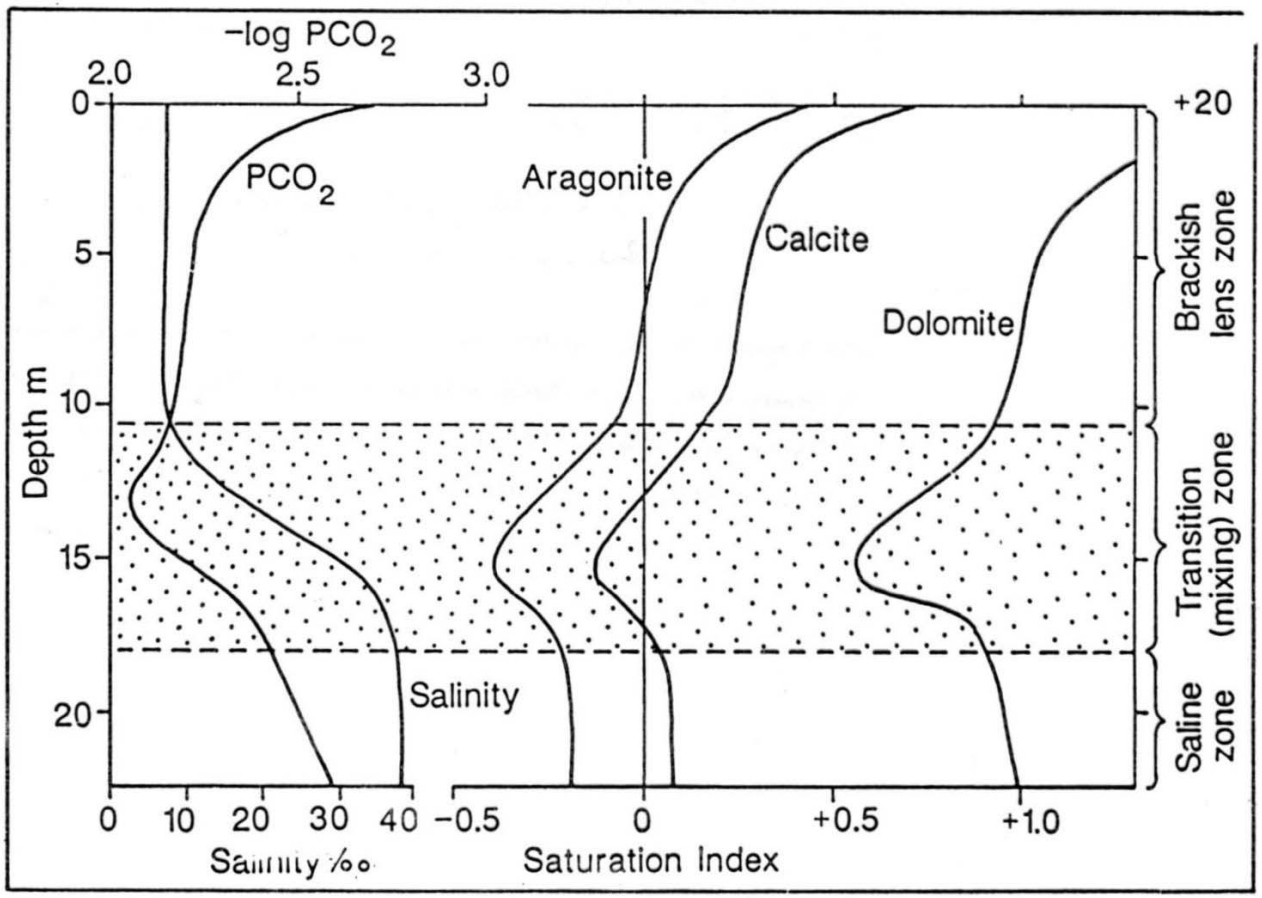

Fig. 7.21 *Vertical variation of salinity, P_{CO_2}, and the saturation indices of aragonite, calcite and dolomite through the meteoric–marine mixing zones within a 'blue hole', Andros Island. After Smart et al. (1988).*

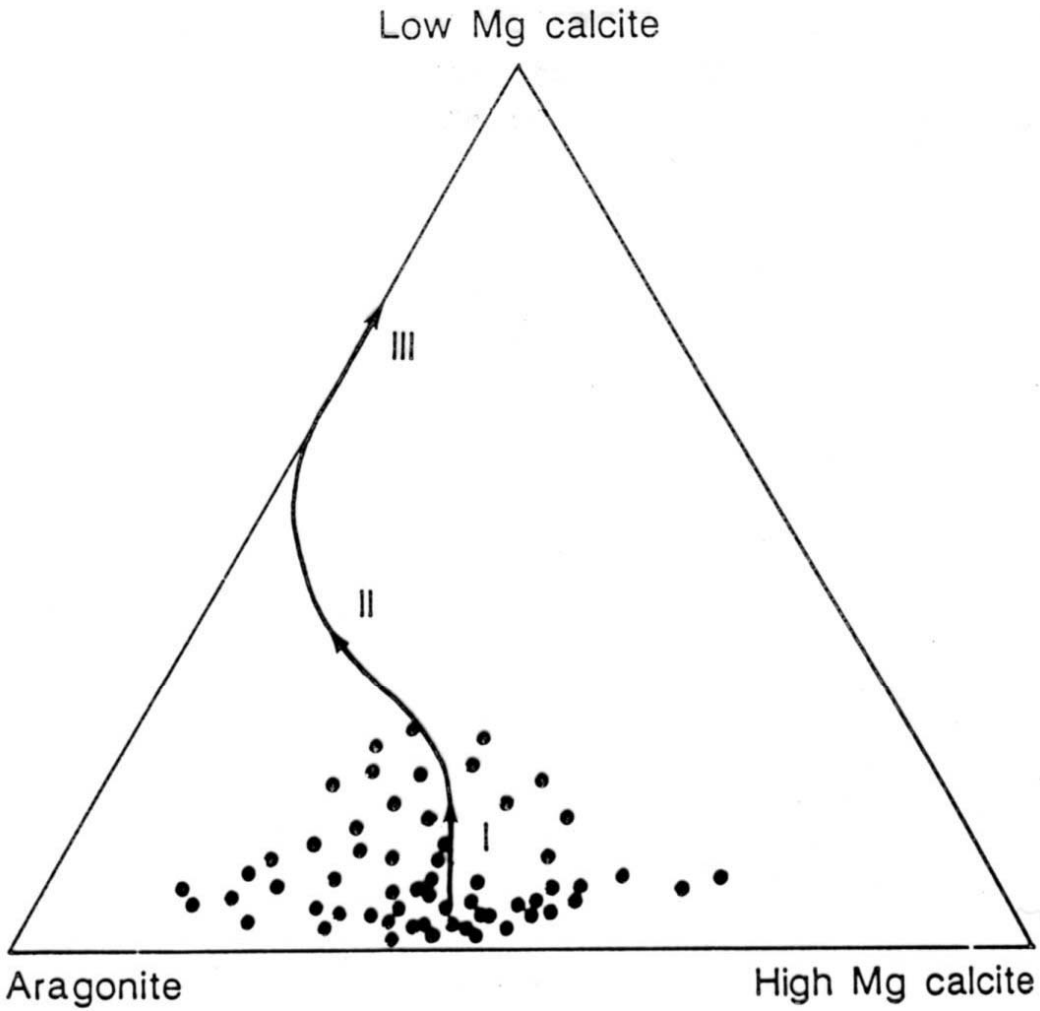

Fig. 7.22 *Triangular diagram showing the typical mineralogical evolution of Quaternary marine sediments during prolonged meteoric diagenesis. Stippled area represents range of marine sediments. I, initial cementation by low-Mg calcite. II, loss of Mg from high-Mg calcites. III, dissolution of aragonites and cementation by low-Mg calcite. Modified from Tucker (1981).*

mořská diageneze

diageneze ve starších horninách

raná d. – na mořském dně n. blízko pod povrchem sedimentu; pozdní d. – při pohřbení

kritéria identifikace mořských tmelů: 1) nejranější (1.generace), 2) často izopachové lemy kolem zrn, 3) vláknitá/sloupcovitá struktura, 4) následná generace je sparit

aragonitové tmely – často kalcitizované, **izopachové** lemy

kalcitové tmely – vláknitý (**jehlicovitý, sloupcovitý**) kalcit, kolmo na substrát; útesy – **mikritický a peloidální HMC**; hardgoundy – syntaxiální nárůsty, stejnozrnný sparit – oba jinak typické pro meteorickou diagenezi a pro pohřbení

procesy: mikritický tmel – rapidní nukleace, pomalé přírůstky; jehlicovitý/sloupcovitý – rychlejší přírůstky kolmo na substrát; stejnozrnný sparitový – velmi pomalá nukleace


250 μm
(a)

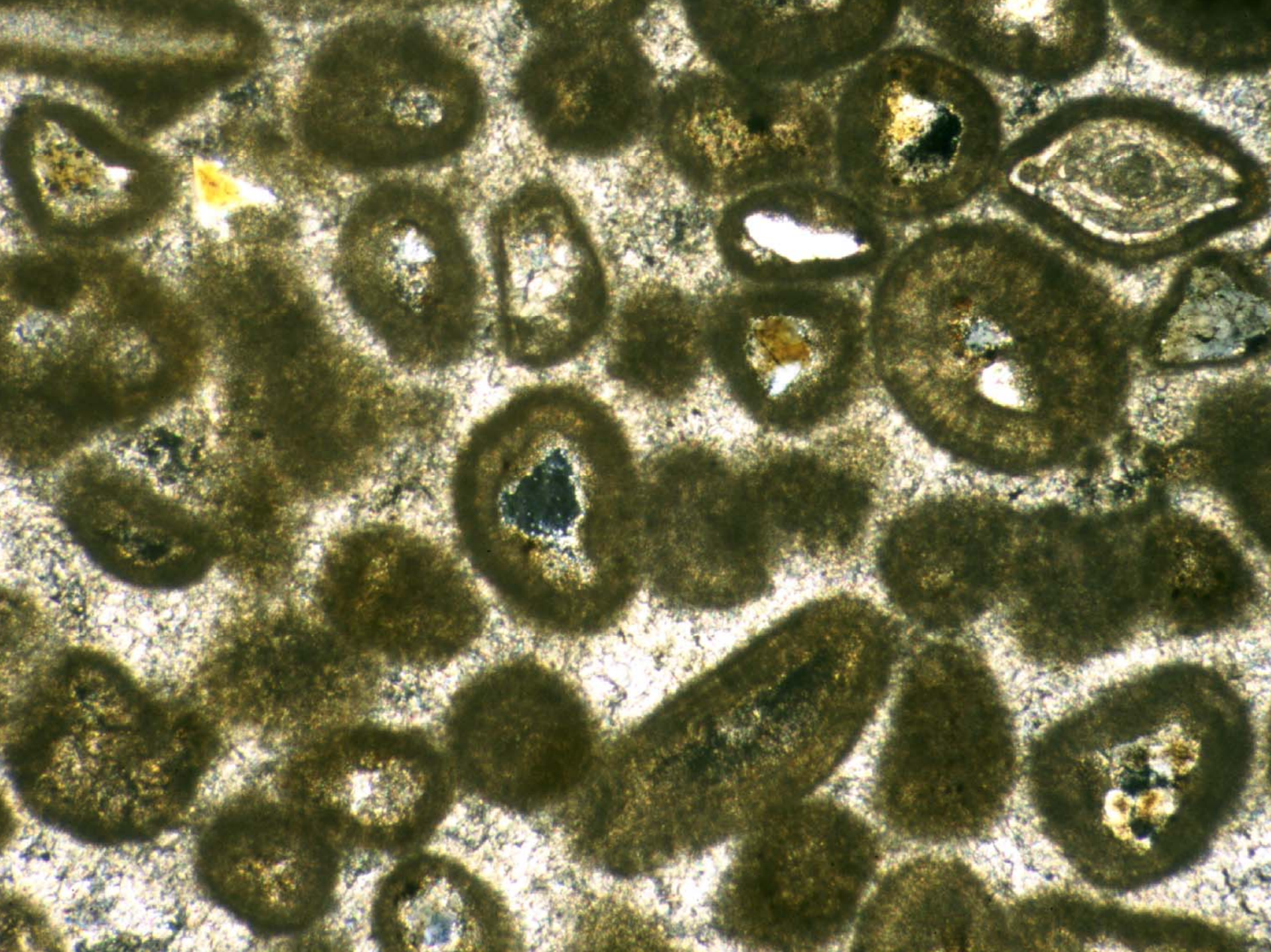

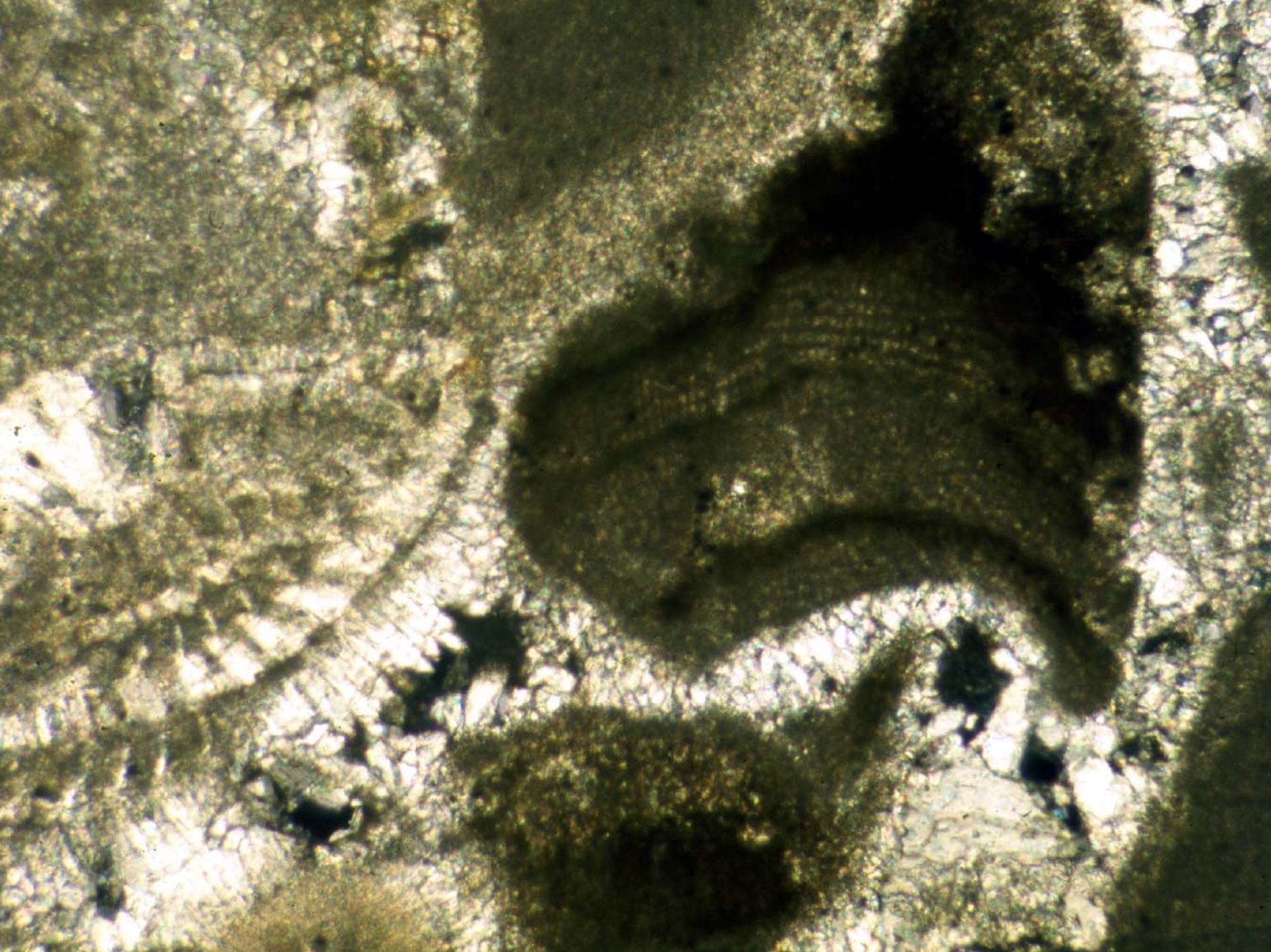

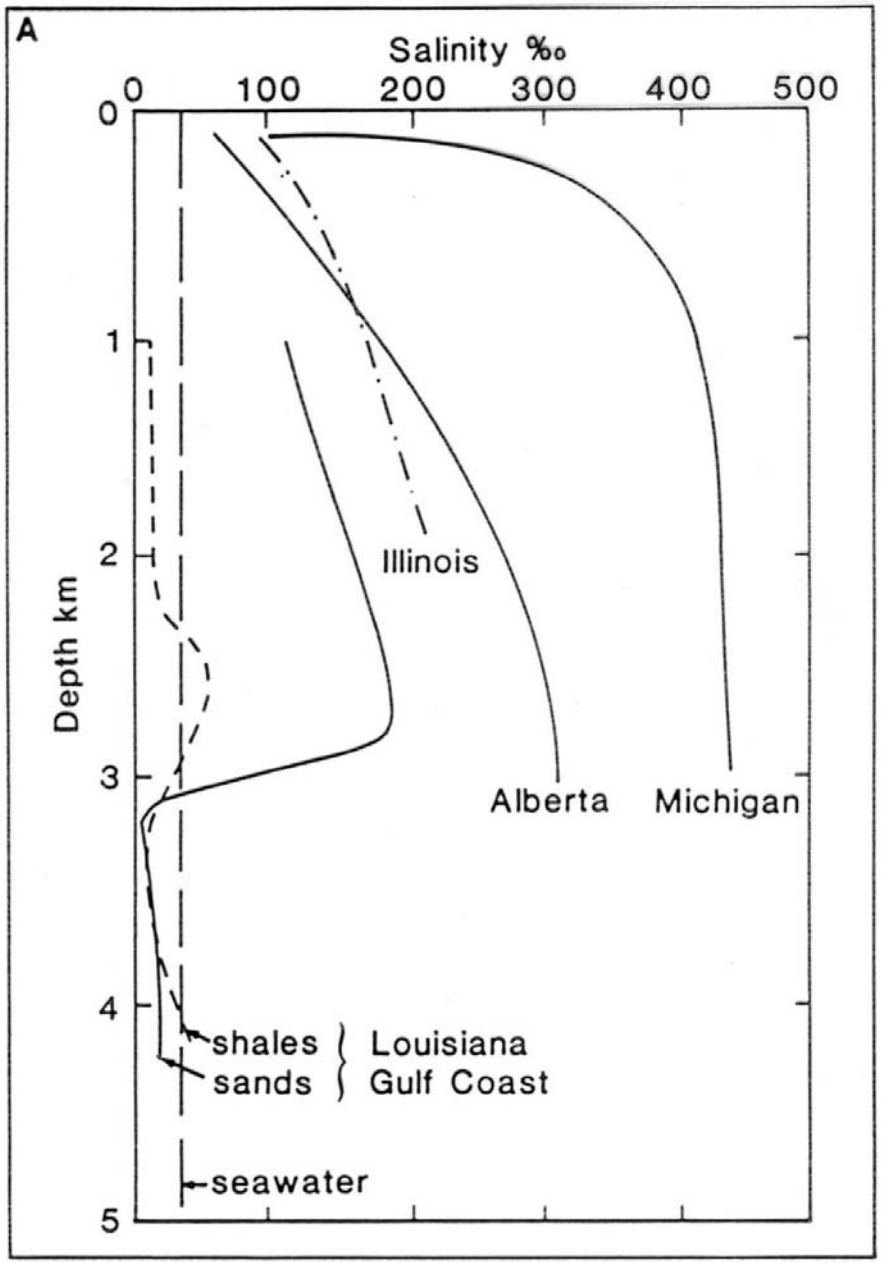
A
Salinity ‰
0
100
200
300
400
500
0
1
2
3
4
5
Depth km
Illinois
Alberta
Michigan
shales
sands
Louisiana
Gulf Coast
seawater

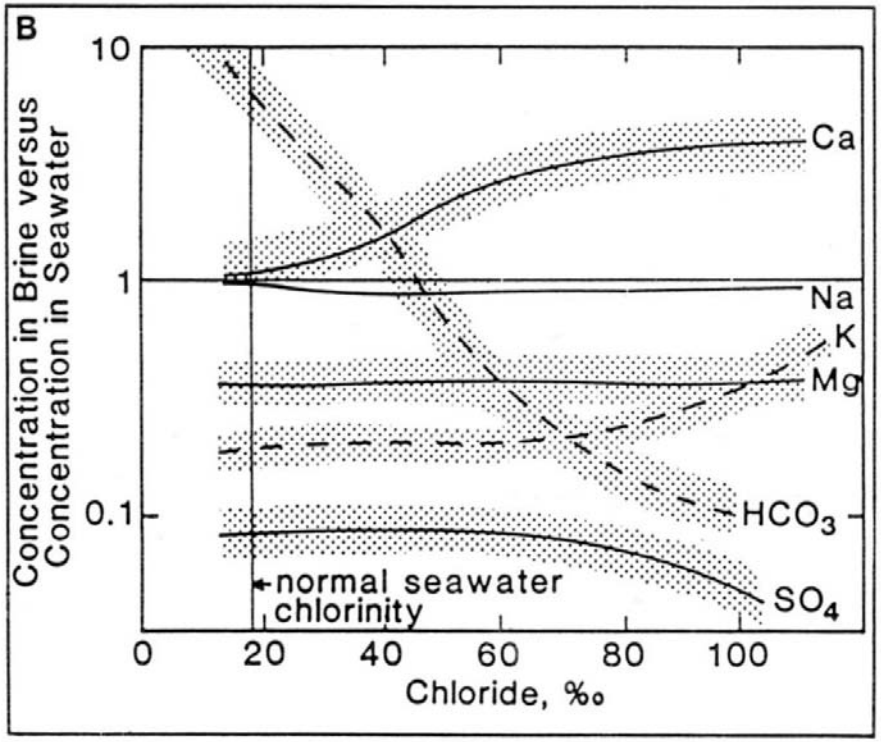

Fig. 7.30 *(A) Generalized salinity variations with depth for formation waters from the Alberta, Illinois, Louisiana Gulf Coast and Michigan Basins (B) Generalized variations in chemical composition of subsurface brines in the Illinois Basin with increasing chlorinity. Values are normalized with respect to seawater of the same chloride content. From Hanor (1983).*

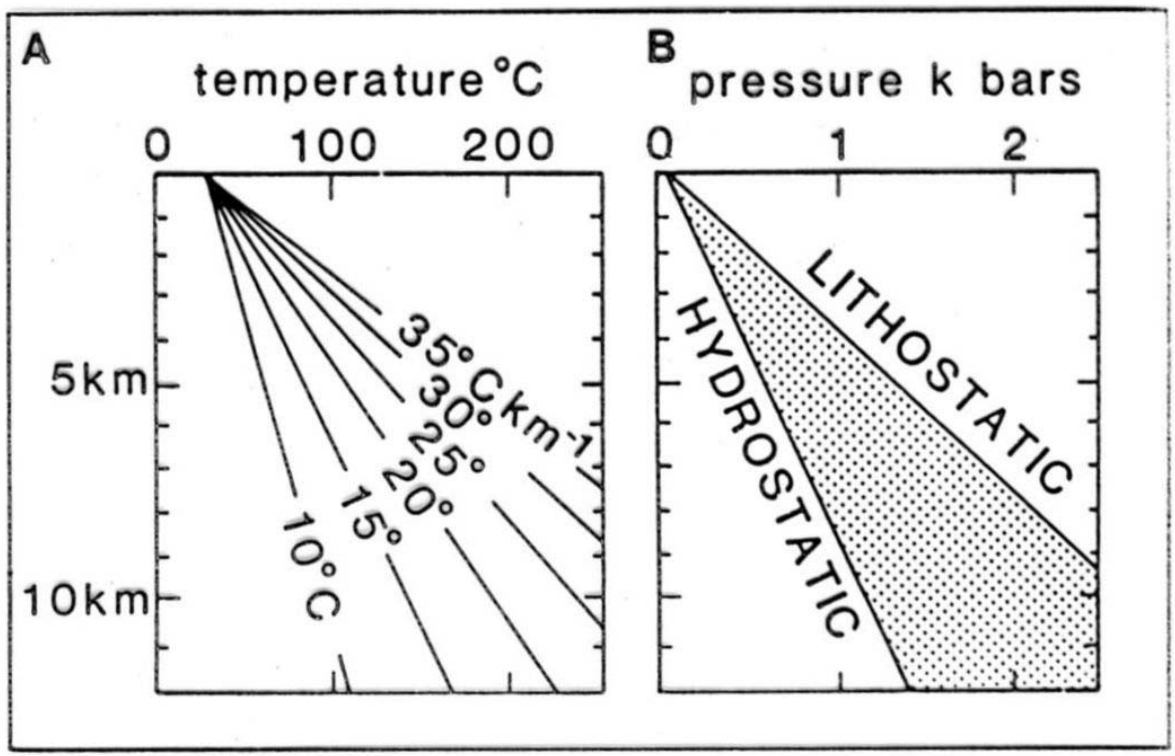
A
temperature °C
0
100
200
5km
10km
35°C km⁻¹
30°
25°
20°
15°
10°C
B
pressure k bars
0
1
2
LITHOSTATIC
HYDROSTATIC

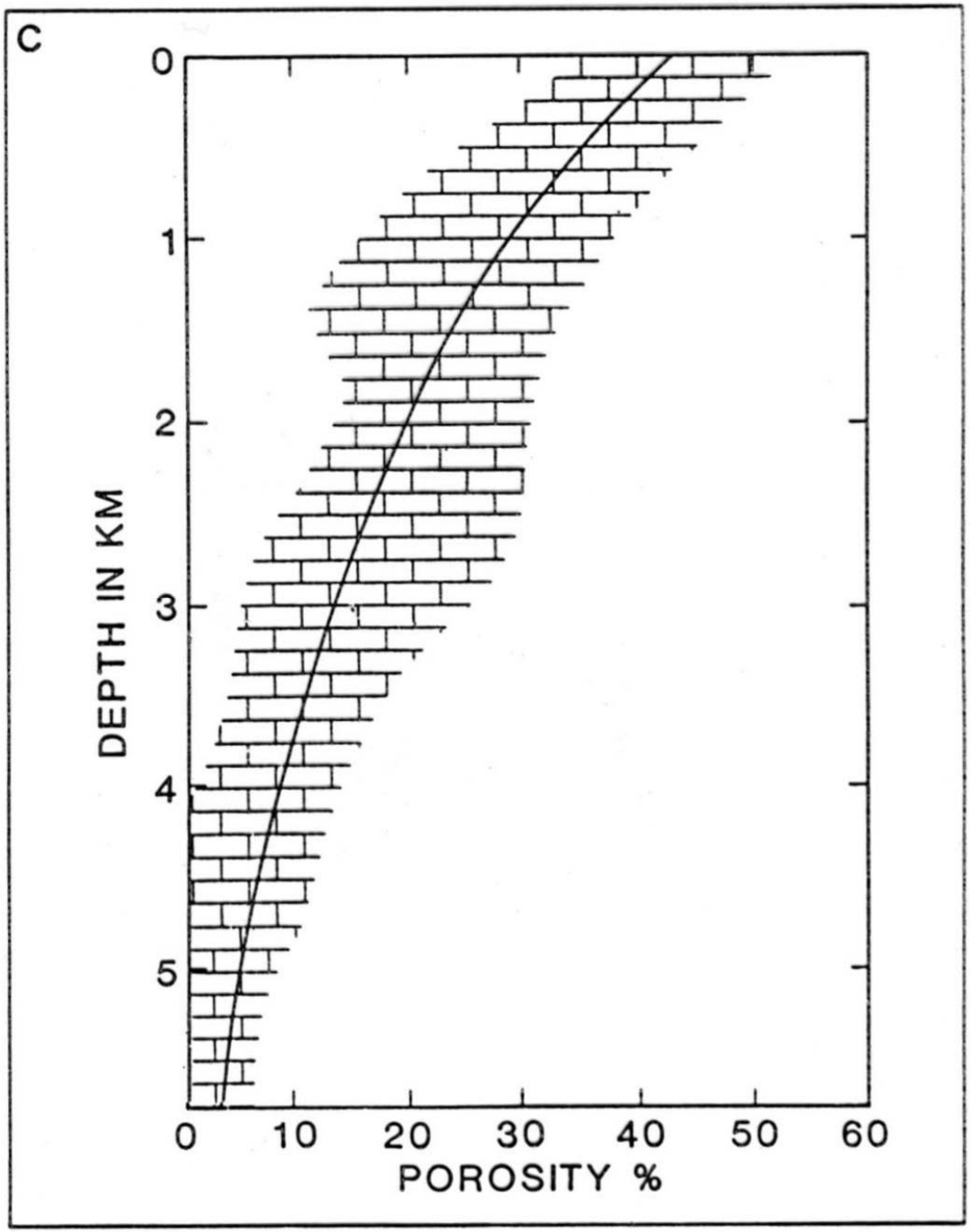
C
0
1
2
3
4
5
DEPTH IN KM
0
10
20
30
40
50
60
POROSITY %

meteorická diageneze

rozpouštění (sekundární porozita, krasovění), tmelení, pedogeneze
vadózní zóna – svrchní – infiltrace, spodní – perkolace
freattické **- syntaxiální nárůsty, stejnozrnný sparit**
vadózní – asymetrické : **meniskový, gravitační**;

---

izopachový tmel – freatický — rané stádium
asymetrický – vadózní
syntaxiá
lní nárůsty
náhrada A kalcitem – sparitový tmel — pozdní stádium
výplně pórů LMC

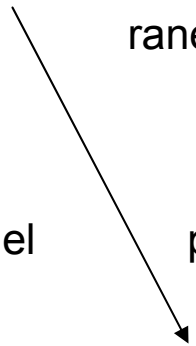

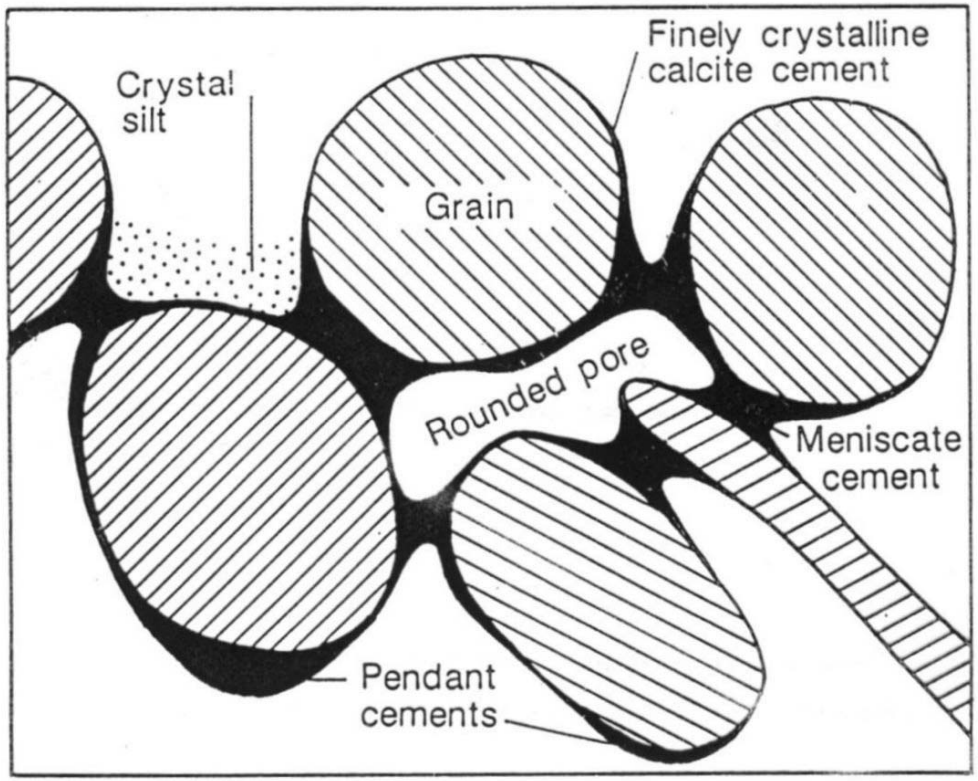

Fig. 7.27 *Common cement geometries in vadose zones (see text).*

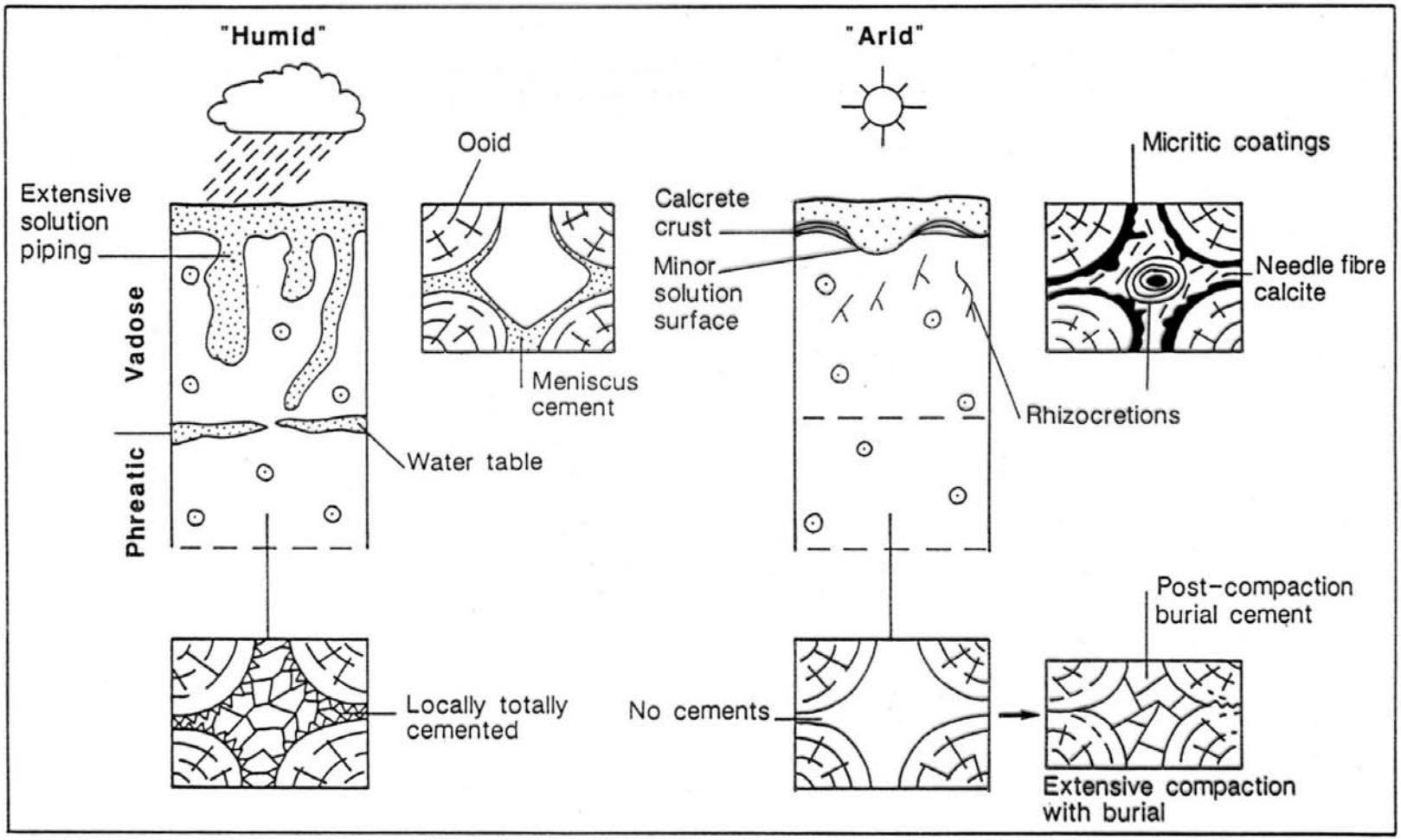

Fig. 7.24 *Contrasting styles of karstification, meteoric cementation and porosity evolution in Early Carboniferous oolitic limestones from south Wales. Based on Hird & Tucker (1988) and Wright (1988).*

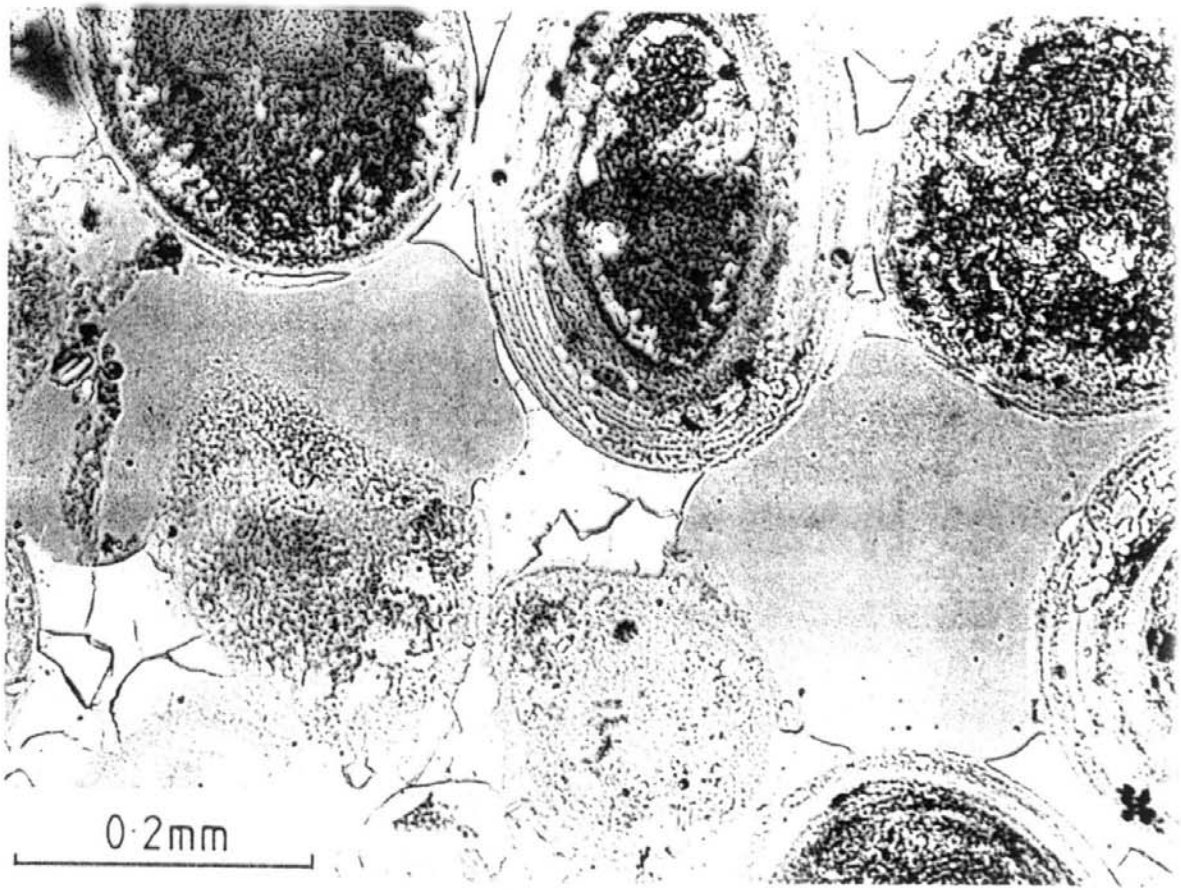

Fig. 7.28 *Meniscus cement, vadose zone, Joulter's Cay, Bahamas.*

kalcitový sparit

stejnozrnná mozaika, syntaxiální nárůsty, poikilotopický sparit

-meteorická freatická zóna, zdroj $CaCO_3$ – pórové vody

-pohřbení, zdroj $CaCO_3$ – tlakové rozpouštění

stratigrafie tmelů, katodová luminiscence, stabilní izotopy, fluidní inkluze

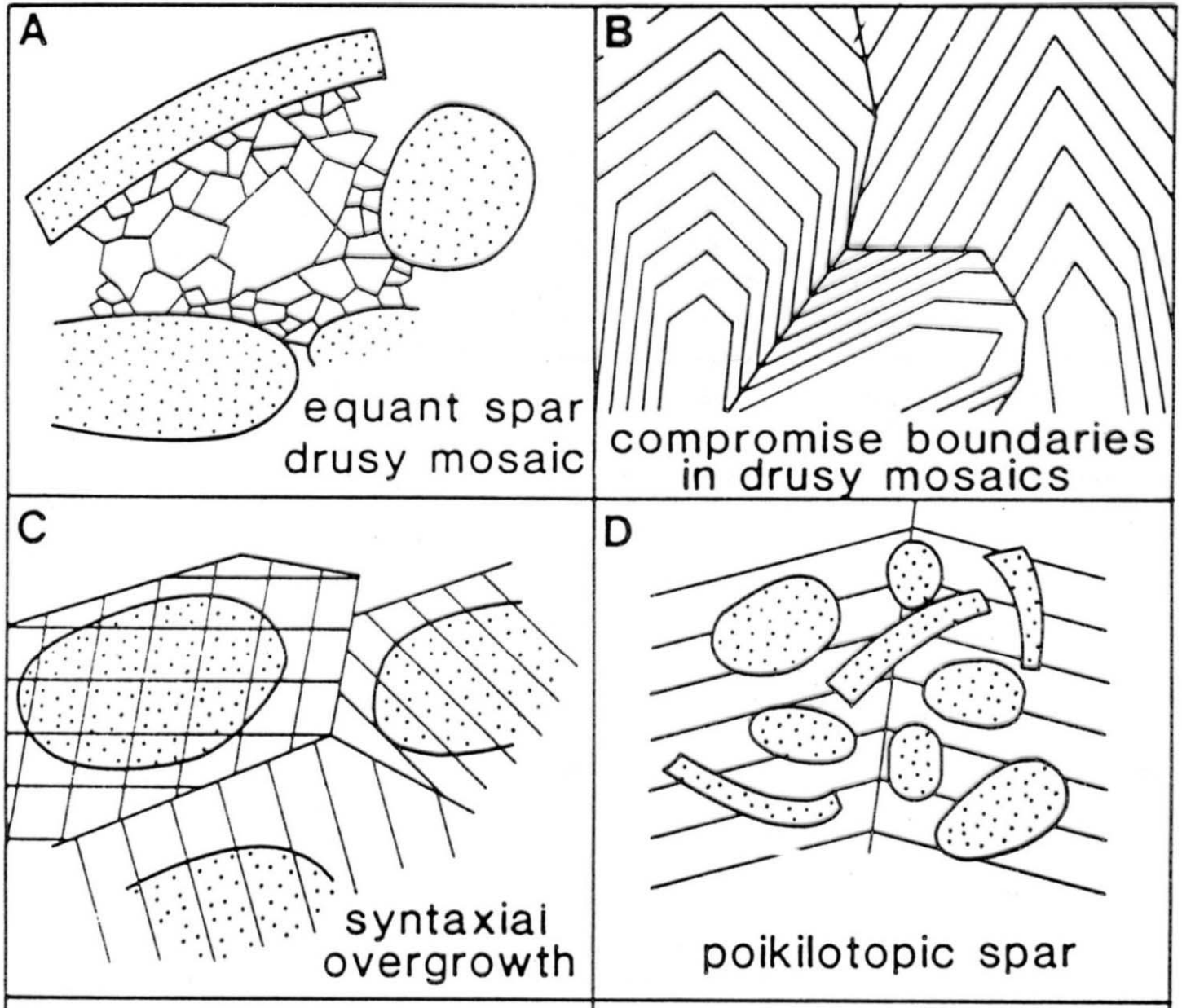
A
equant spar
drusy mosaic
B
compromise boundaries
in drusy mosaics
C
syntaxiai
overgrowth
D
poikilotopic spar

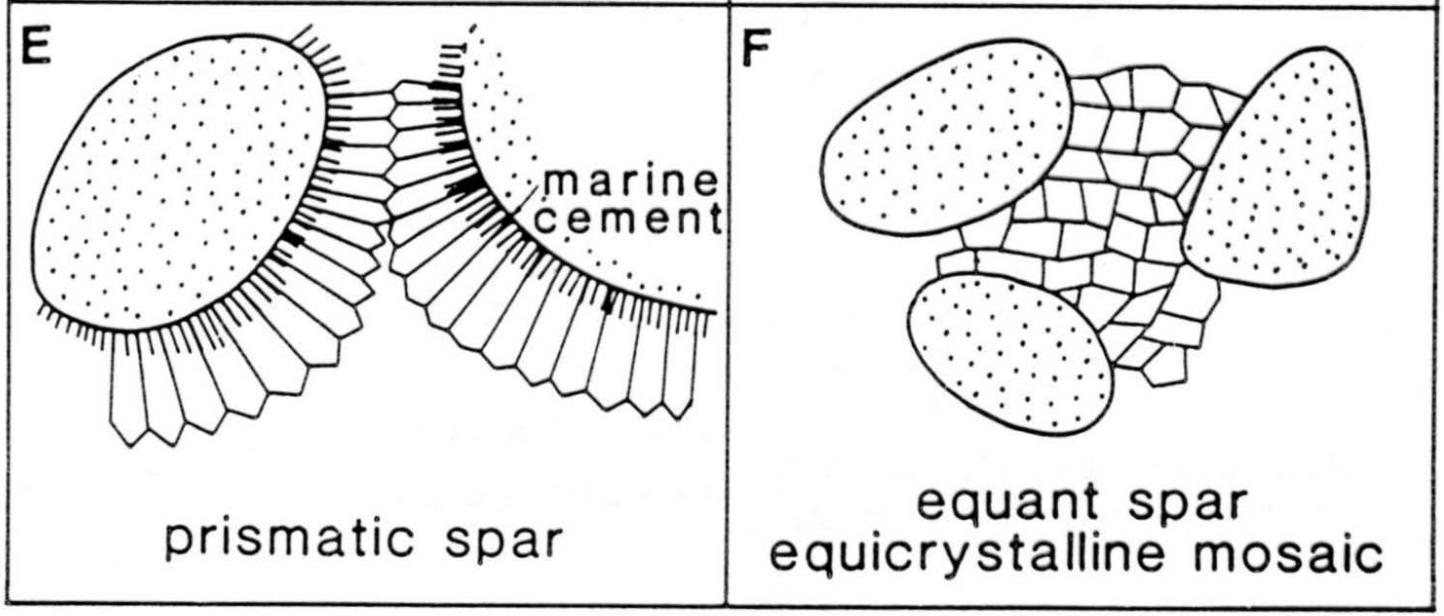

Fig. 7.32 *Calcite spar: sketches illustrating the common types.*

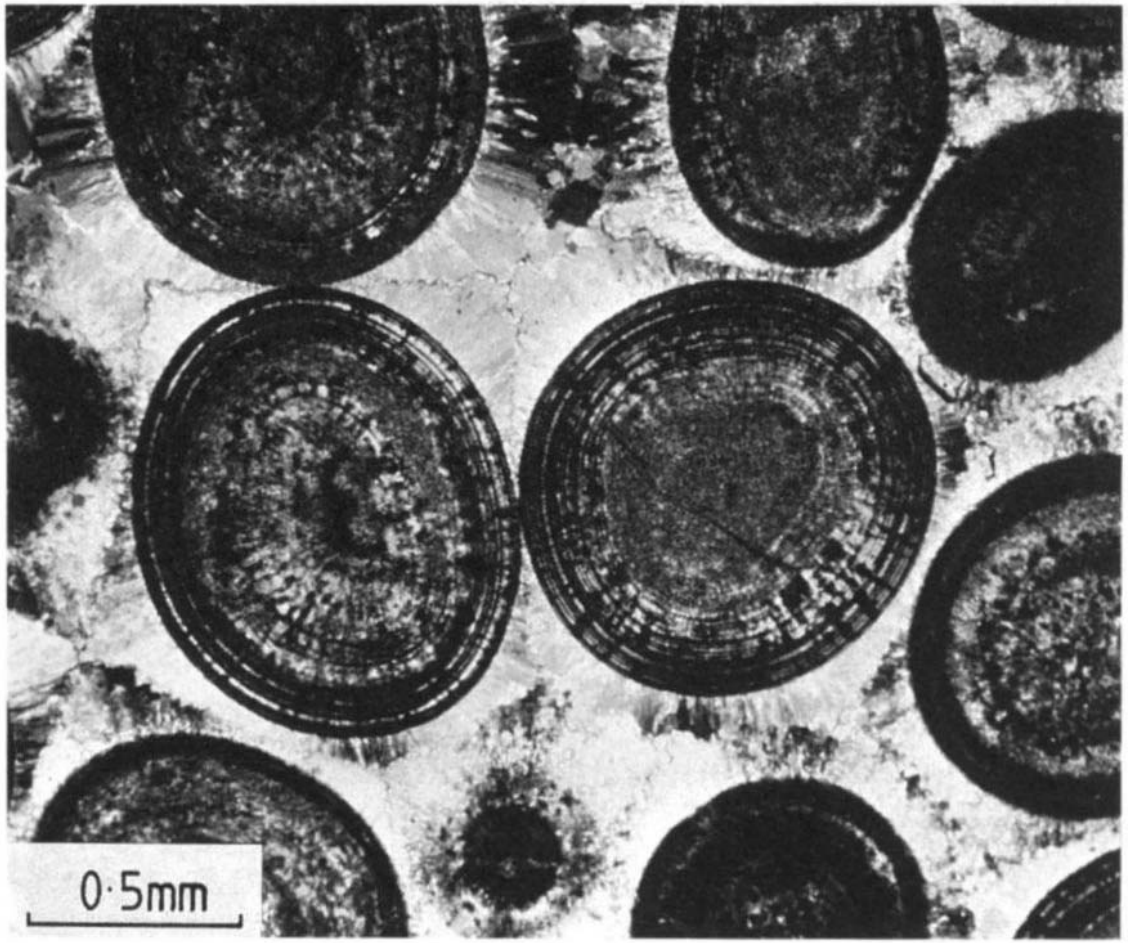

Fig. 7.14 *Fibrous calcite marine cement (primary) around ooids (also primary calcite) with prominent polygonal compromise boundary between fringes. These more acicular crystals are in optical continuity with radial-fibrous crystallities of the ooids. Jurassic Smackover Formation, subsurface Arkansas. Crossed polars.*

neomorfismus

A→C, C→C, rozpouštění + reprecipitace

agradační neomorfismus – následná fáze hrubozrnější; a) mikrit → mikrosparit, pseudosparit, b) kalcitizace aragonitu

kalcilutity: **mikrosparit** (4-10 mm), **pseudosparit** (10-50 mm); nepravidelné nerovné hranice mezi zrny, nepravidelné velikostní rozložení zrn, skelet plove ve sparitu; pseudobrekcie

kalcitizace A zrn a tmelů – **drůzový sparit**; a) relikty pův. struktur schránky, b) nepravidelná mozaika krystalů růz.velikosti, c) hnědavé zbarvení neomorfního sparitu (relikty org.hmoty) - pseudopleochroismus

degradační neomorfismus – klesá zrnitost; zřídka; obvykle při metamorfóze nebo při tlakovém postižení

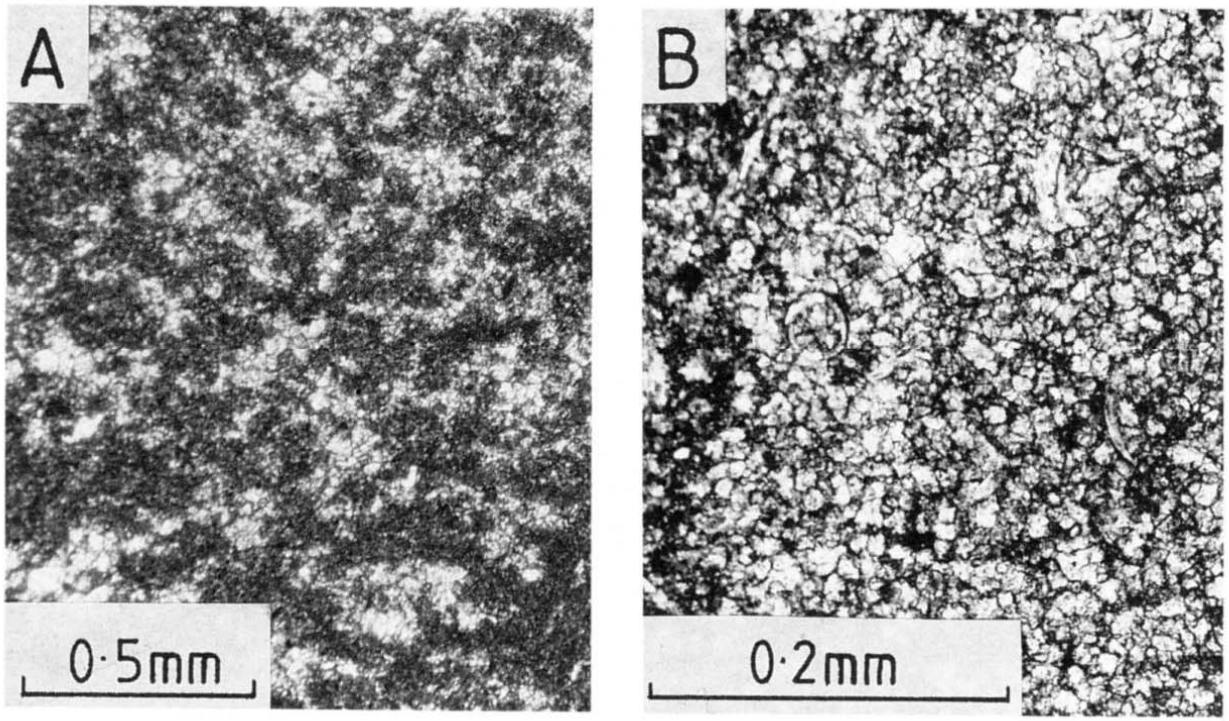

Fig. 7.41 *Neomorphic spar. (A) Patches of microspar in a micritic pelagic limestone resulting from aggrading neomorphism. Upper Devonian, West Germany. (B) Coarse microspar mosaic of equant crystals with floating skeletal debris. Pseudobreccia, Lower Carboniferous, northwest England.*

kompakce

mechanická k. – už v raných stádiích; přeuspořádání částic do prostorově úspornější, stabilnější vzájemné pozice; deformace velkých klastů, tmelů, mikritických obálek; bioklastický wackestone → b. packstone

chemická k. – při hlubším pohřbení (stovky m); rozpouštění základní hmoty → fitted fabric; stylolity, švy tlakového rozpouštění

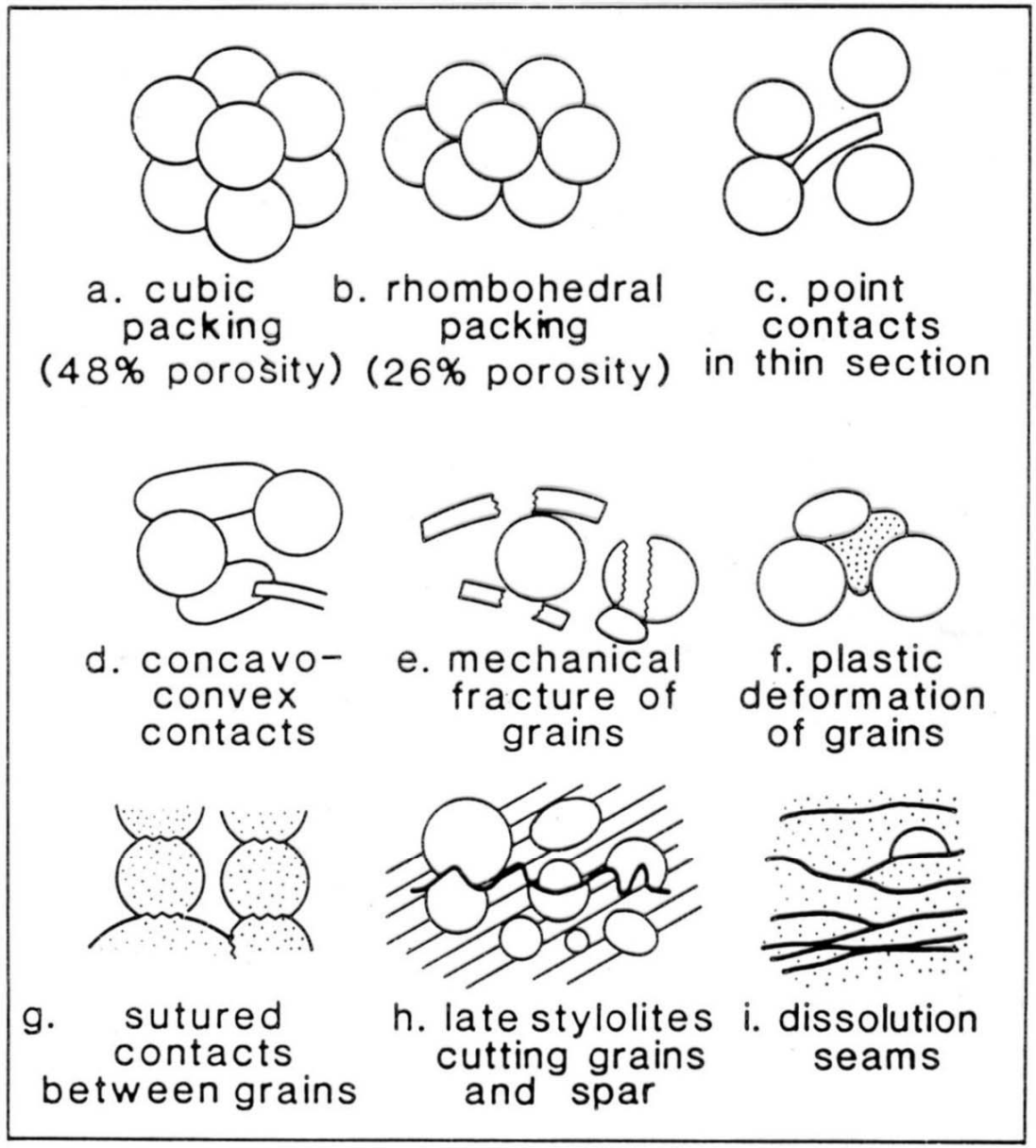

Fig. 7.37 *Grain packing, grain contacts and mechanical and chemical compaction textures in limestones.*

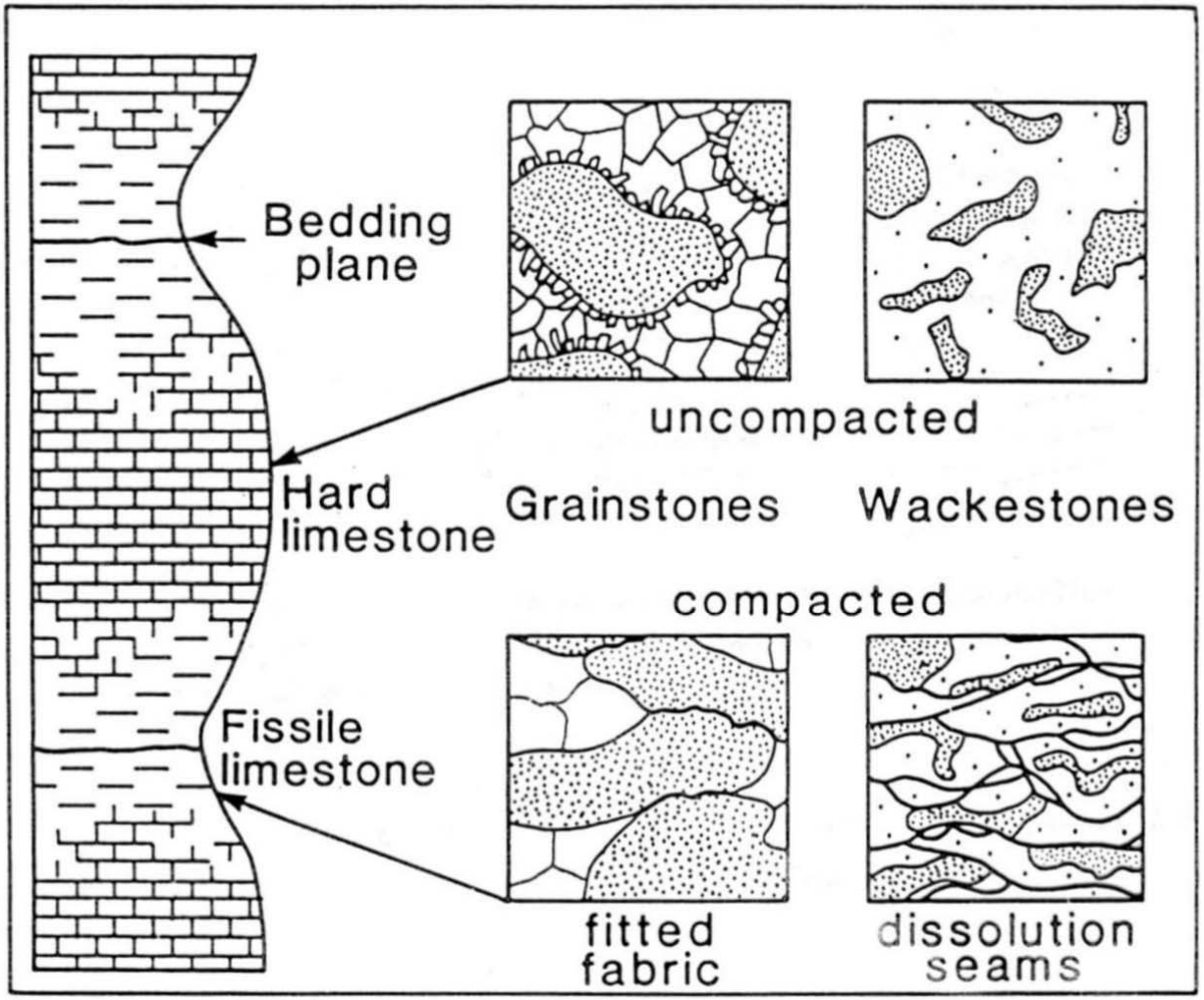

Fig. 7.40 *Uncompacted, hard limestones alternating with fissile limestones showing fitted fabrics and dissolution seams. This is the result of episodic subseafloor cementation. After Bathurst (1987).*

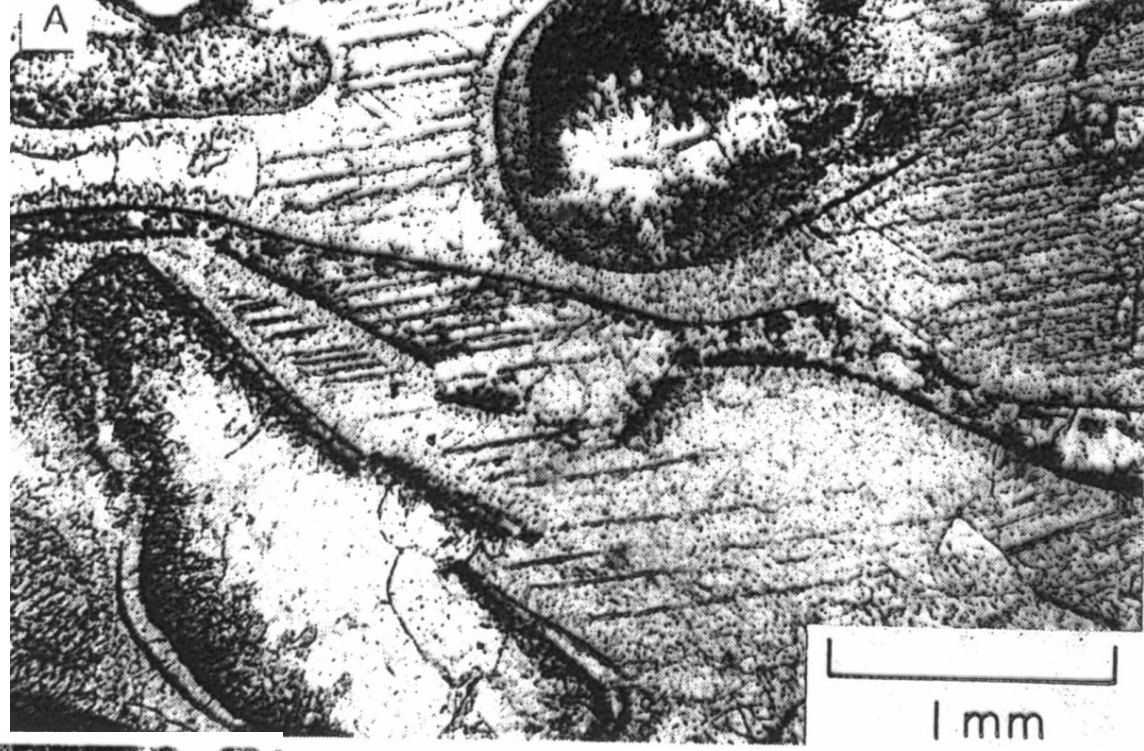
A
1 mm


B
1 mm

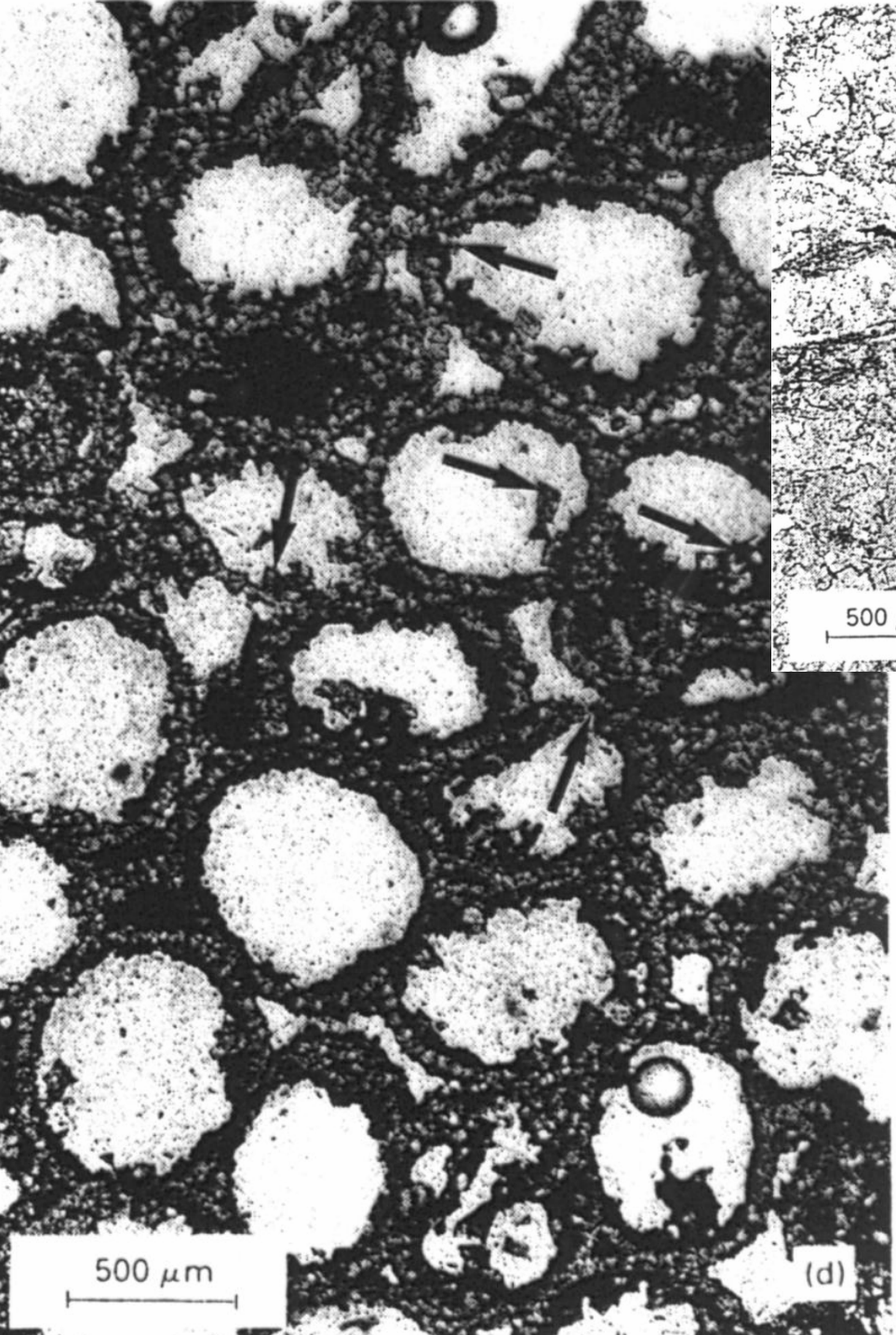
500 μm
(d)

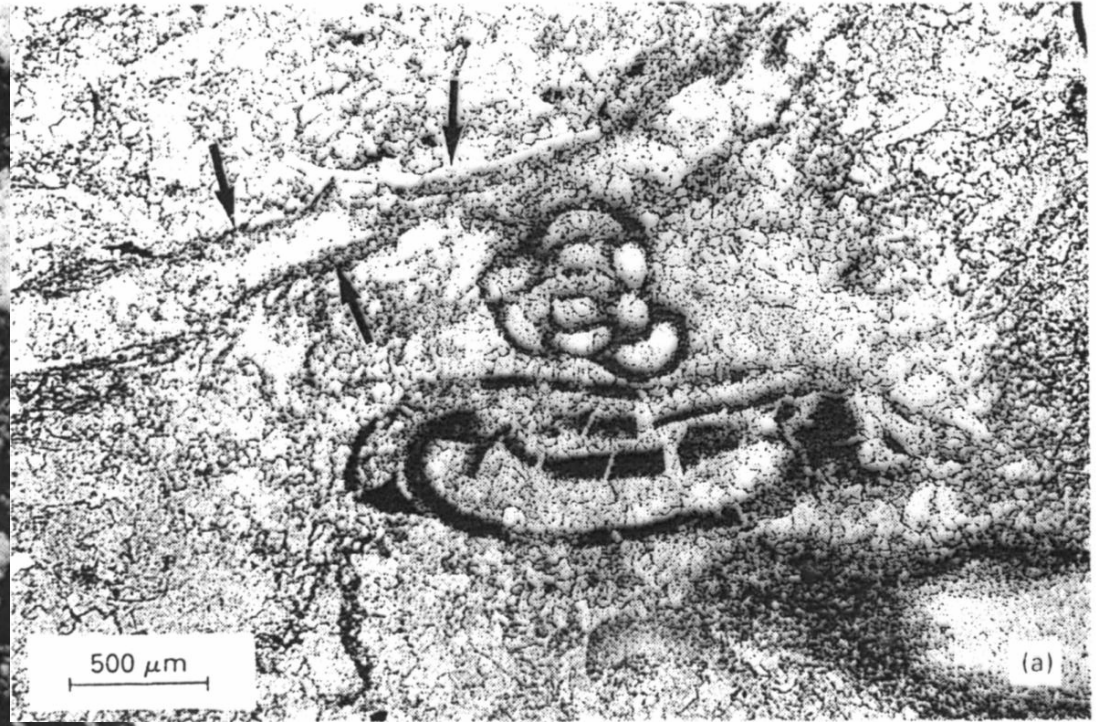
500 μm
(a)

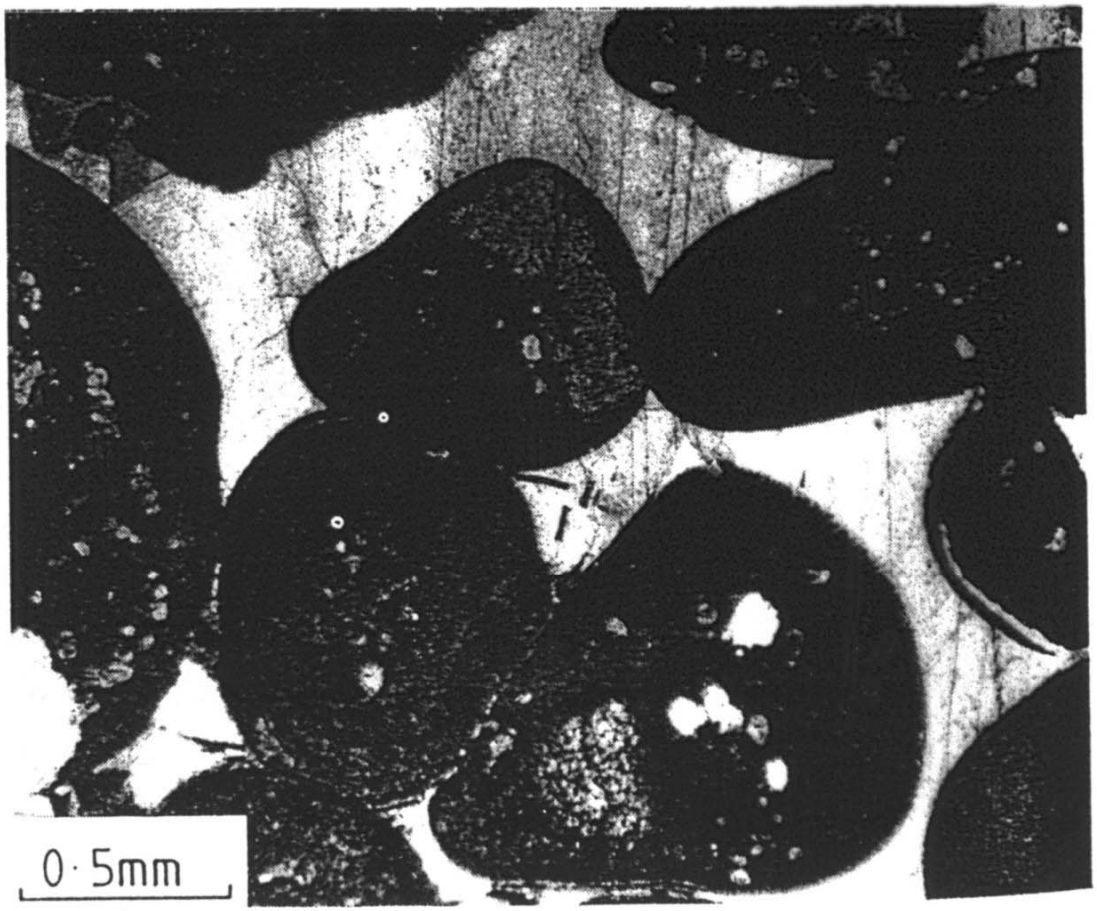

Fig. 7.38 *Concavo-convex and microstylolitic contacts in Smackover Oolite, Jurassic, Louisiana subsurface. Notice also the spalling and fracture of thin oolitic coating off the central grain. Intergranular porosity later filled by very coarse, poikilotopic calcite spar (white).*

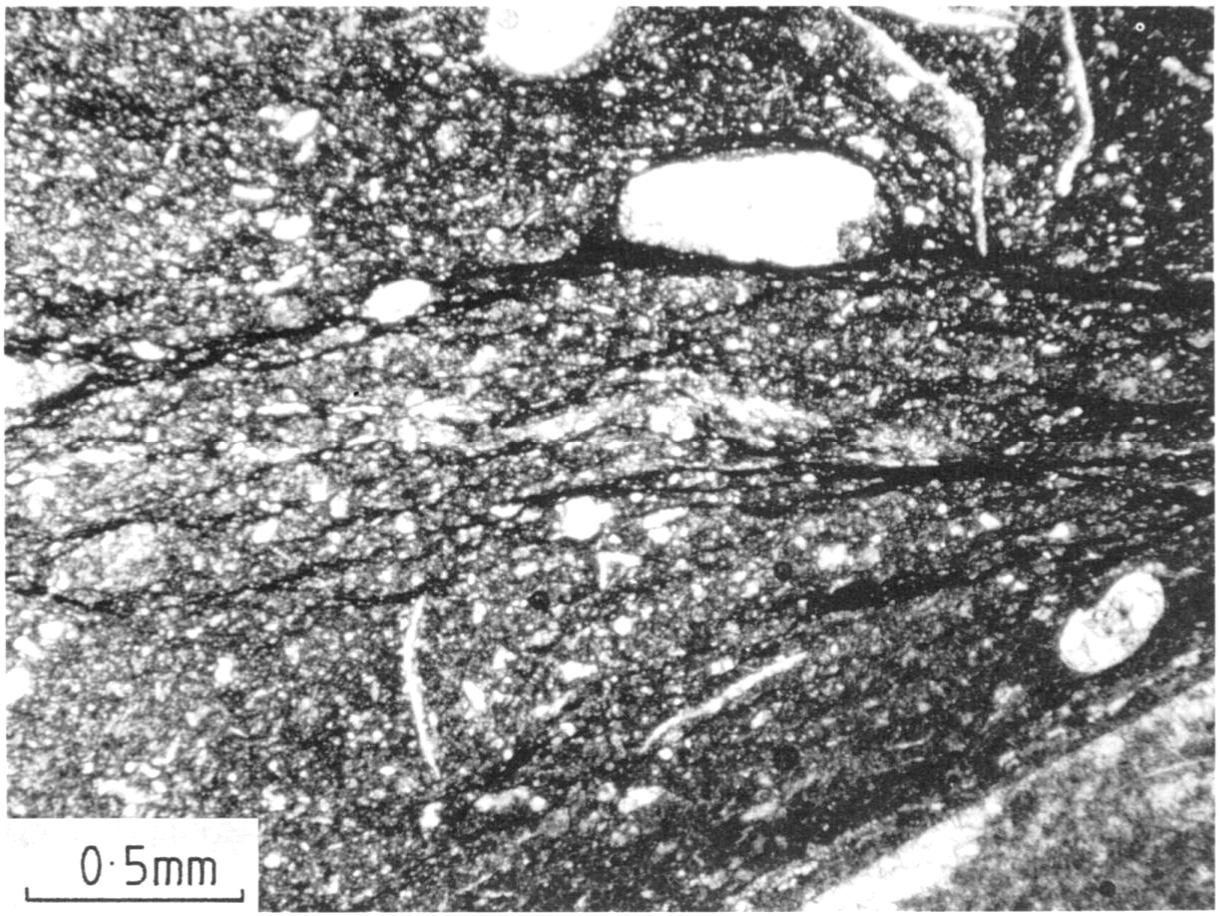

Fig. 7.39 *Dissolution seams with insoluble residue (clay) concentrated along them. Upper Devonian, Griotte (pelagic limestone), southern France.*

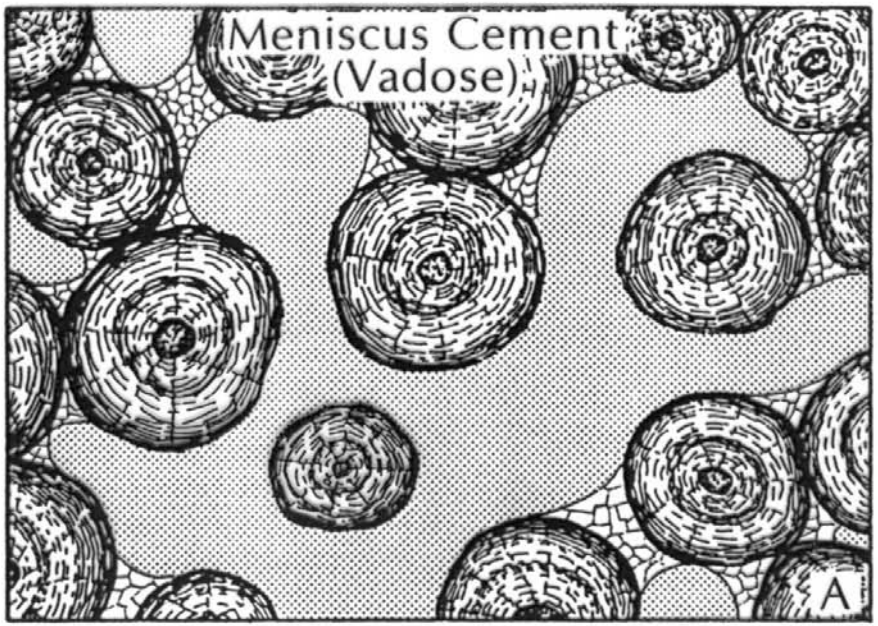
Meniscus Cement
(Vadose)
A

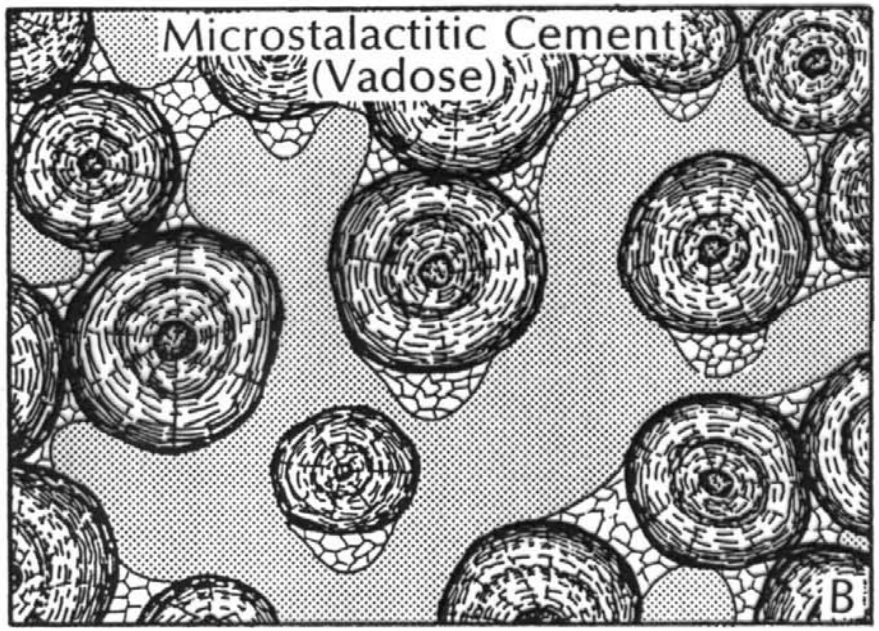
Microstalactitic Cement
(Vadose)
B

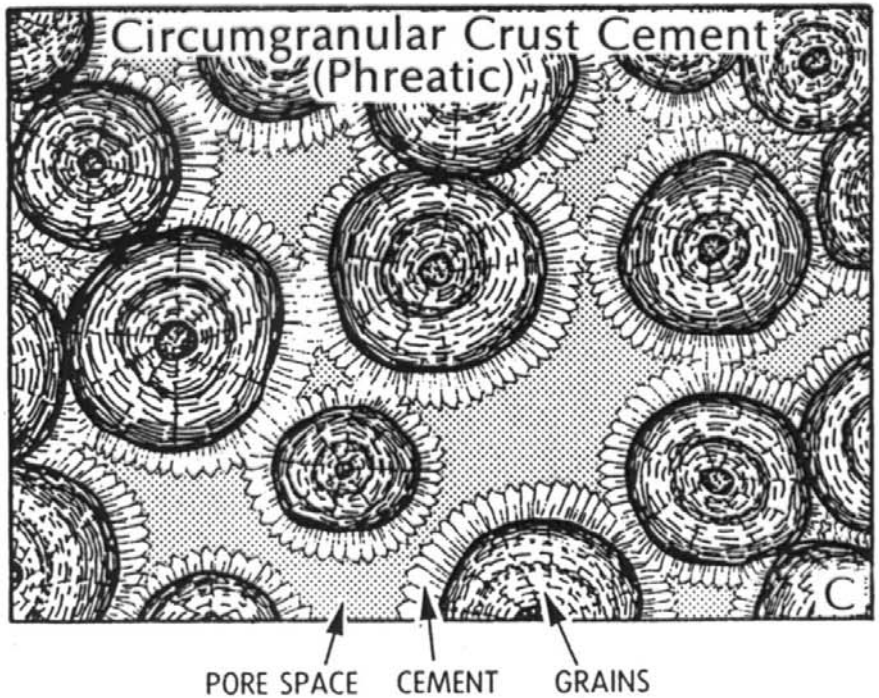

Fig. 3.6. Cement distributional patterns as a function of diagenetic environment. A. In the vadose zone, cements are concentrated at grain contacts and the resulting pores have a distinct rounded appearance due to the meniscus effect . The resulting cement pattern is termed meniscus cement. B. In the vadose zone immediately above the water table there is often an excess of water that accumulates at the base of grains as droplets. These cements are termed microstalactitic cements. C. In the phreatic zone, where pores are saturated with water, cements are precipitated as circumgranular crusts.

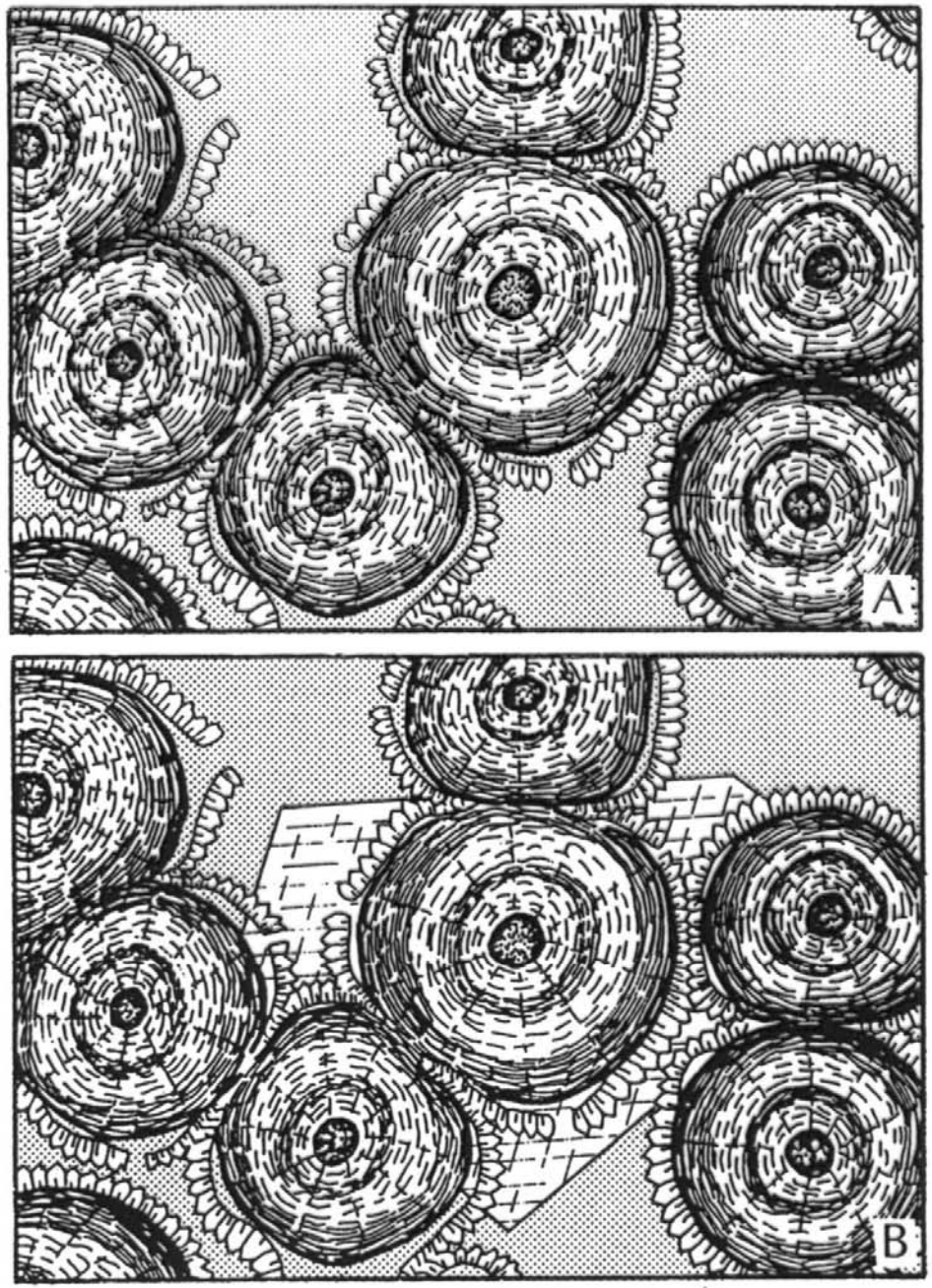
A
B

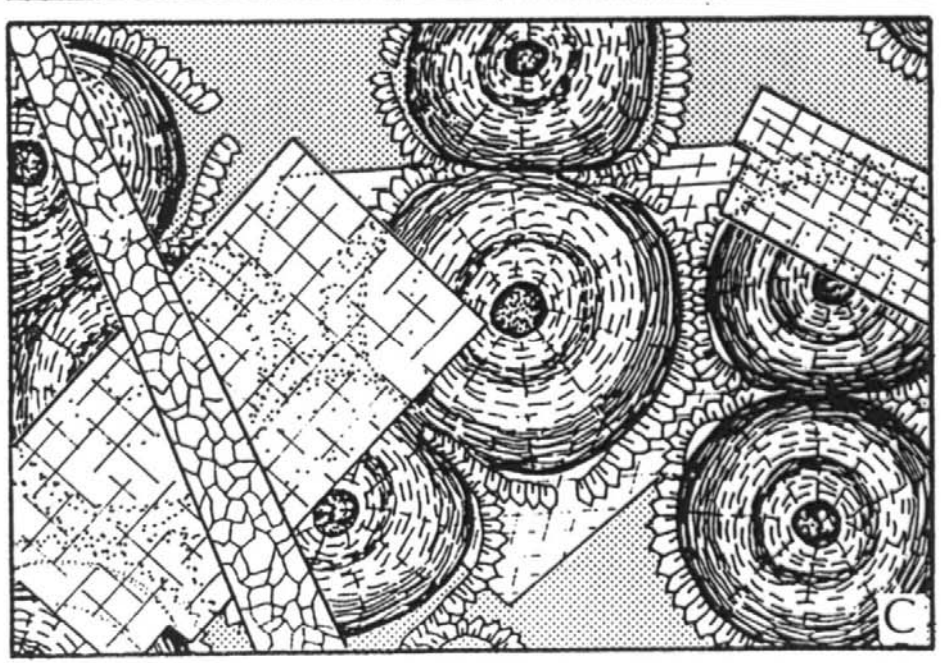

Fig. 3.8. Timing of diagenetic events by petrographic relationships. A. Involvement of isopachous cement in compaction indicates that cement was early. B.Cement that encases compacted grains and spalled isopachous cement is relatively late. C. Cross cutting relationships of features such as fractures and mineral replacements are useful. Calcite filling fracture is latest event, replacement anhydrite came after the late poikilotopic cement, but before the fracture, while the isopachous cement was the earliest diagenetic event.

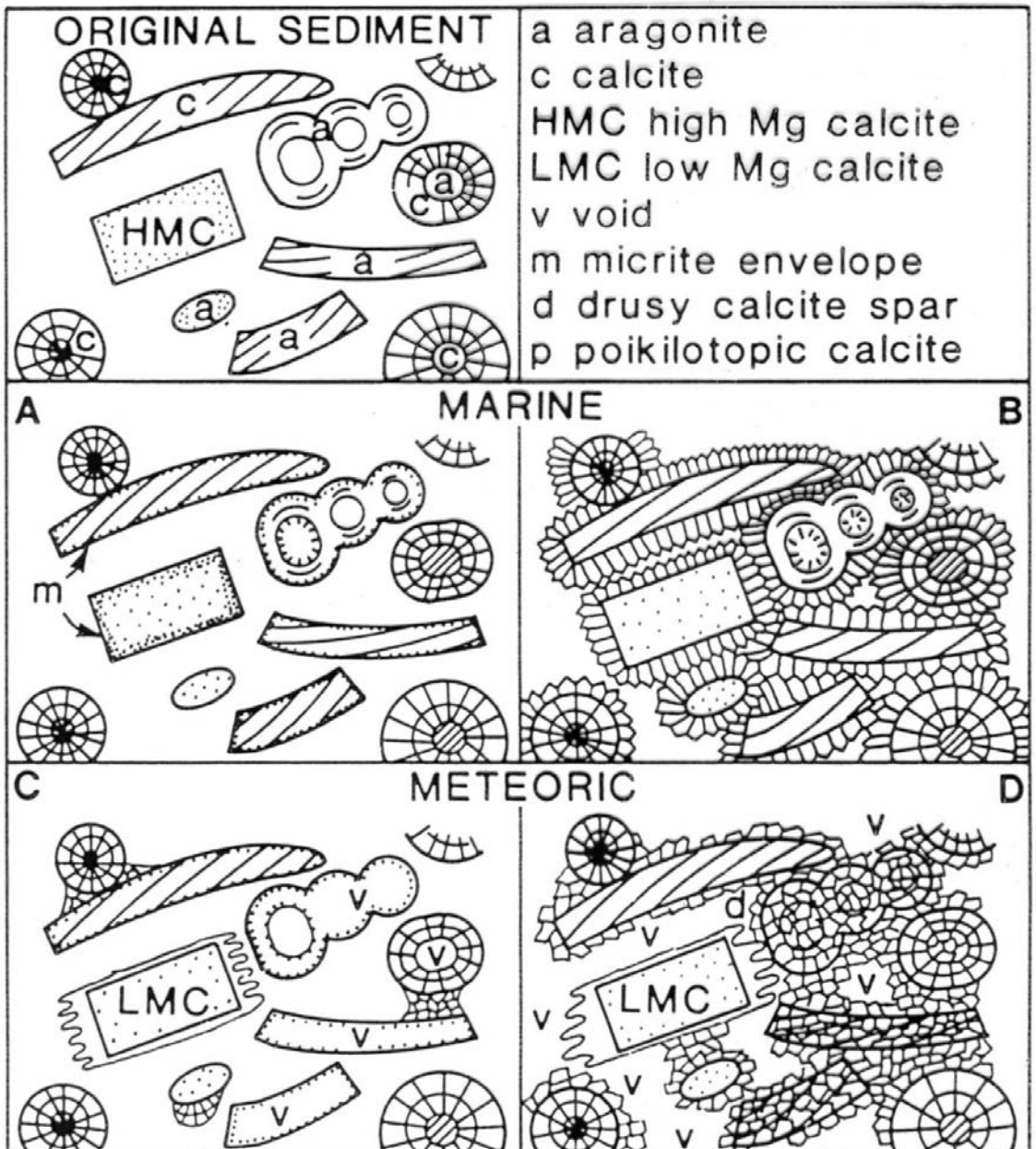
ORIGINAL SEDIMENT
a aragonite
c calcite
HMC high Mg calcite
LMC low Mg calcite
v void
m micrite envelope
d drusy calcite spar
p poikilotopic calcite
HMC
MARINE
A
B
m
METEORIC
C
D
LMC
LMC
v
d

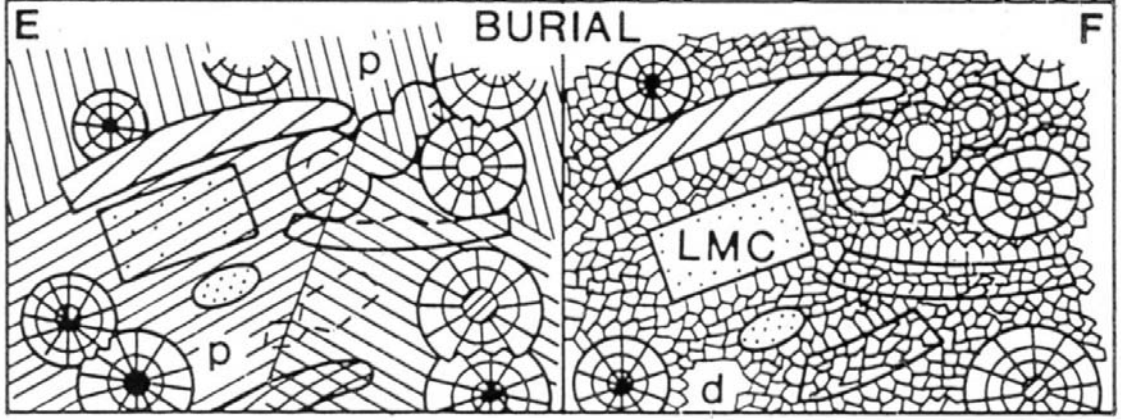

Fig. 7.42 *End-member diagenetic models for marine, meteoric and burial environments. Model A is for marine diagenesis in a poorly agitated or stagnant location where grain micritization is dominant. Model B is for marine diagenesis in a high-energy location where there is much cementation through seawater pumping. Model C is for meteoric diagenesis in an active zone of much dissolution, whereas model D applies to a zone of more $CaCO_3$-saturated meteoric water where cementation and grain replacement are features. Model E applies to the burial diagenesis of sediments which have little near-surface cement and so compaction is extensive, whereas model F is appropriate for sediments which have been well lithified before any significant compaction. See text for further discussion.*

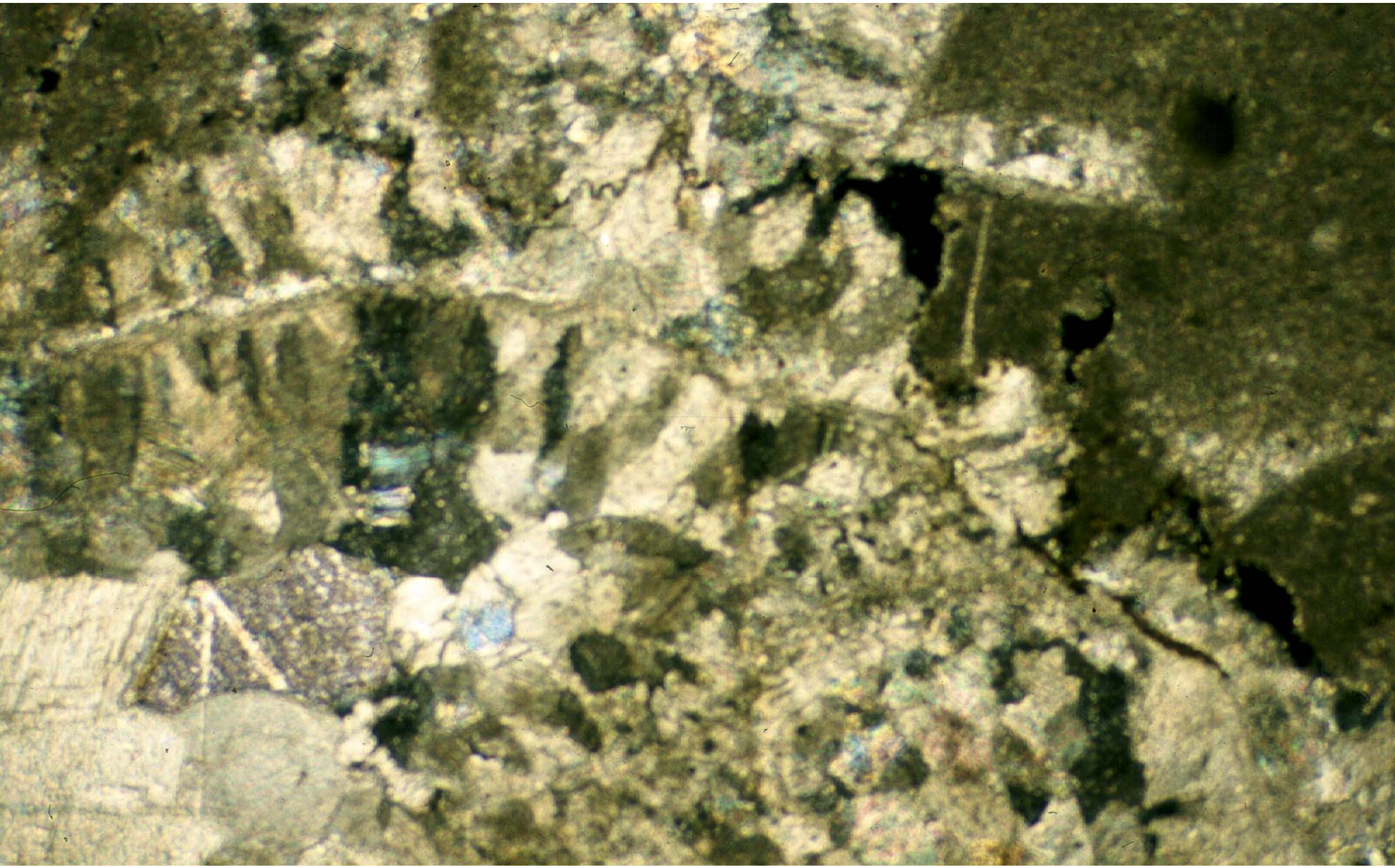

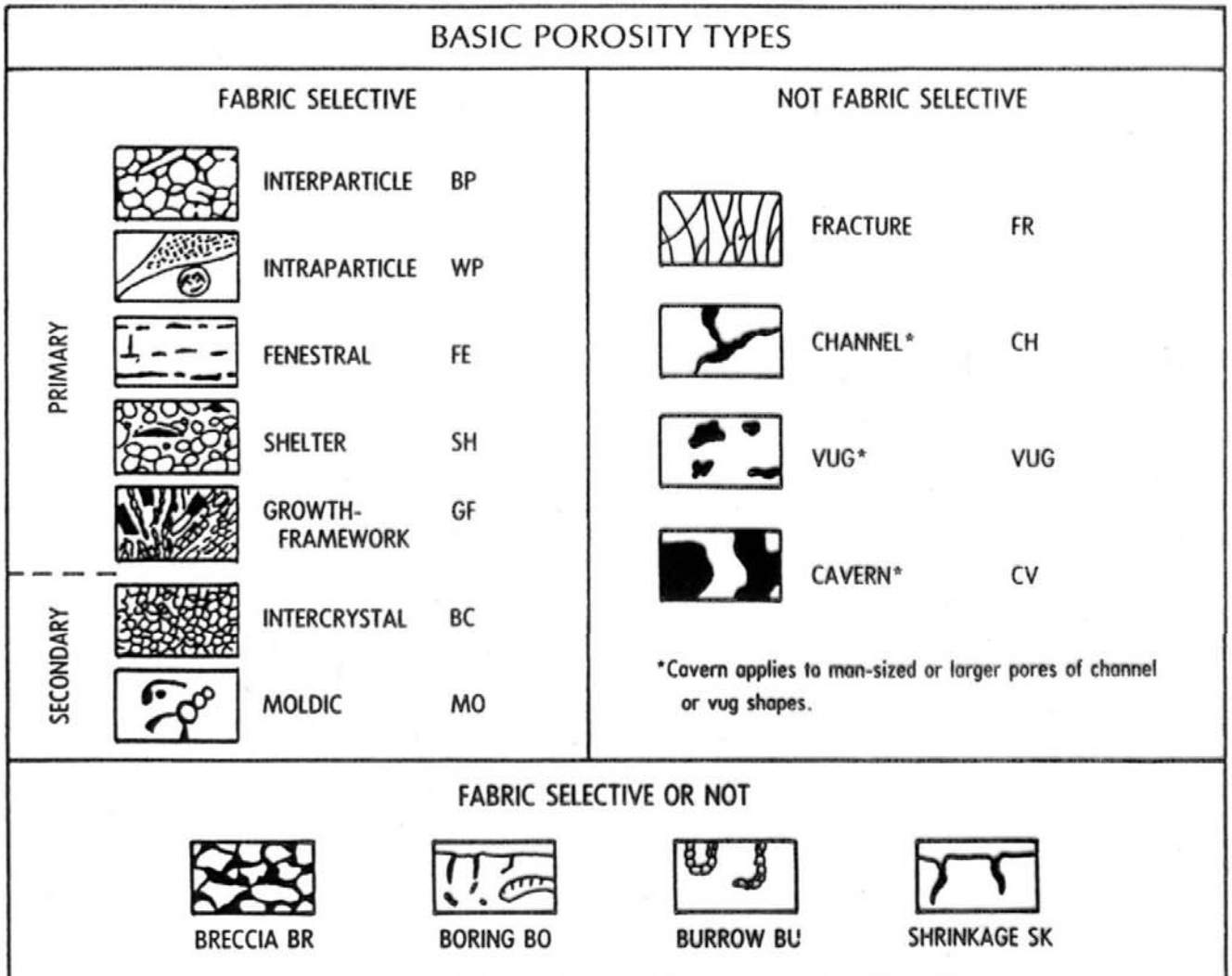
BASIC POROSITY TYPES
FABRIC SELECTIVE
NOT FABRIC SELECTIVE
PRIMARY
SECONDARY
INTERPARTICLE BP
INTRAPARTICLE WP
FENESTRAL FE
SHELTER SH
GROWTH-FRAMEWORK GF
INTERCRYSTAL BC
MOLDIC MO
FRACTURE FR
CHANNEL* CH
VUG* VUG
CAVERN* CV
*Cavern applies to man-sized or larger pores of channel or vug shapes.
FABRIC SELECTIVE OR NOT
BRECCIA BR
BORING BO
BURROW BU
SHRINKAGE SK

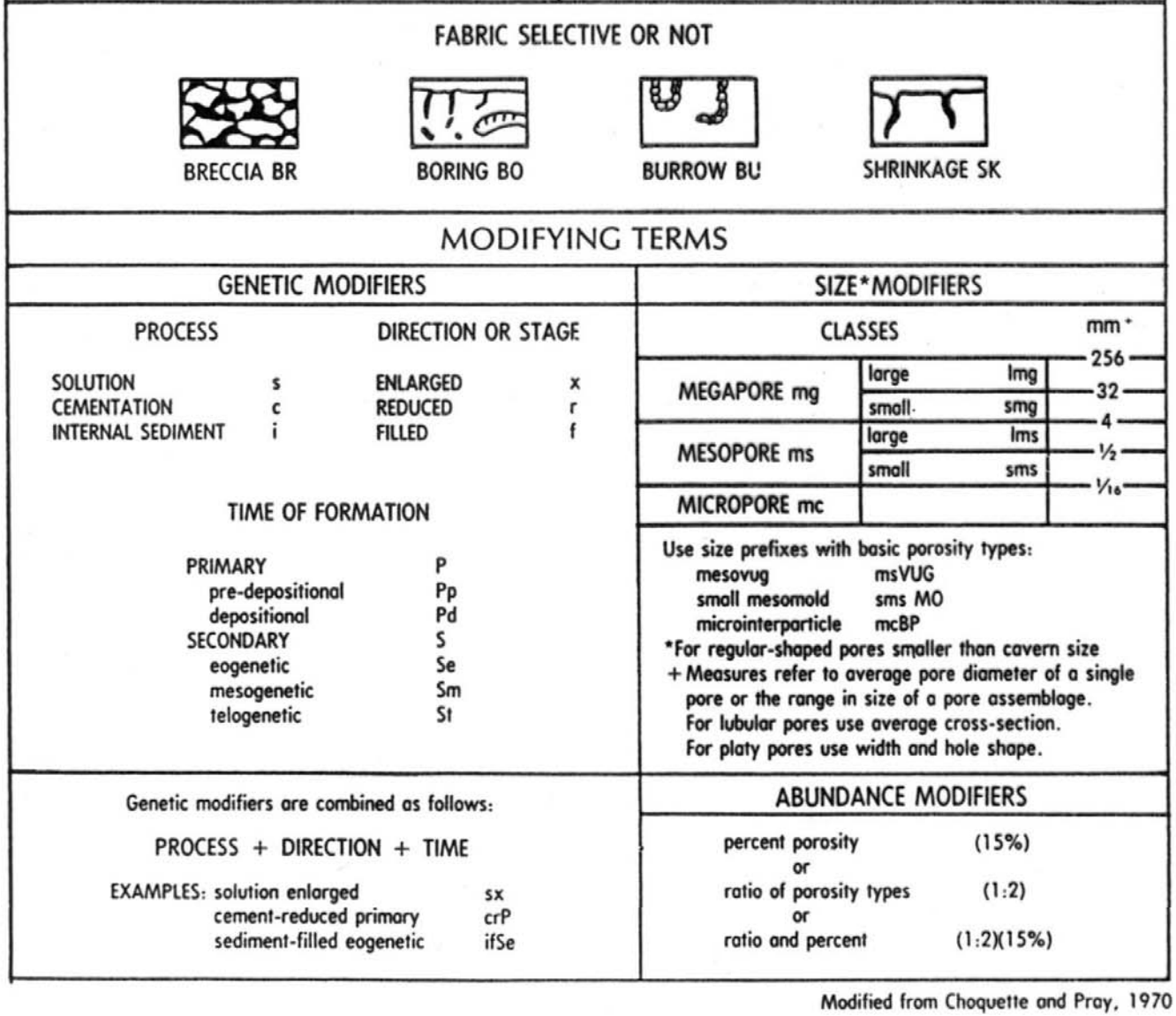

Fig. 2.1. Classification of carbonate porosity. Classification consists of basic porosity types, such as moldic. Each type is represented by an abbreviation (MO). Modifying terms include genetic modifiers, size modifiers and abundance modifiers. Each modifier also has an abbreviation. Reprinted by permission of the American Association of Petroleum Geologists.

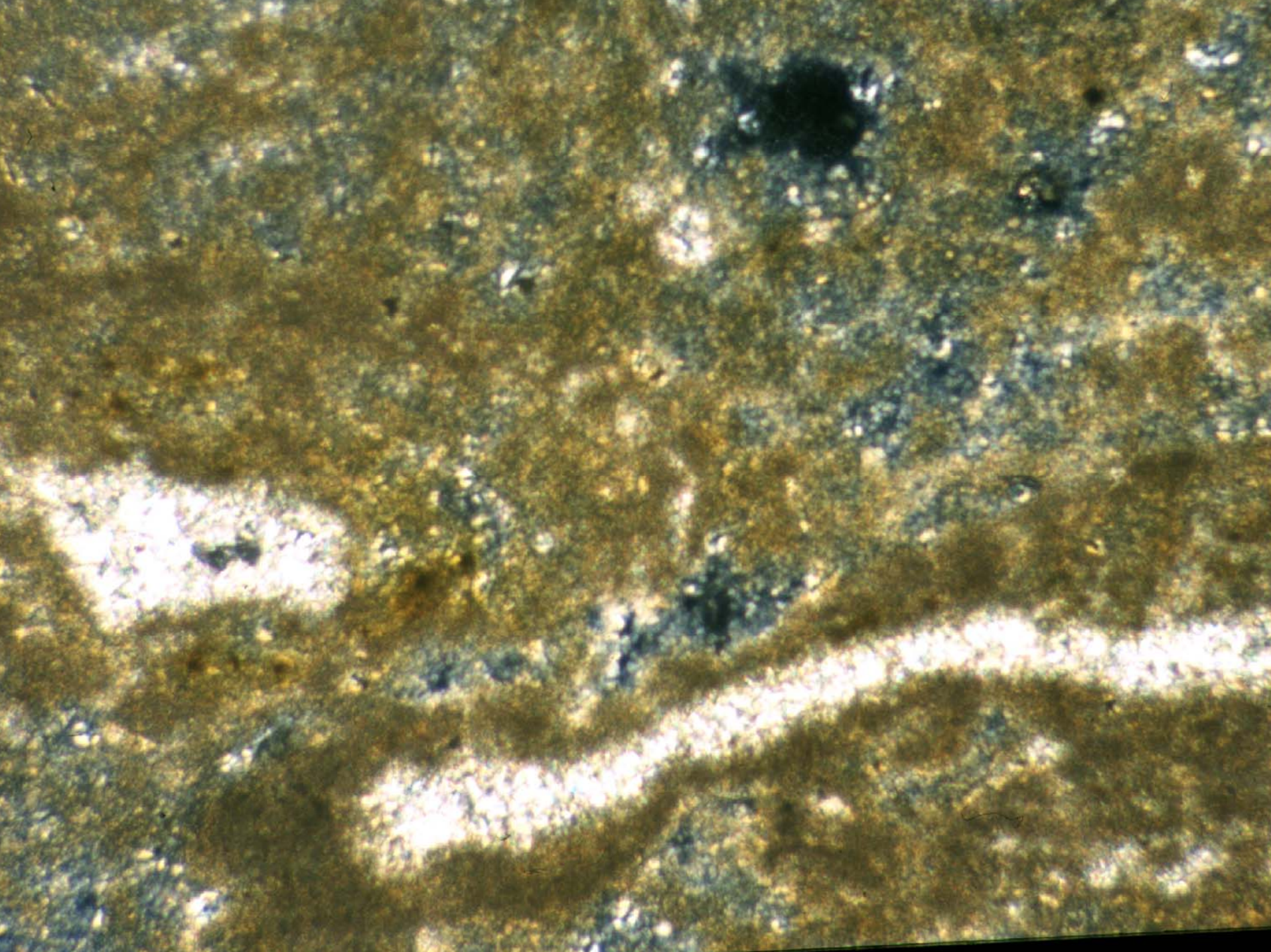

Dolomitizace

vápenec → dolomitizace → dolomit → dedolomitizace → vápenec

dolomit, protodolomit, Fe-dolomit

dolomitizace - velmi raná - penekontemporánní dolomit

- pozdní - po cementaci, při pohřbení (epigenetická d.)

strukturně selektivní d., např. postihující pouze matrix nebo bioklasty

dolomitizace HMC - zachovává pův. struktury; dol. A - rekrystalizace, destrukce pův. struktur

barokní, sedlový dolomit - velké kr., zakřivené tvary zrn a štěpnost, undulózní zhášení → pohřbení (HT, uhlovodíky, sulfidová mineralizace)

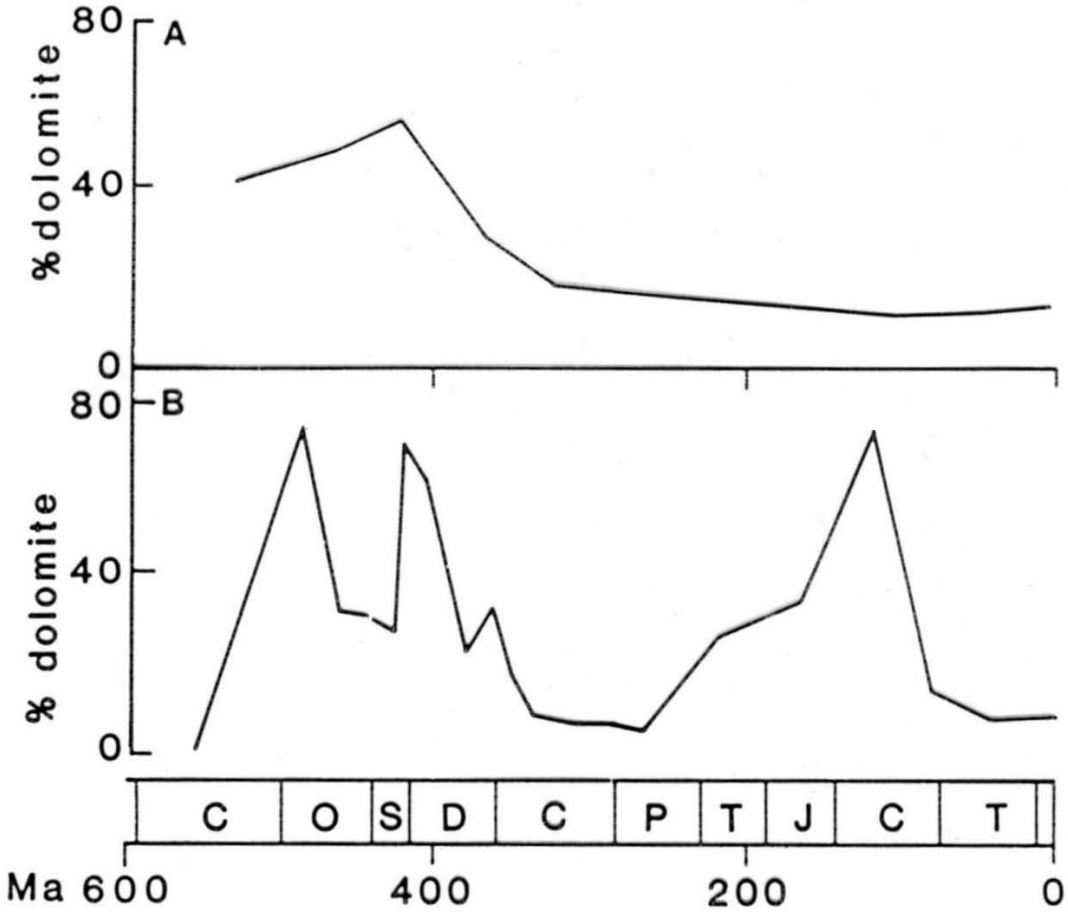

Fig. 4.65 Geological record of dolomites through the Phanerozoic. A, Increasing dolomite occurrence back in time as suggested by many earlier workers. B, A recent compilation showing a more variable trend, which broadly corresponds with the global sea-level curve (greater abundance of dolomite coinciding with higher sea-level stand). The global sea-level curve is given in Fig. 4.4. After Given & Wilkinson (1987).

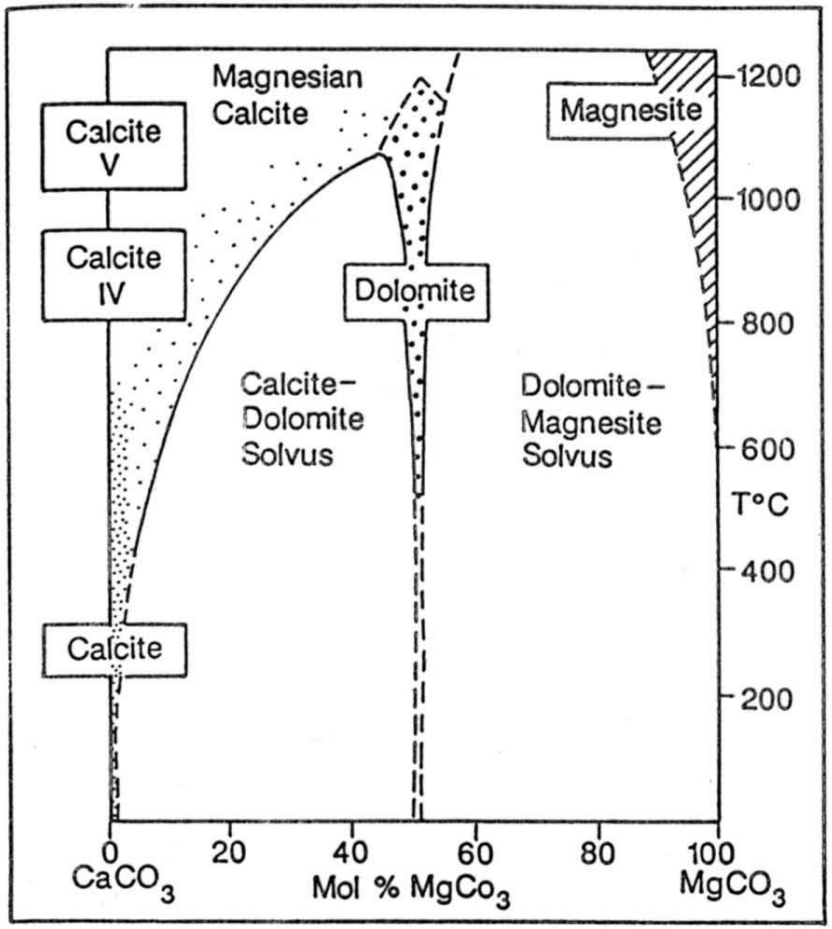

Fig. 6.7 *Phase relations of the $CaCO_3$–$MgCO_3$ system. High temperature margin to dolomite field conjectural. After Goldsmith & Heard (1961a).*

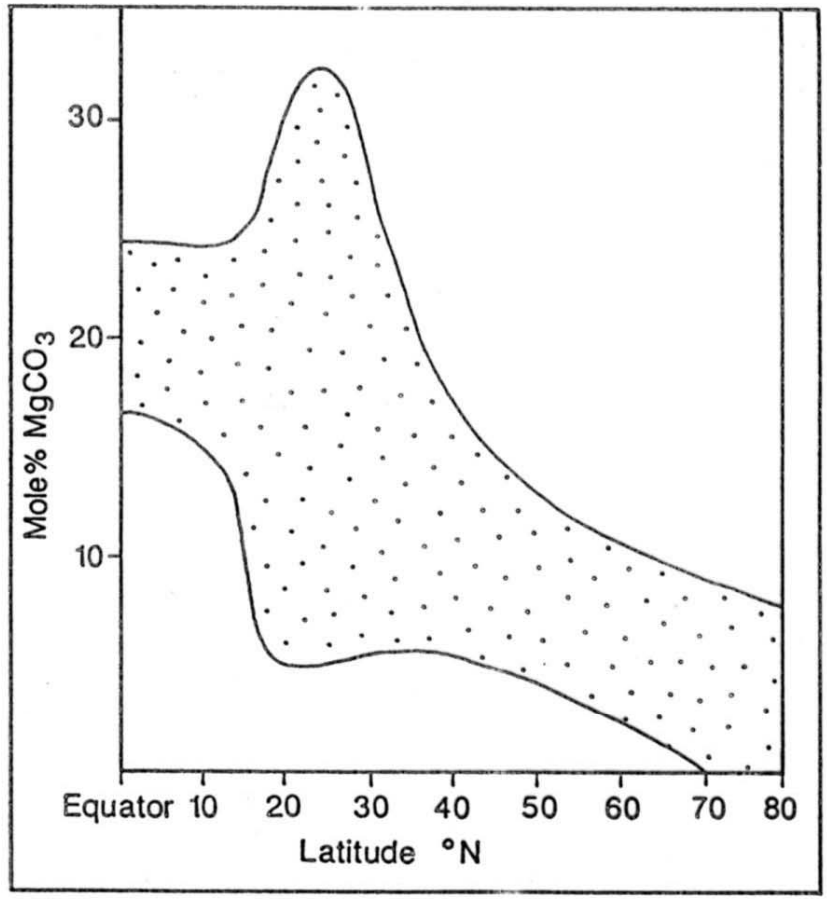

Fig. 6.8 *Range of mole % $MgCO_3$ in skeletal magnesian calcites plotted against latitude. Data (from Chave, 1954) include red algae and a variety of invertebrate phyla.*

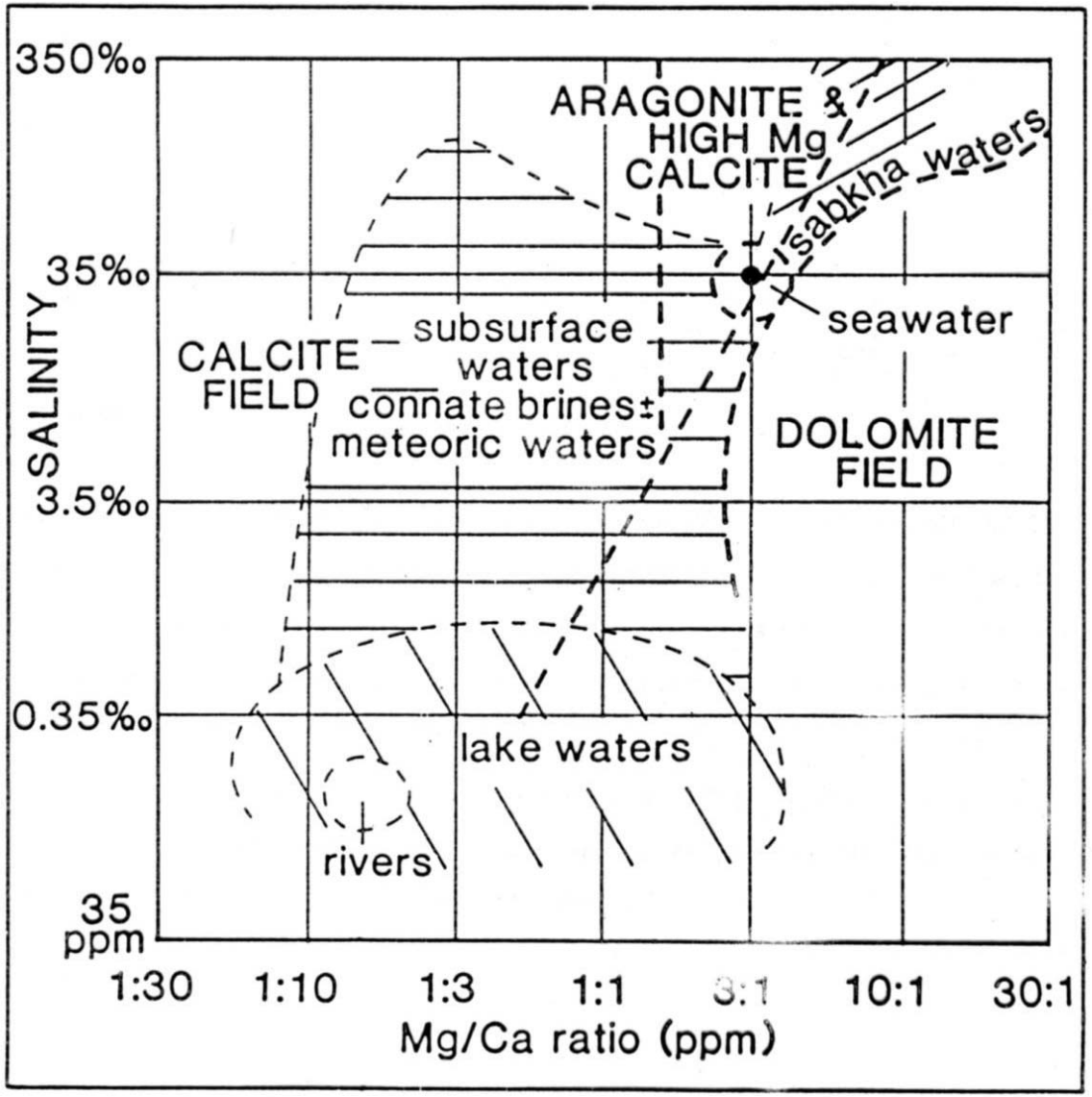

Fig. 8.2 *The precipitational fields of calcite, dolomite and aragonite plus high-Mg calcite in terms of salinity and Mg/Ca ratio of natural waters. After Folk & Land (1975).*

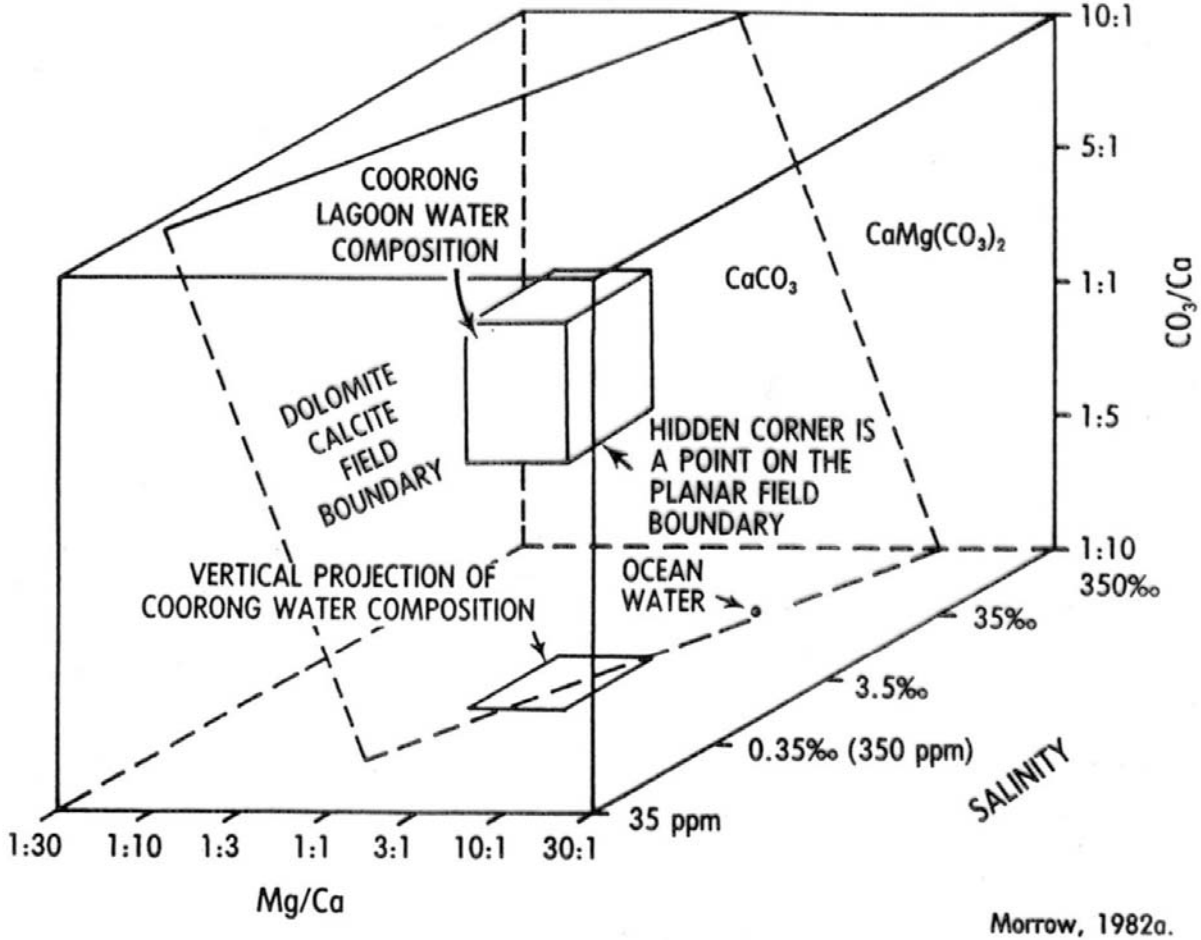

Fig. 6.1. Block diagram showing the effect of variation in the three parameters, the Mg/Ca solution ratio, the salinity, and the CO_3 / Ca ratio. The plane represents the kinetic boundary between dolomite and calcite or aragonite and it includes the hidden corner of the Coorong Lagoon waters as a point on the plane. The basal plane is after Folk and Land (1975). Note that the vertical projection of Coorong Lagoon waters falls largely on the calcite-aragonite side of the stability boundary on the basal plane. A decrease in salinity, an increase in the Mg/Ca ratio or an increase in the CO_3 / Ca ratio favours the precipitation of dolomite. Reprinted with permission of the Geological Association of Canada.

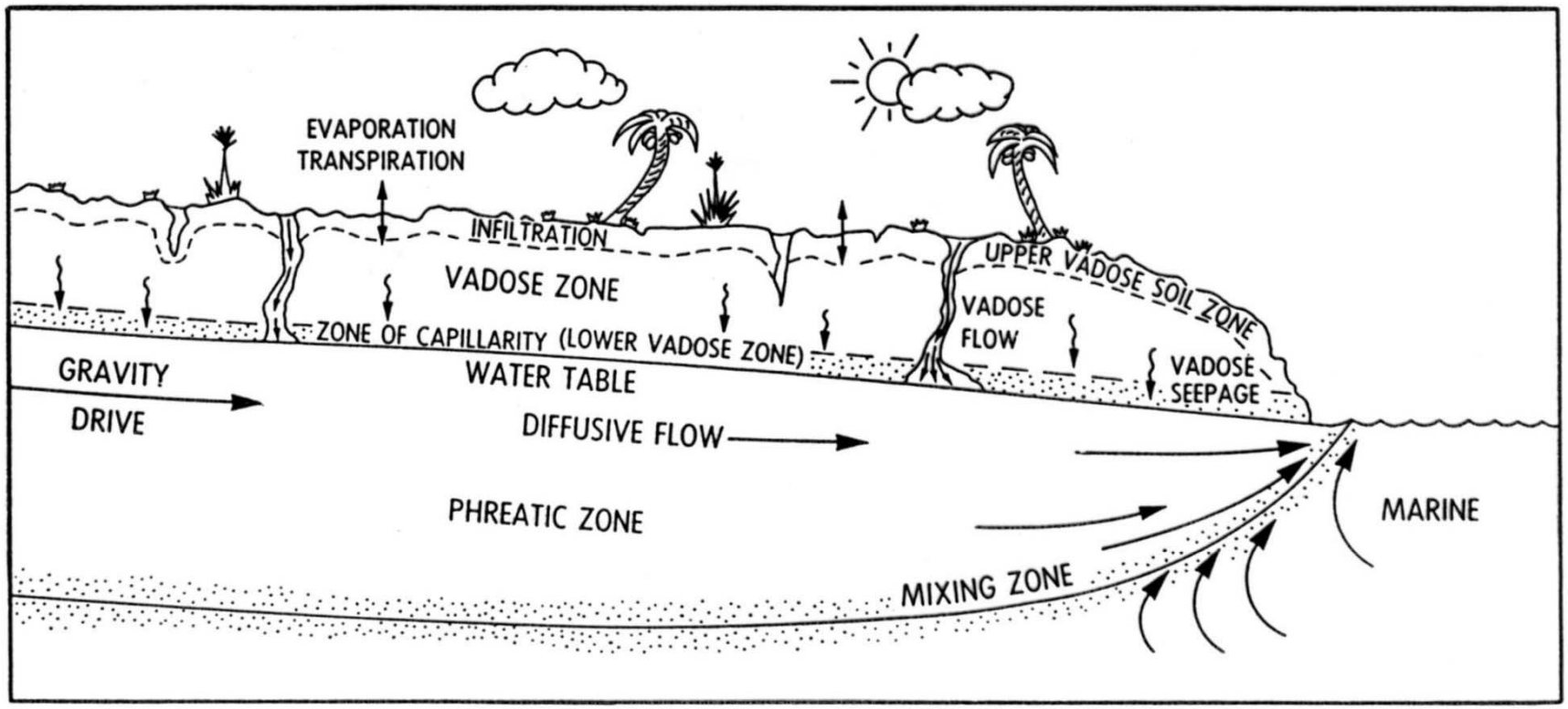

Fig. 6.8. Conceptual model of the major diagenetic environments, and hydrologic conditions present in the meteoric realm.

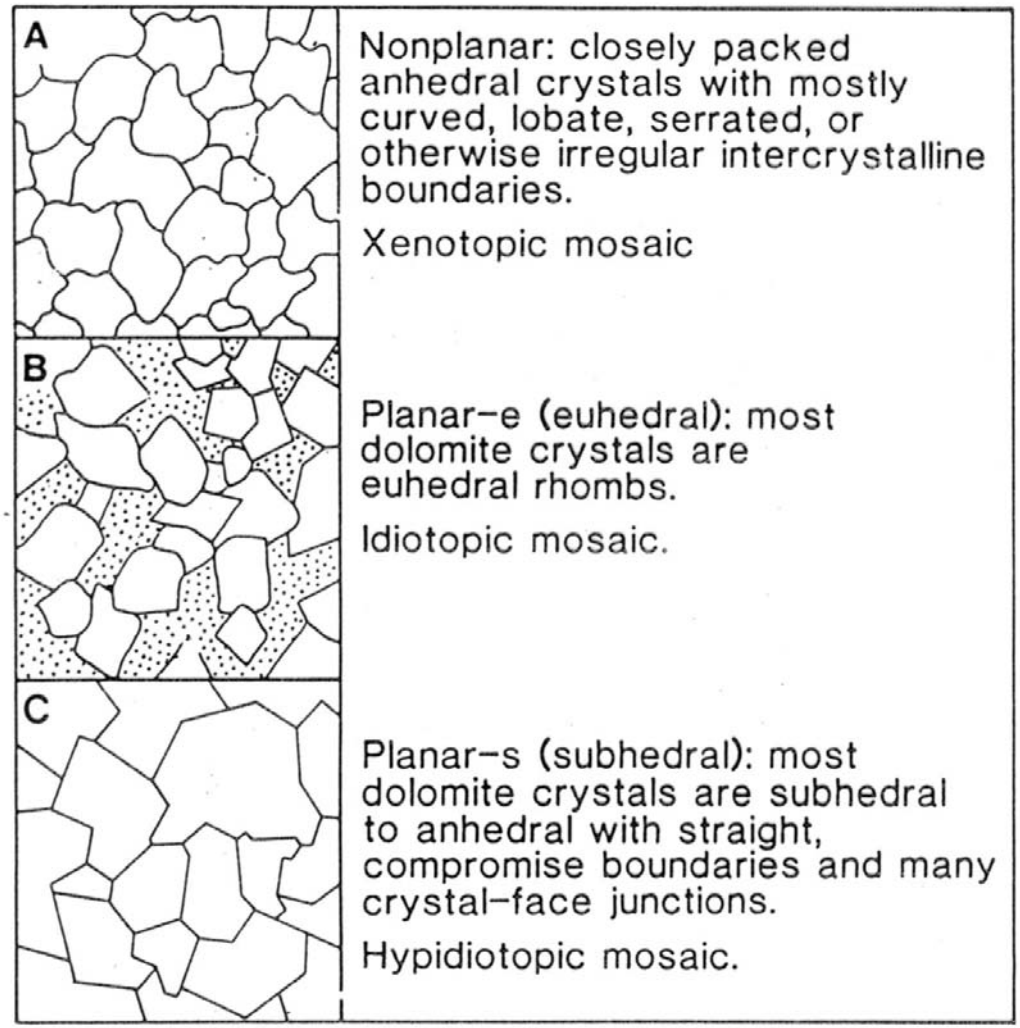

Fig. 8.6 *Three common dolomite textures. (A) Non-planar crystals in a xenotopic mosaic. (B) Planar-e crystals (e for euhedral) in an idiotopic mosaic. (C) Planar-s crystals (s for subhedral) in a hypidiotopic mosaic. After Sibley & Gregg (1987).*

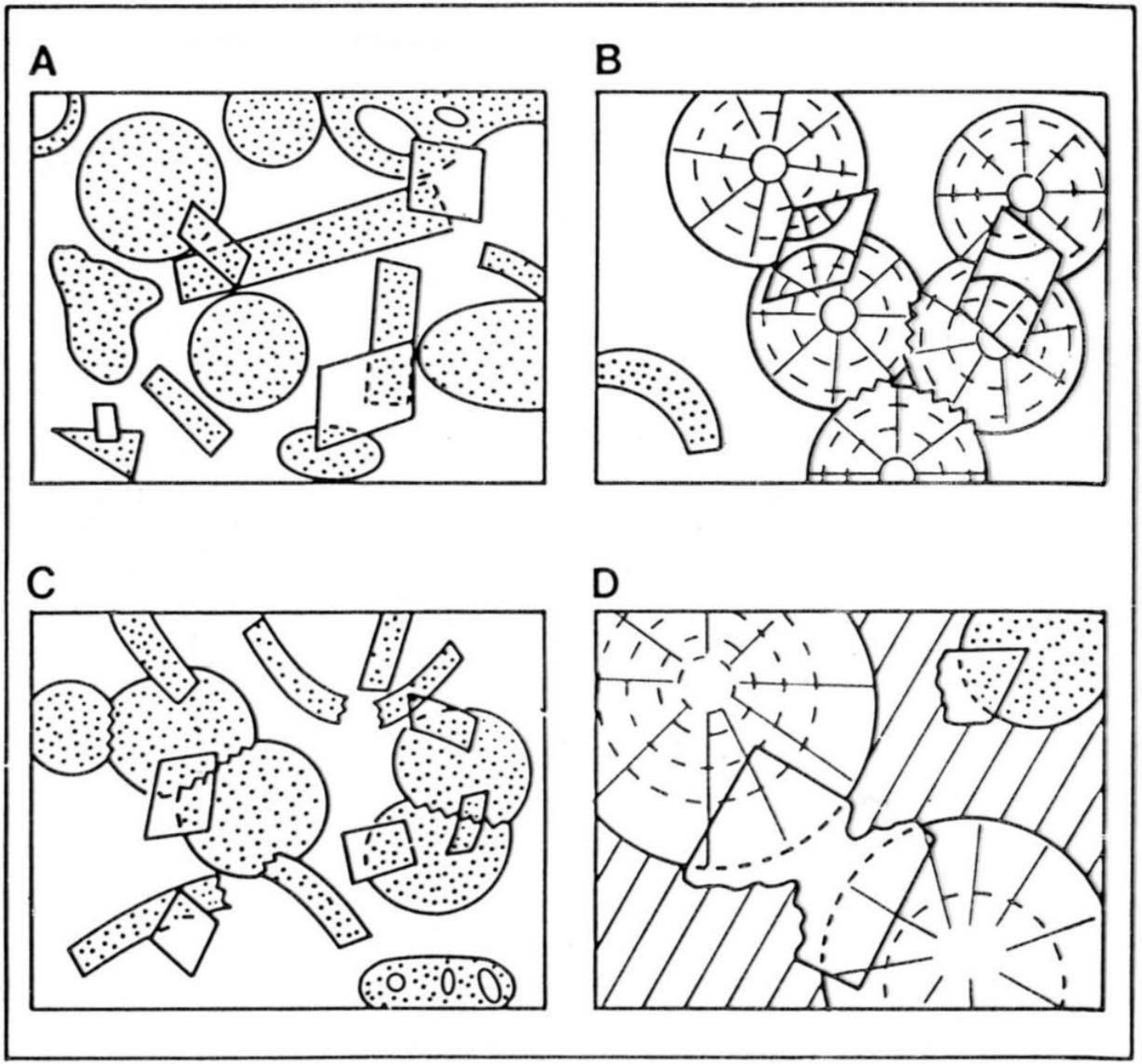
A
B
C
D

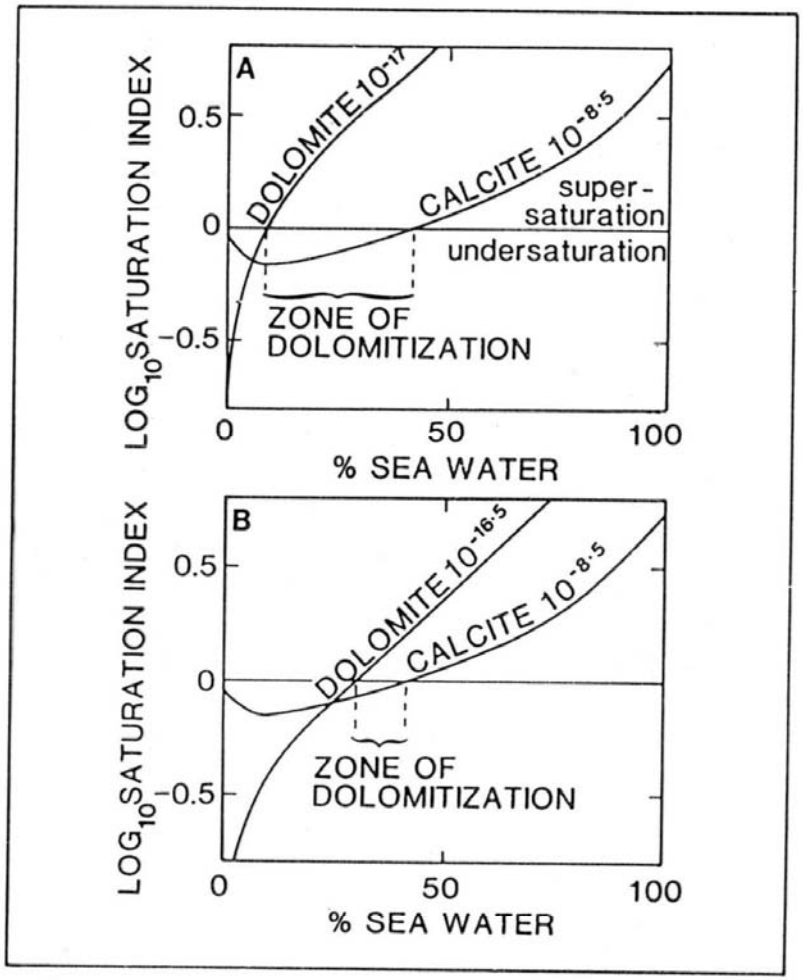

Fig. 8.3 *Mixing-zone dolomitization. Solubility curves for dolomite and calcite in meteoric water with increasing content of seawater. Dolomitization is considered to take place in waters supersaturated with respect to dolomite but undersaturated with respect to calcite. (A) For dolomite with solubility product* $K = 10^{-17}$, *as used by Badiozamani (1973). (B) For disordered dolomite with* $K = 10^{-16.5}$, *as used by Hardie (1987). Note that in (B) the zone of dolomitization is much reduced. After Hardie (1987).*

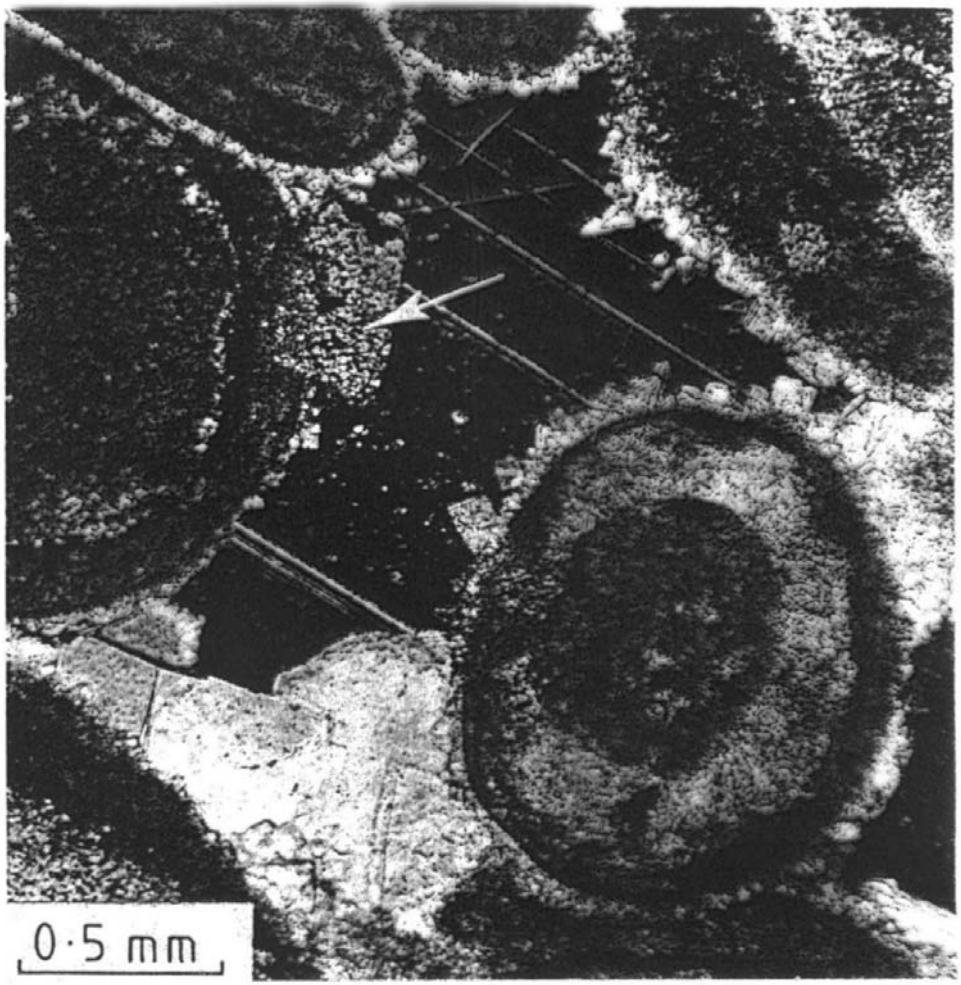

Fig. 4.54 Calcite cement at grain contacts and irregularly around grains. This geometry indicates precipitation in the near-surface, meteoric vadose environment. Later precipitation of large poikilotopic calcite (black, in extinction) took place during burial. Isolated dolomite rhombs (arrowed) were precipitated after the meteoric and before the burial cements. Crossed polars. Lower Carboniferous oolitic grainstone. Glamorgan, Wales.

Fig. 8.13 *Pre-compaction dolomite rhomb. Notice that the edge of the ooid is displaced within the rhomb. Gully Oolite, Lower Carboniferous, south Wales.*

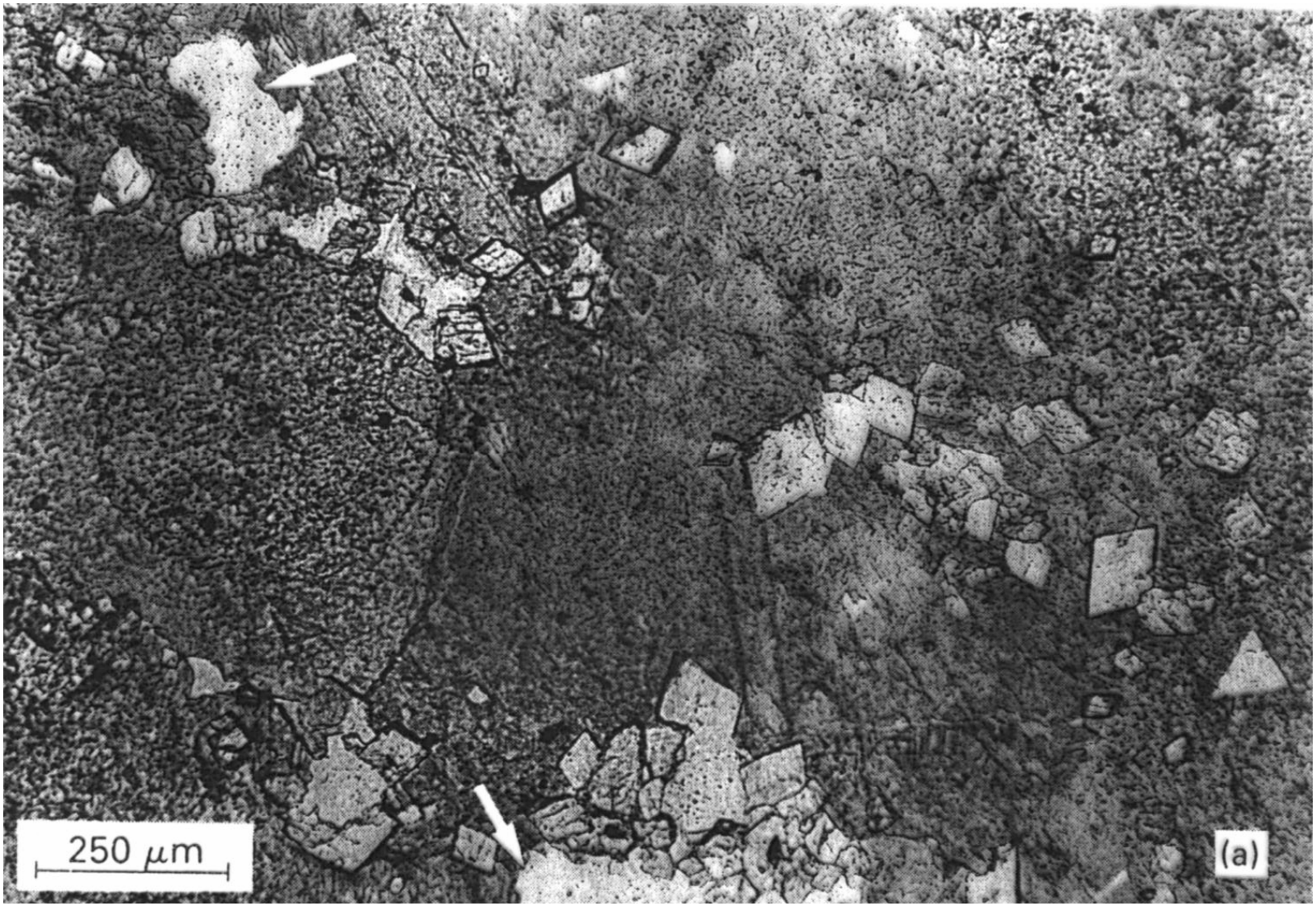
250 μm
(a)

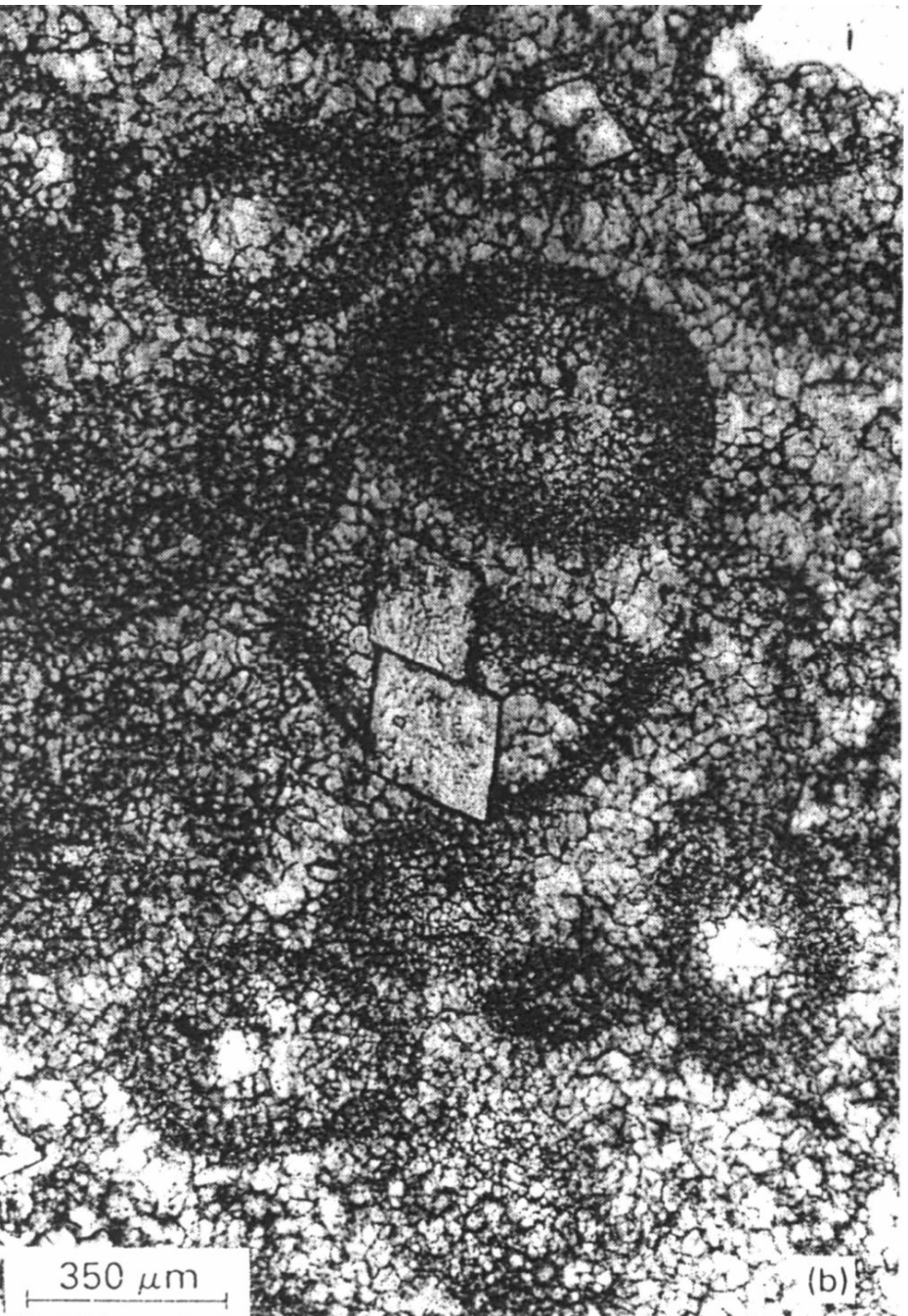
350 μm
(b)

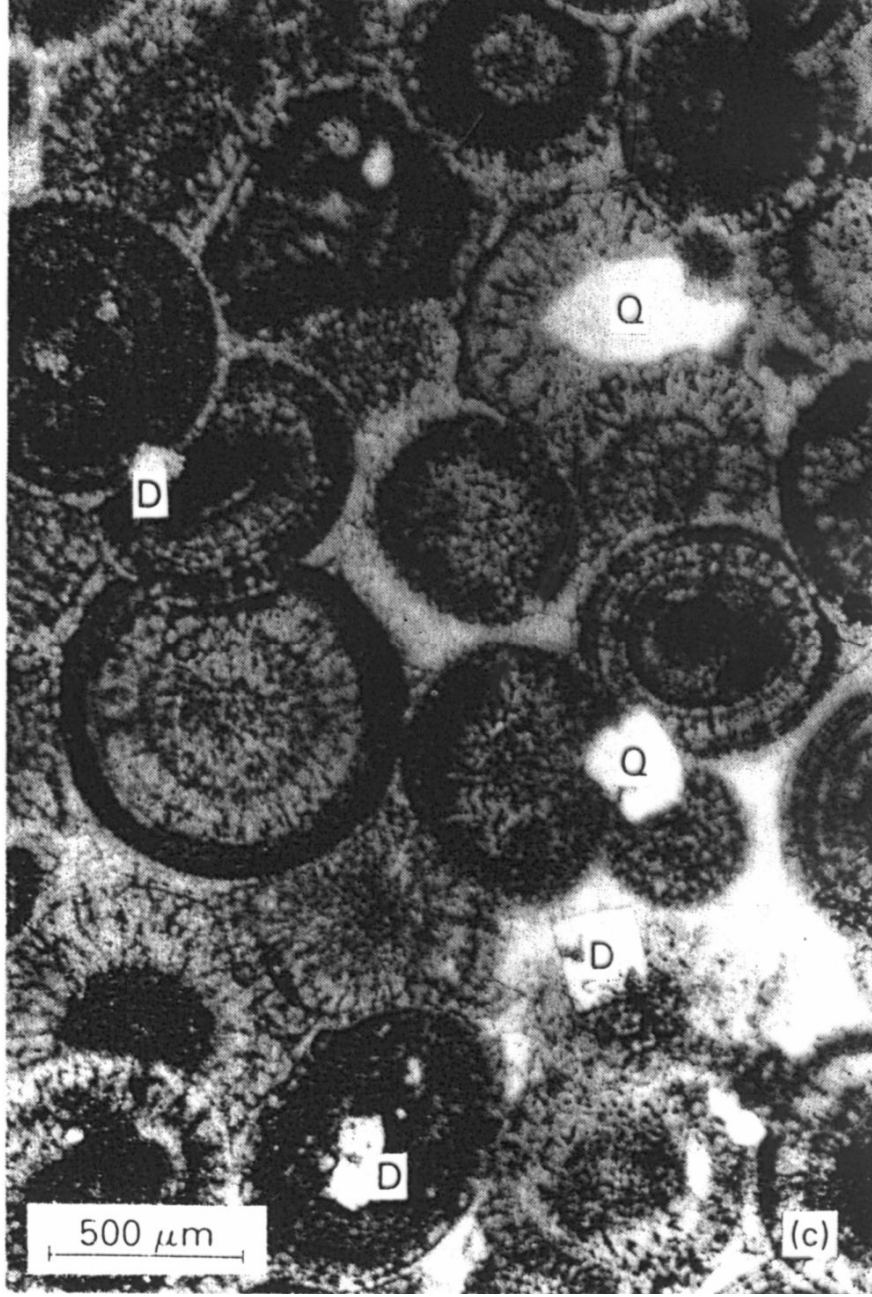
Q
D
Q
D
D
500 μm
(c)

modely dolomitizace

mořská voda přesycena d., ale jeho přímá precipitace je inhibována řadou kinetických faktorů, proto se z mořské vody přednostně sráží A a HMC

z pórových vod, Bahamy, Florida, Arab. zál., 1-4 mm klence, povrch krusty; nárůst Mg/Ca v pór.vodách díky precipitaci A a sádrovce-anhydritu, také evaporace

Viktoriino jez., **přímé srážení d. z jez. vody**, vysoký Mg/Ca díky zvětrávání blízkých bazaltů

Coorong, j.Austrálie, přímé srážení d. při mísení kontinetálních Mg bohatých podz.vod se slanou vodou příbřežních jezer

laguny, periodicky hyperslané, evaporace

intertidál-supratidál, evaporitická dolomitizace, zachování sed.struktur (teepee, ptačí oči)

mělký subtidál a útes, prosakování a zpětné proudění lagunárních vod s evaporiticky zvýšeným Mg/Ca zpět do bariéry/útesu

zóna míšení meteorické a marinní vody, poměr 2:1 → pokles nasycení kalcitem a nárůst nasycení dolomitem; nižší salinita, Mg/Ca stejný

během **pohřbení**, při kompakci pelagických kalů migrace Mg bohatých fluid do vápenců; Mg z jíl.min., pór.vod, příp. z org.hm., část Mg také při přechodu HMC na LMC

subrecentní dolomitizace pod atoly a karb. platformami (v hl. 1200-1400m) proudí chladná mořs.voda → nízká tep., nízké nasyc. kalcitem, ale stabilní nasycení dolomitem; cirkulace díky tidálnímu pumpování a mořským proudům → vysoký geotermální gradient …. **Kohoutova konvekce**

v **anoxickém** prostředí, bakt. redukce sulfátů - kinetický inhibitor dolomitizace, zdroj Mg zčásti v org. hmotě

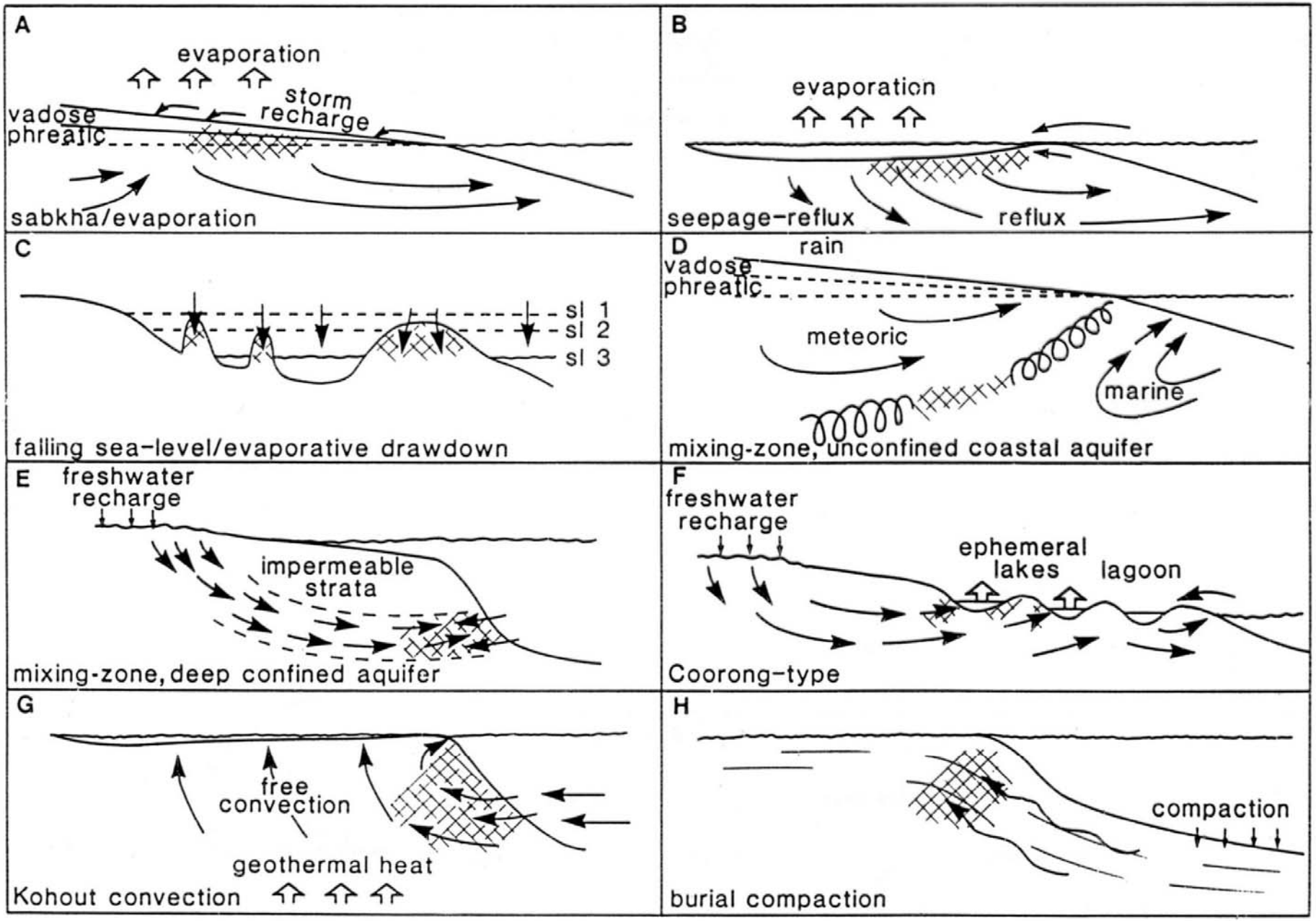

Fig. 8.1 *Models of dolomitization, illustrating the variety of mechanisms for moving dolomitizing fluids through the sediments. In part after Land (1985). Also see Fig. 8.31 for seawater dolomitization models.*

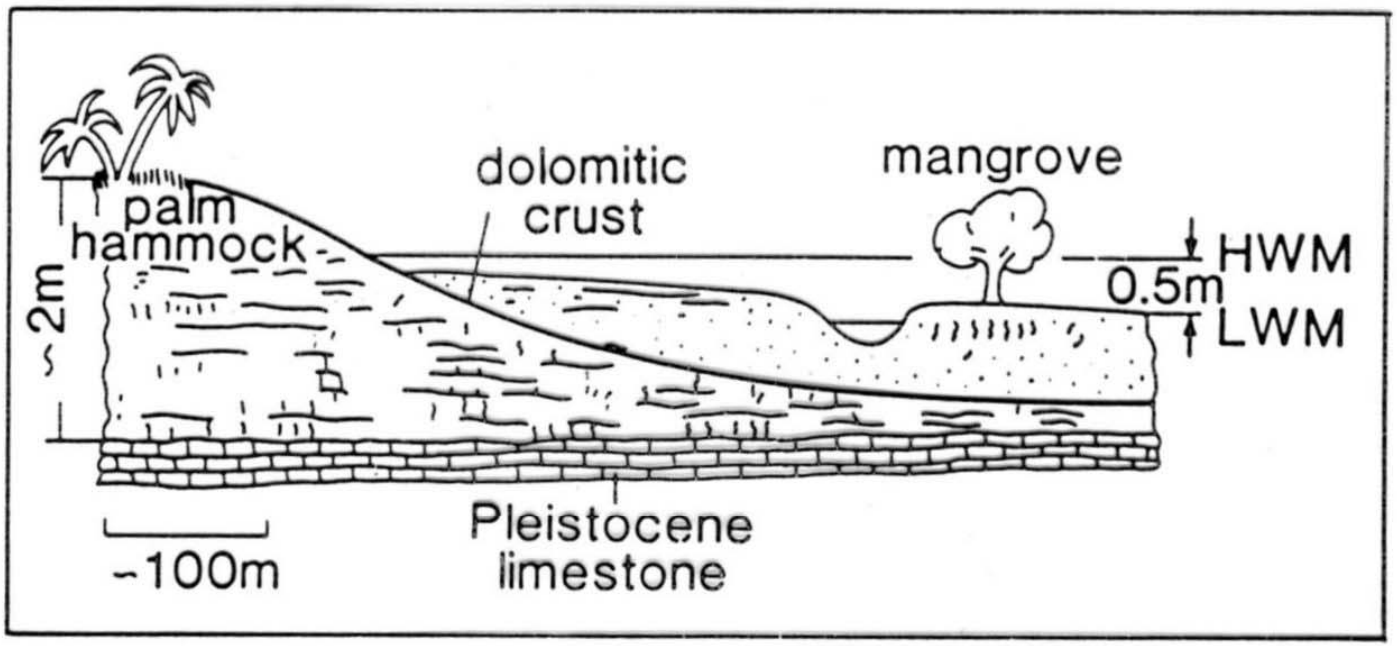

Fig. 8.21 *Schematic cross-section of a palm hammock on the tidal flats of Andros Island, Bahamas, showing dolomitic crust, now forming in the upper intertidal/low supratidal zone, with earlier crust occurring beneath the low intertidal–shallow subtidal sediments. After Shinn* et al. *(1965).*

Fig. 8.22 *Dolomites of the Coorong region, South Australia. (A) The coastal plain of Quaternary barriers and interdu flats where ephemeral lakes occur and dolomite is being precipitated. (B) Stratigraphic log of a core from an epheme Coorong lake. After Von der Borch (1976) and Von der Borch & Lock (1979).*

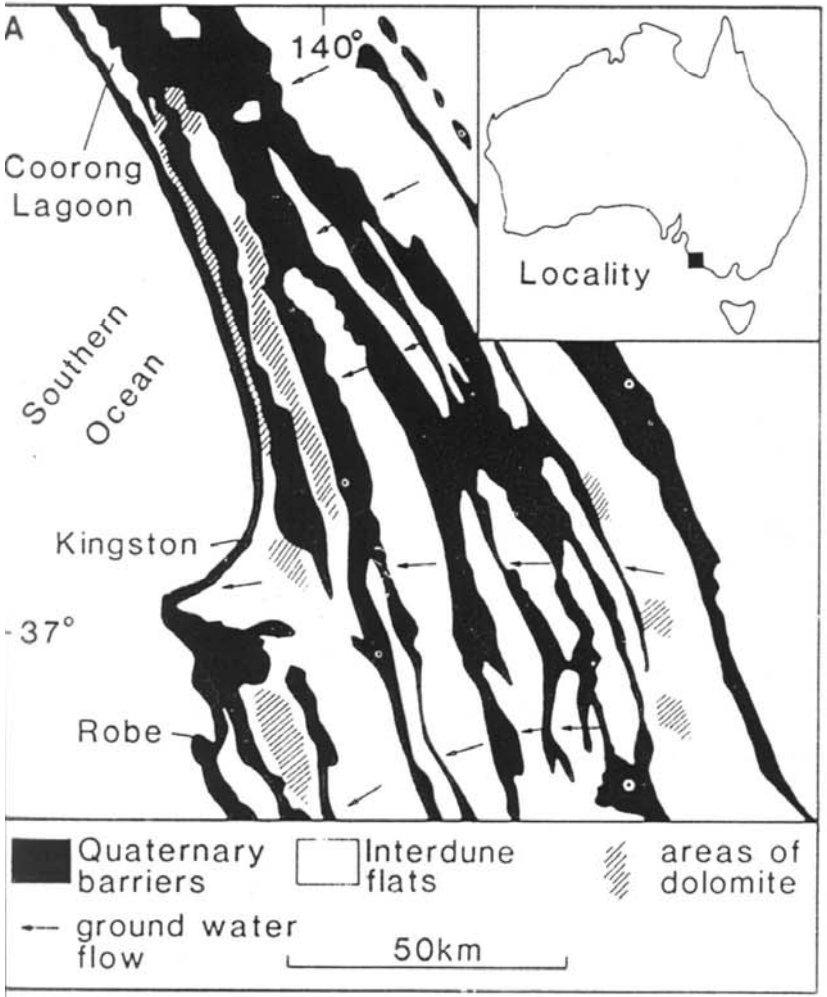

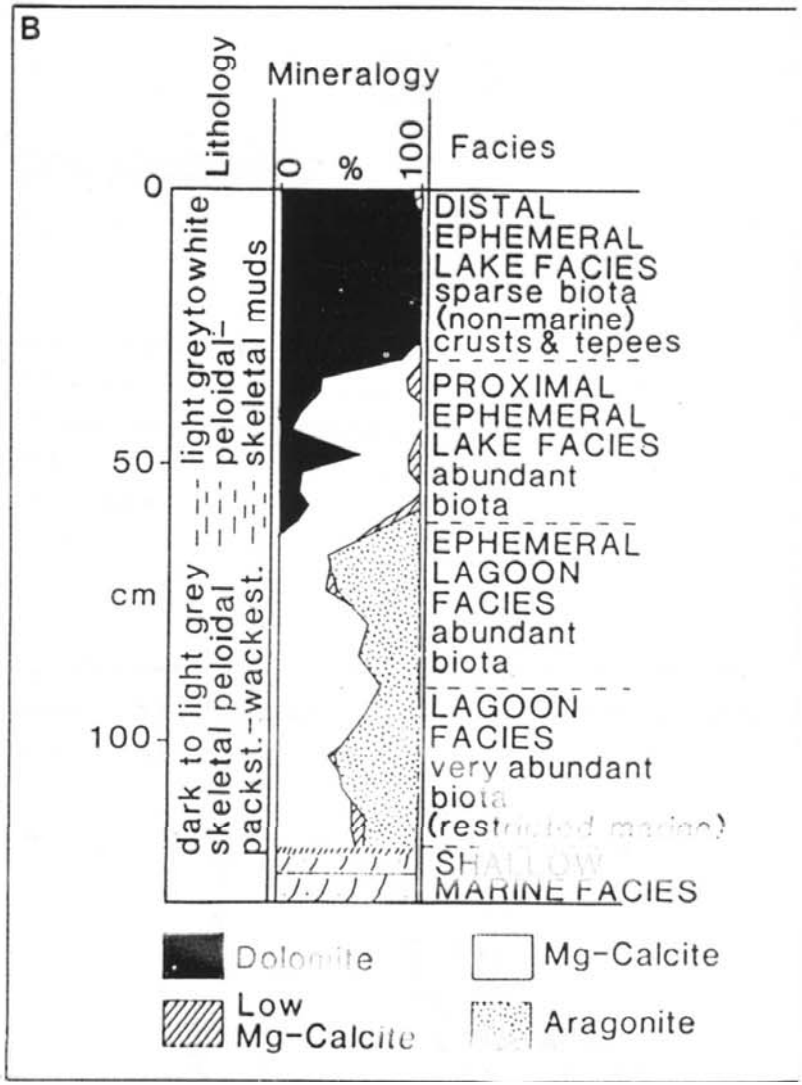

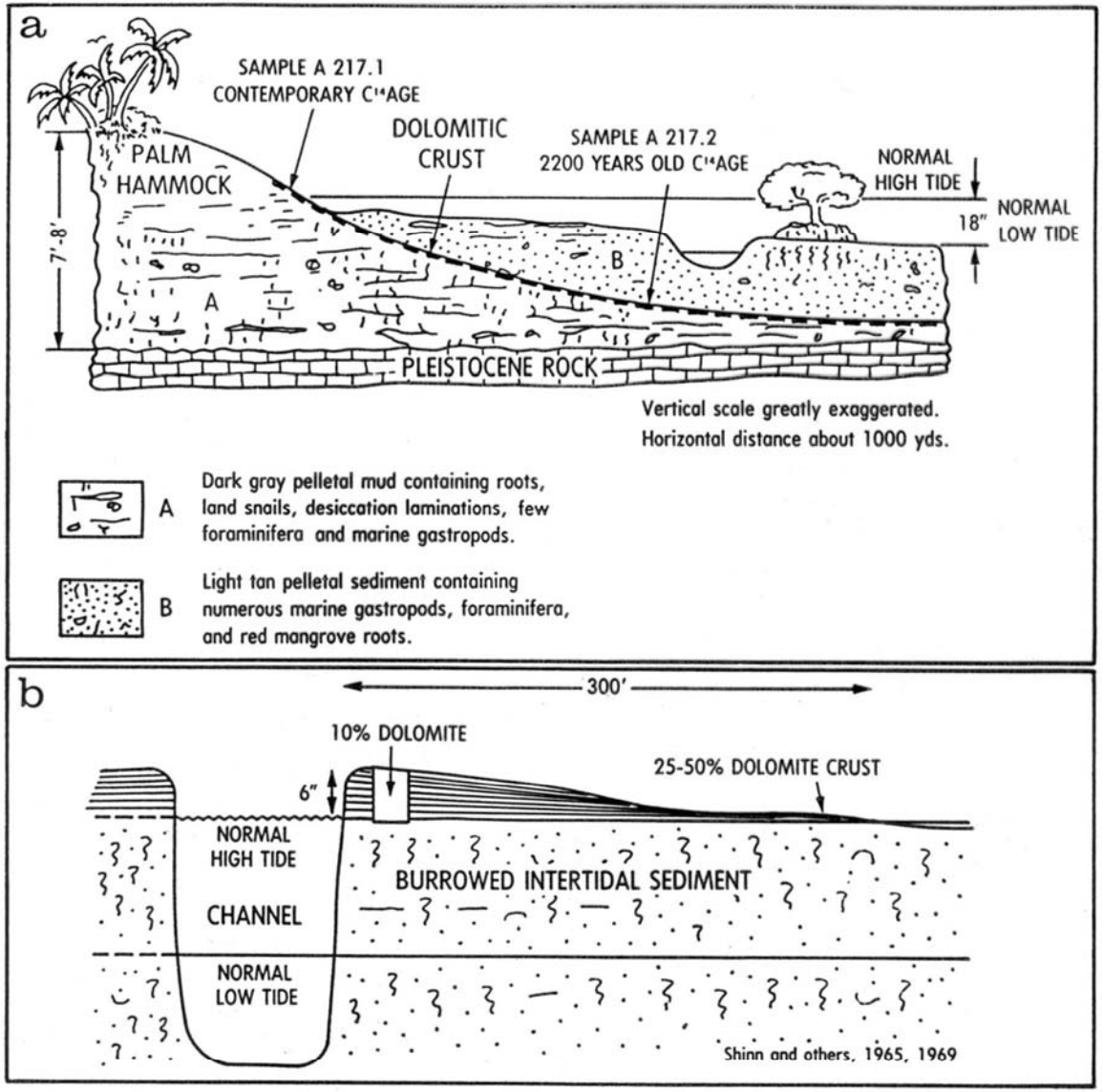

Fig. 5.7. a. Stratigraphic cross section across the flank of a palm hammock on Andros Island, the Bahamas. Note variation in age along the dolomitic crust. b. Schematic cross section across a tidal channel natural levee on the Andros Island tidal flats. Note that dolomite % is greater in the thin flanks of the levee than in the thicker channel margin part of the levee due to a dilution effect caused by the greater rate of sedimentation along the channel margins. Used with permission of SEPM.

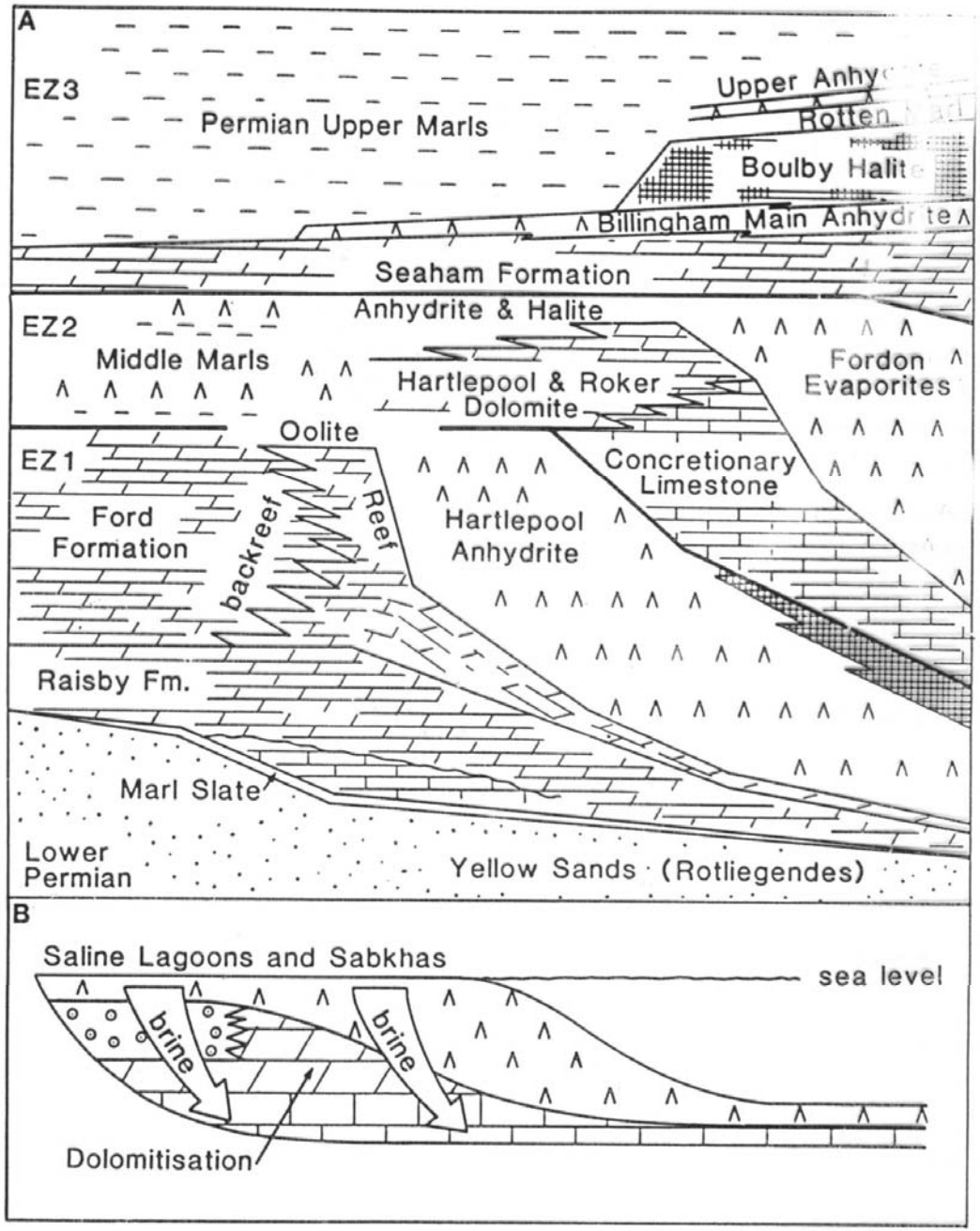

Fig. 8.23 *Dolomites of the Upper Permian (Zechstein) of northeast England. (A) Stratigraphy–lithology showing three carbonate–evaporite cycles. The lower part of the Raisby Formation is still limestone; the Concretionary Limestone is mostly a dolomite. (B) Seepage–reflux model for Zechstein dolomitization. After Smith (1981) and Clark (1980). (C) Coarse dolomite, bryozoan in centre and vuggy porosity. Crossed polars.*

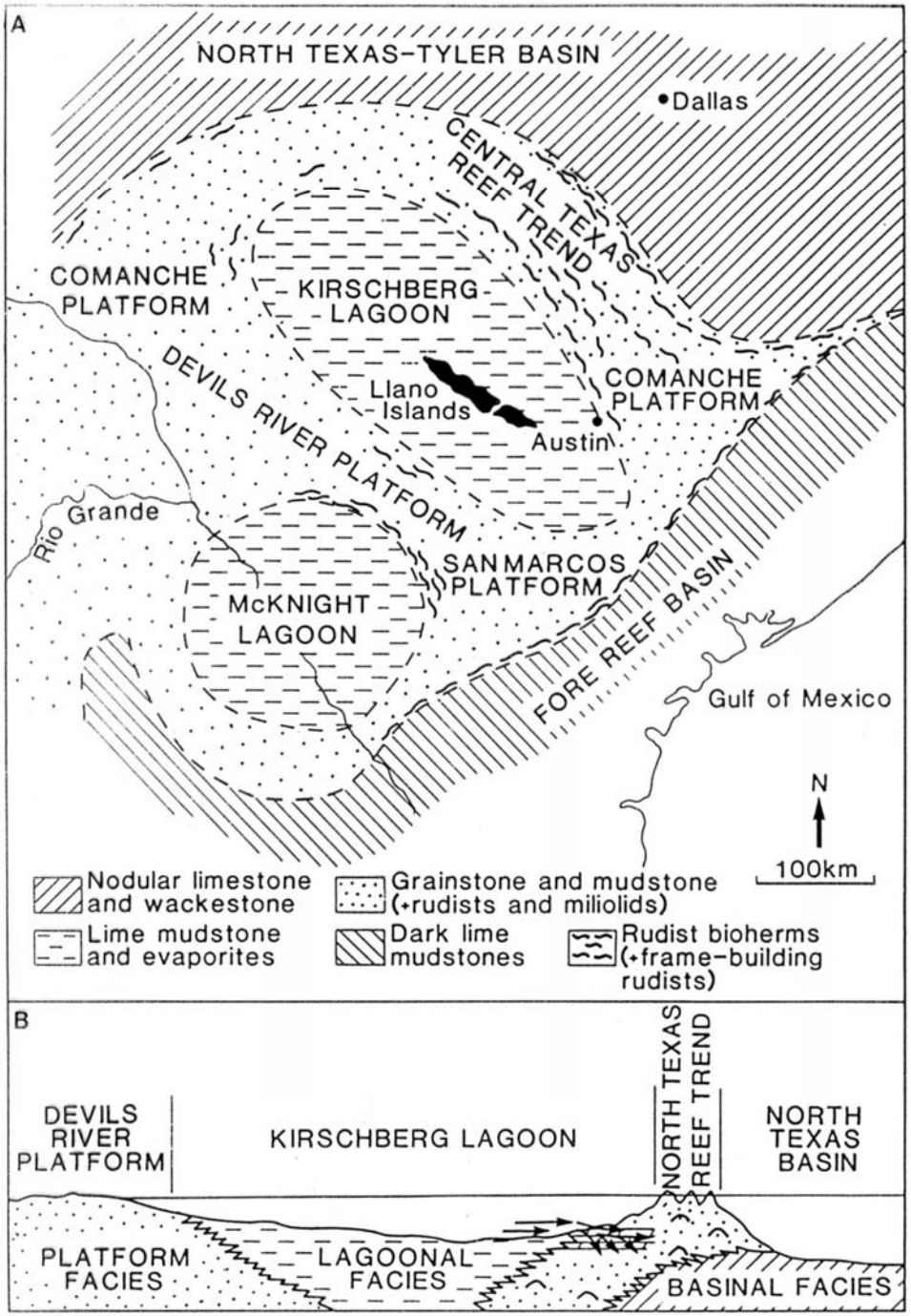

Fig. 8.24 *Dolomites of the Lower Cretaceous (Edwards Formation) of Texas. (A) Palaeogeographic map showing shelf-margin reef trends and two onshelf lagoons. (B) Schematic north–south cross-section and seepage–reflux model for dolomitization of the shelf-margin grainstones. After Fisher & Rodda (1969).*

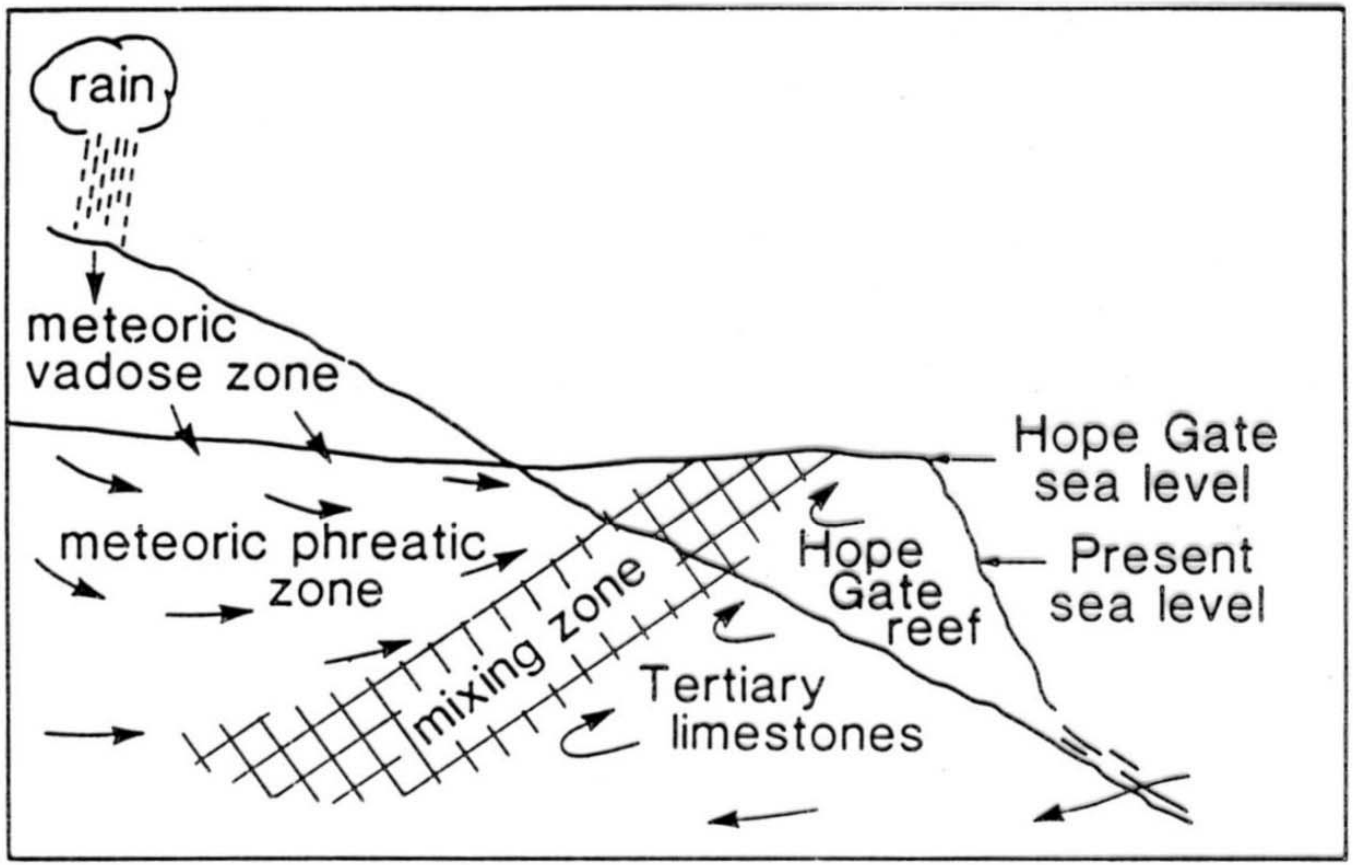

Fig. 8.25 *Mixing-zone model for dolomitization of the Hope Gate Formation of Jamaica. After Land (1973a).*

dolomitizace v mixing zone

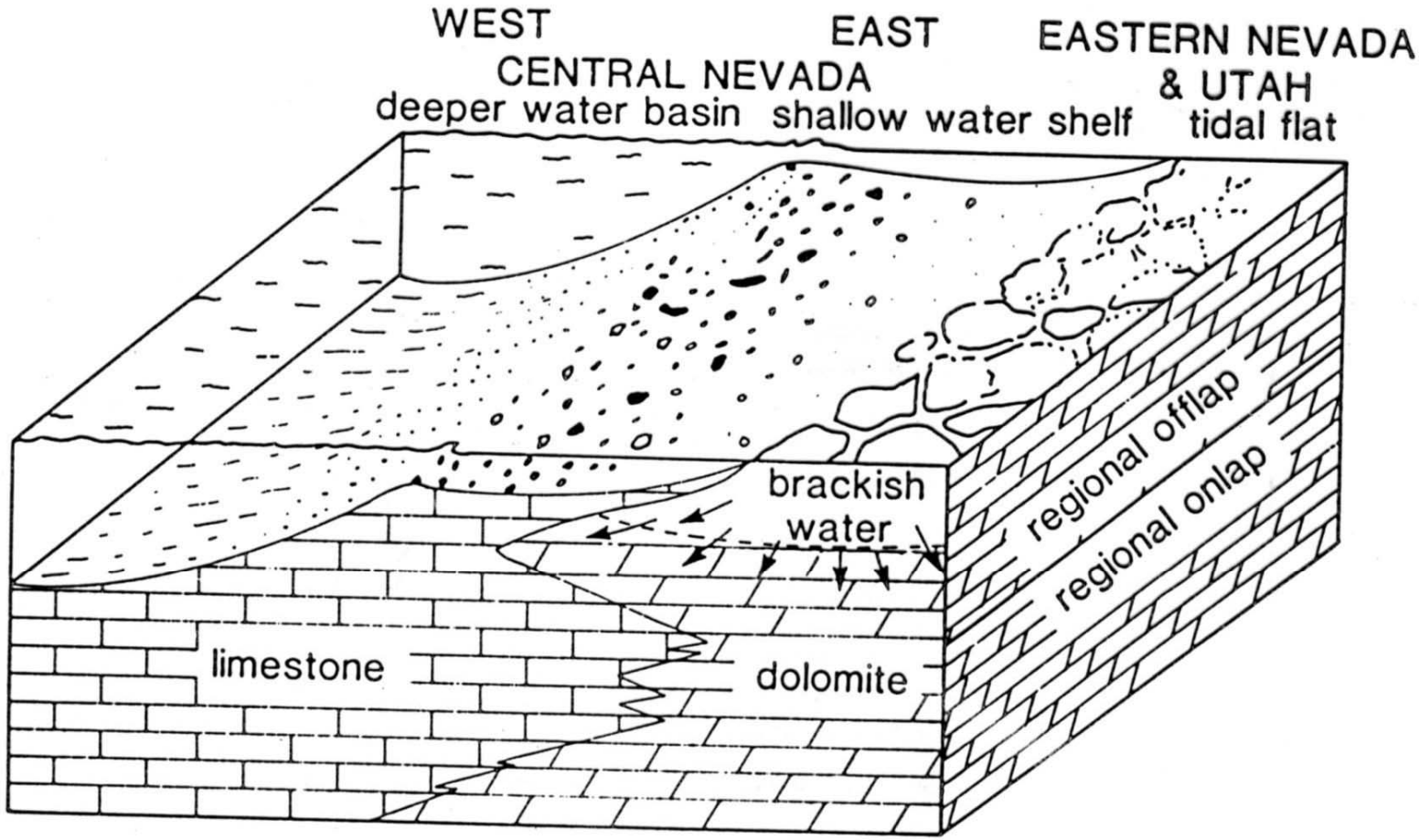

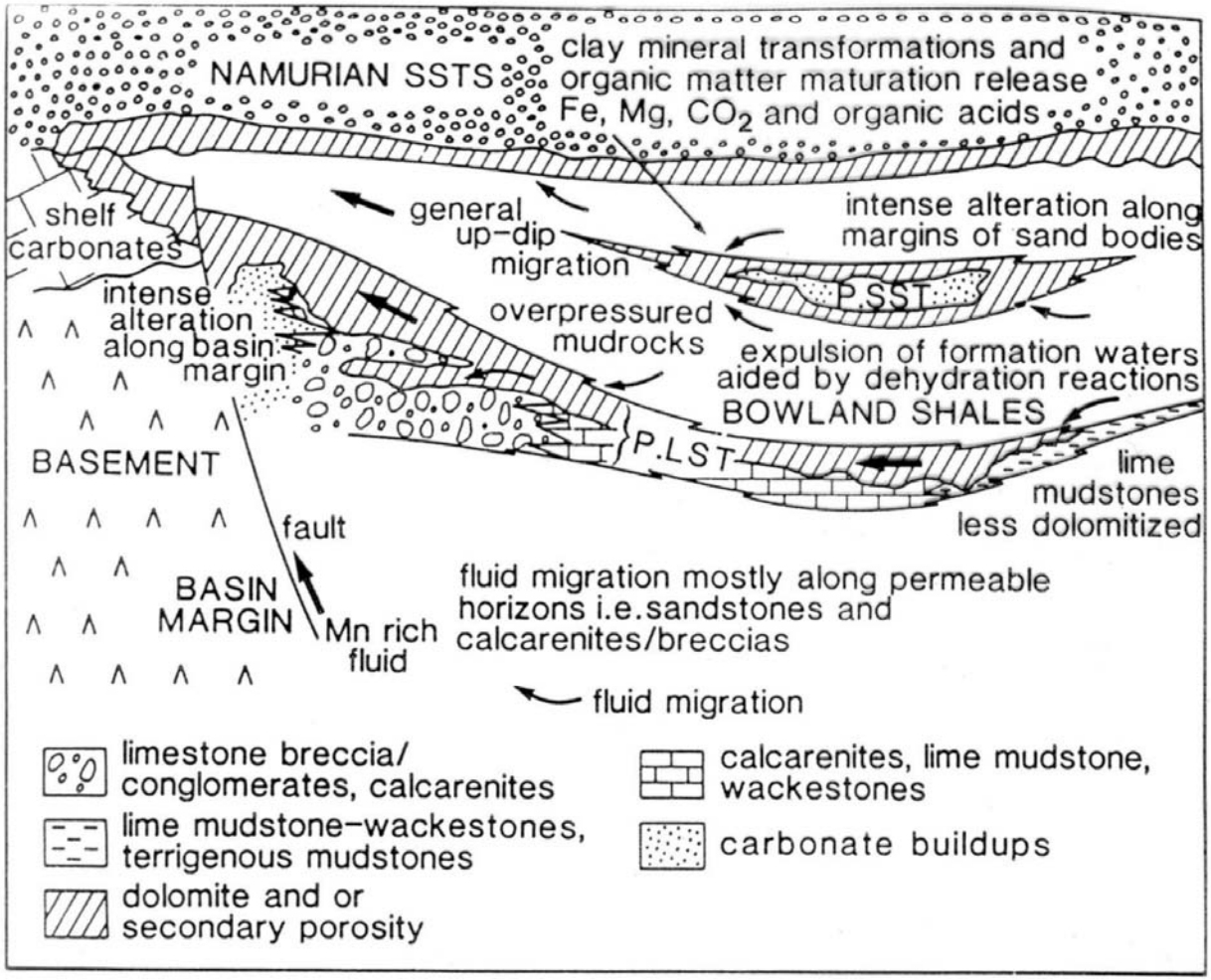

Fig. 8.27 *Burial dolomitization model through mudrock dewatering for Lower Carboniferous sediments, the Pendleside Limestone (P.LST) and Pendleside Sandstone (P.SST), of the Bowland Basin, northwest England. After Gawthorpe (1987).*

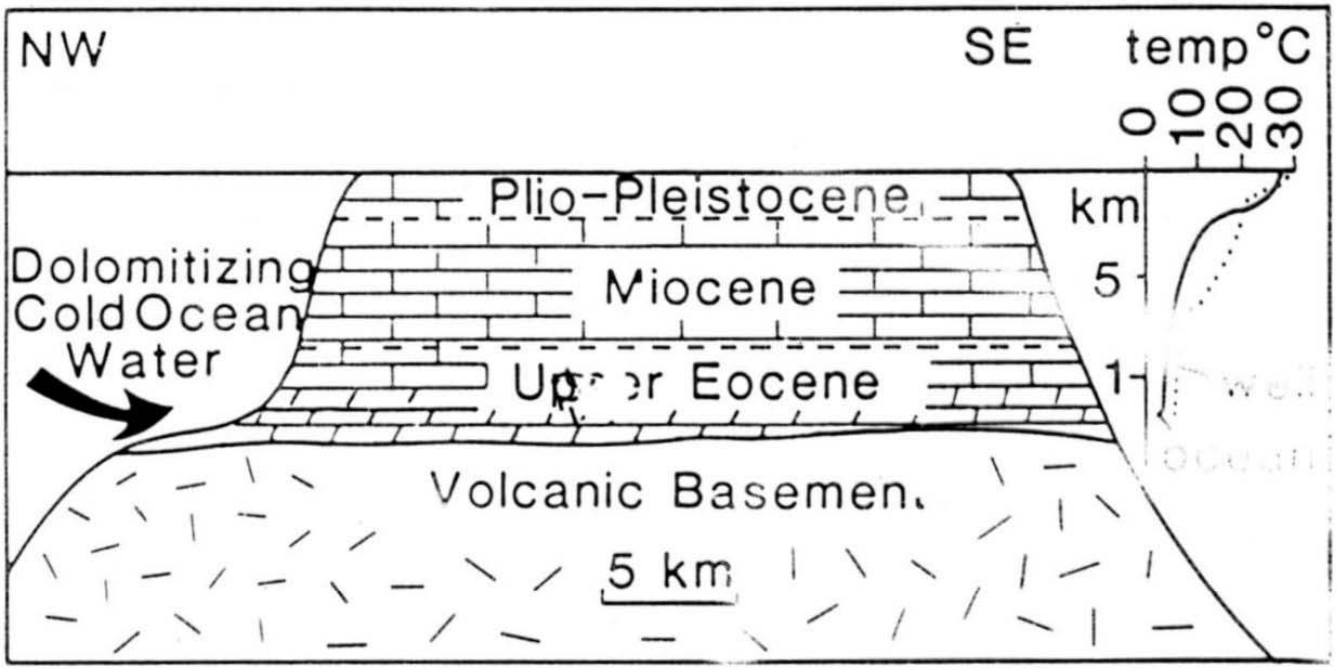

Fig. 8.28 *Model for dolomitization of Eocene limestones of Enewetak Atoll by cold ocean water. The temperature profile of water within the atoll from a deep well is closely parallel to that of the adjacent open ocean, suggesting that ocean water freely circulates through the atoll. There is an increase in temperature near the bottom of the well suggesting that circulating water is removing geothermal heat from Enewetak's volcanic basement. After Saller (1984).*

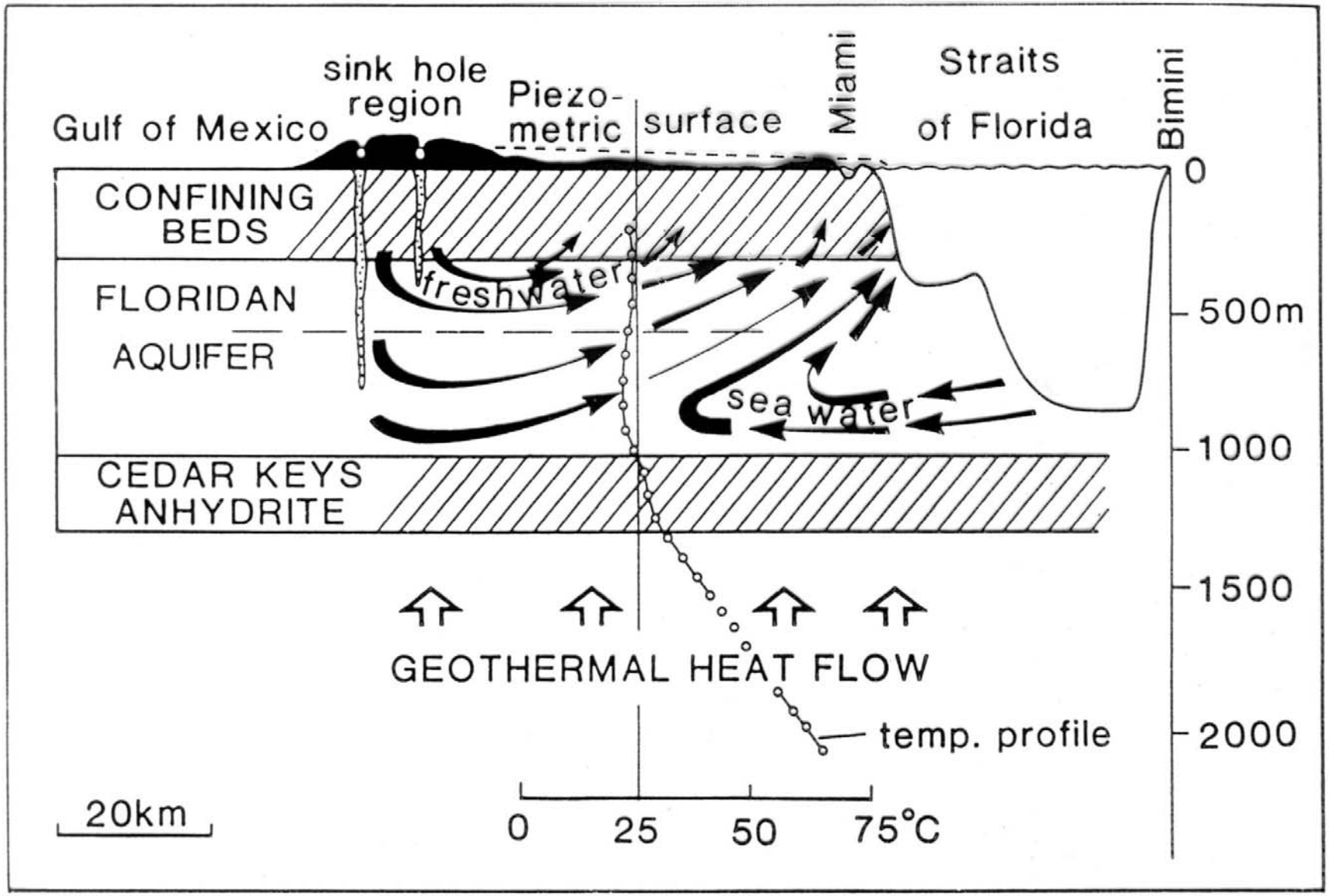
Gulf of Mexico
sink hole region
Piezo-metric surface
Miami
Straits of Florida
Bimini
CONFINING BEDS
FLORIDAN AQUIFER
freshwater
sea water
CEDAR KEYS ANHYDRITE
GEOTHERMAL HEAT FLOW
temp. profile
0
500m
1000
1500
2000
20km
0
25
50
75°C

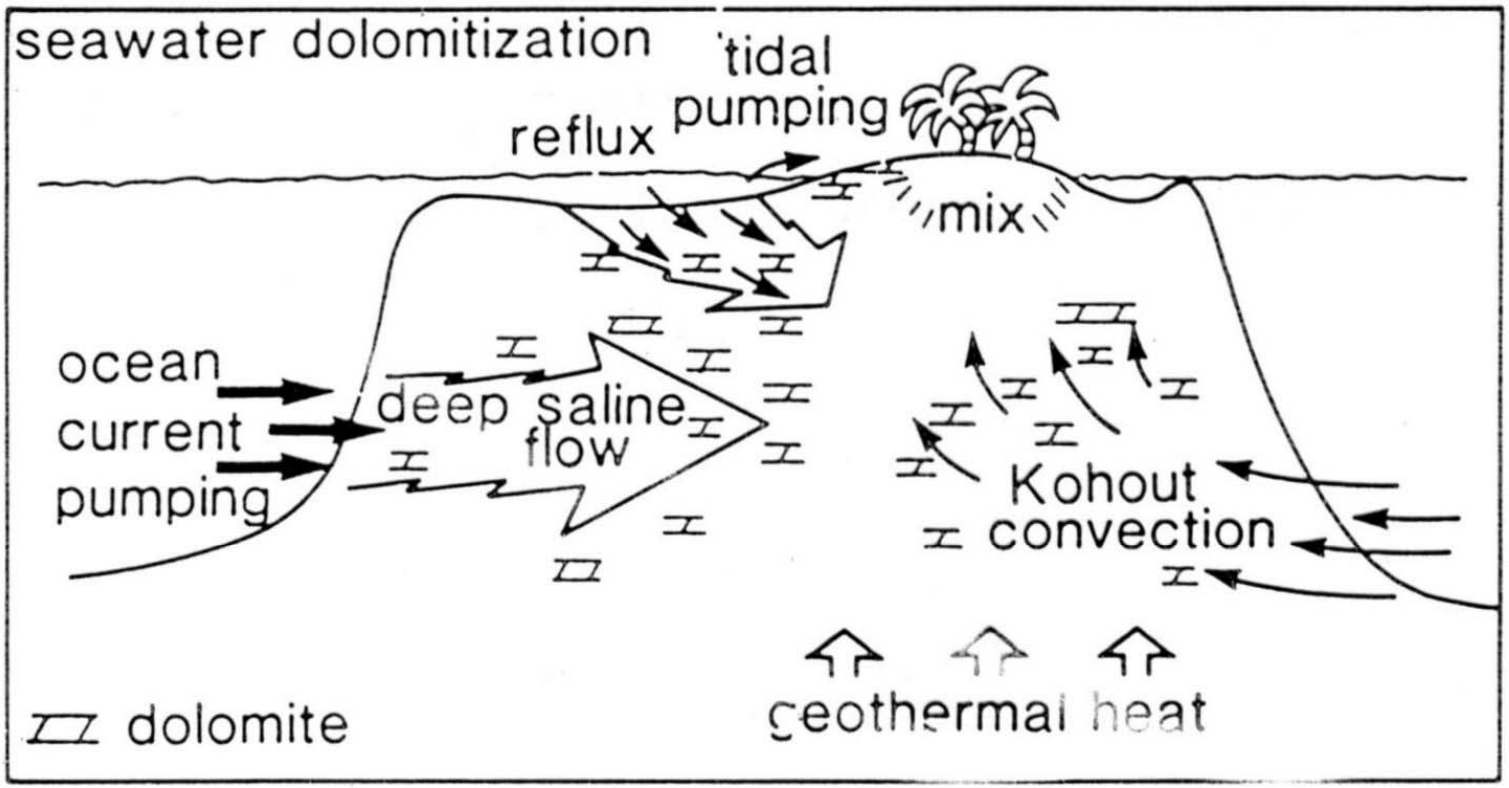

Fig. 4.67 Models for sea-water dolon tization of limestones, all basically different ways of pumping sea water through a carbonate platform. After Tucker & Wright (1990).

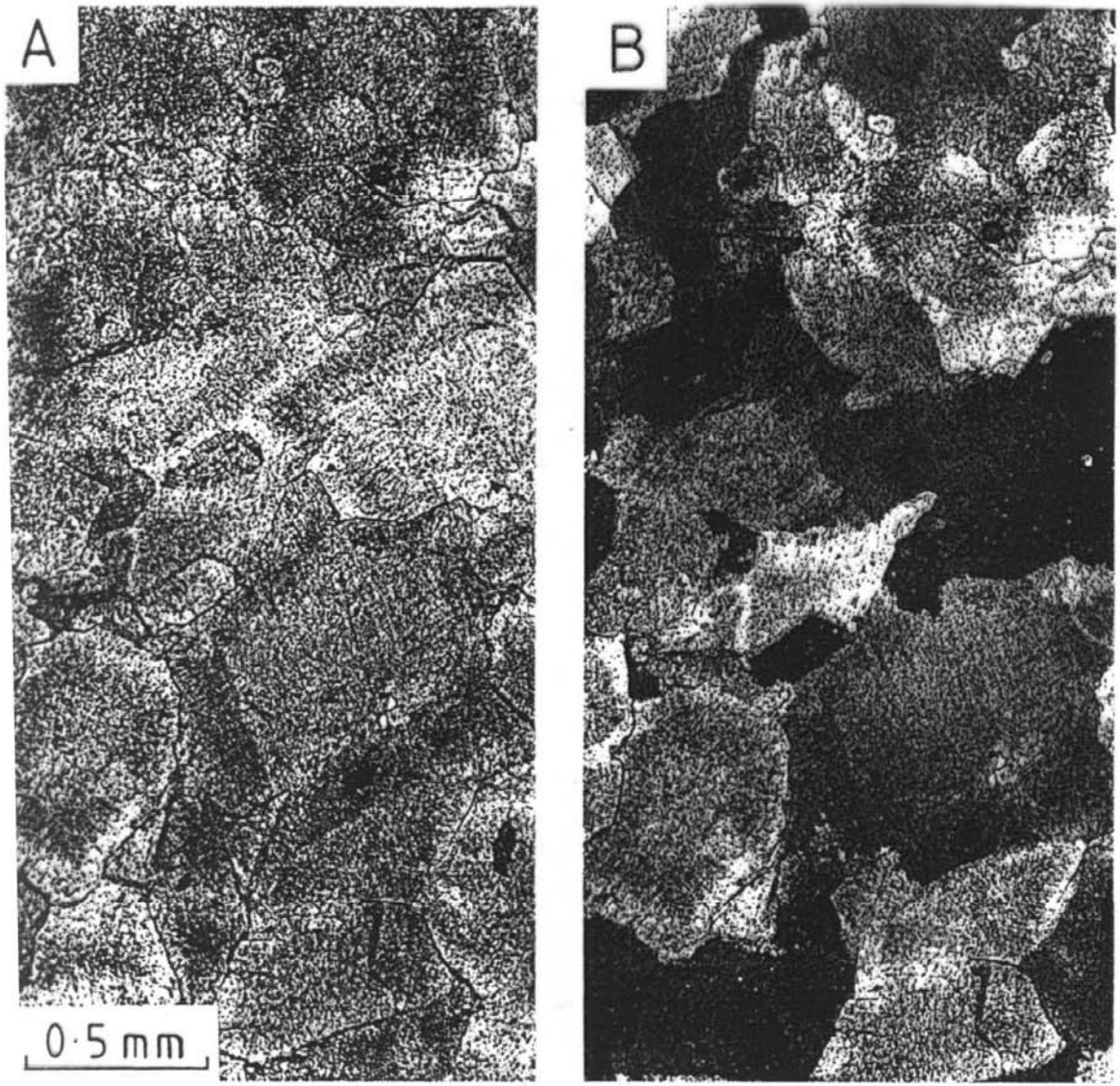

Fig. 4.64 Baroque dolomite; coars crystals with undulose extinction. Plane-polarized light. B, Crossed polars. Lower Carboniferous dolomitized oolite (no relics of structure left). Glamorgan, Wales.

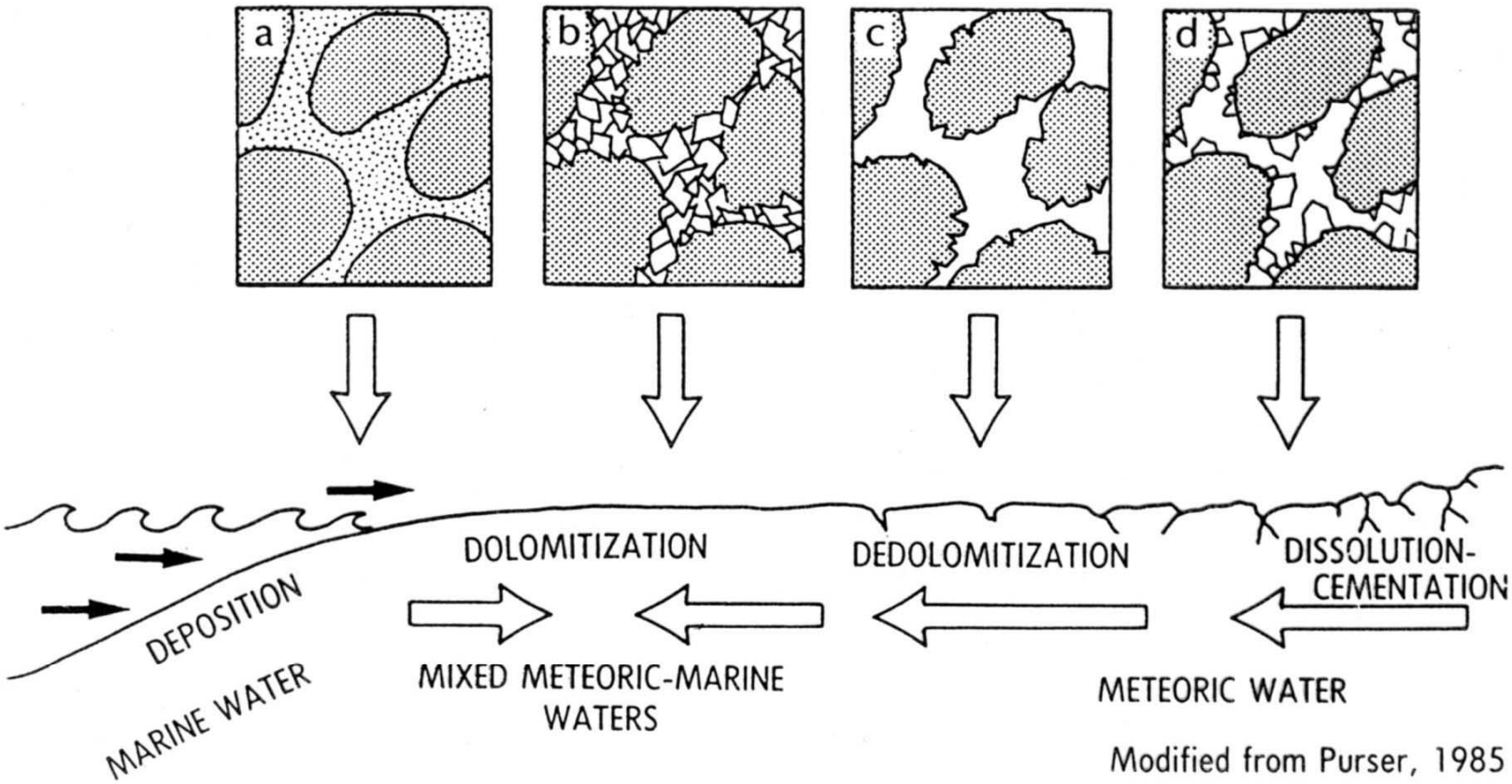

Fig. 2.14. Geologic setting for the dolomitization-dedolomitization of Jurassic ooid packstones from the Paris Basin. Final porosity consists of cement-reduced, dolomite crystal-moldic porosity. Reprinted from Carbonate Petroleum Reservoirs, with permission. Copyright, Springer-Verlag, New York.

porozita

kalcit → dolomit, redukce objemu, nárůst porozity až o 13%

dedolomitizace

dolomit → kalcit; kontakt s meteorickou vodou; povrch. rozpouštění sádrovce-anhydritu; při pohřbení

identifikace: pseudomorfózy kalcitu po dolomitu; neomorfní mozaika

silicifikace karbonátů

raná i pozdní; rekryst. bioklastů, tvorba nodulí, nodulárních horizontů, souvislých poloh; SiO_2 tmel

typy diag. křemene: 1) euhedrální krystaly, 2) mikrokřemen, 3) megakřemen, 4) chalcedonický kř.

zdroj: jehlice hub, diatomity, radiolarie; vulkanický SiO_2

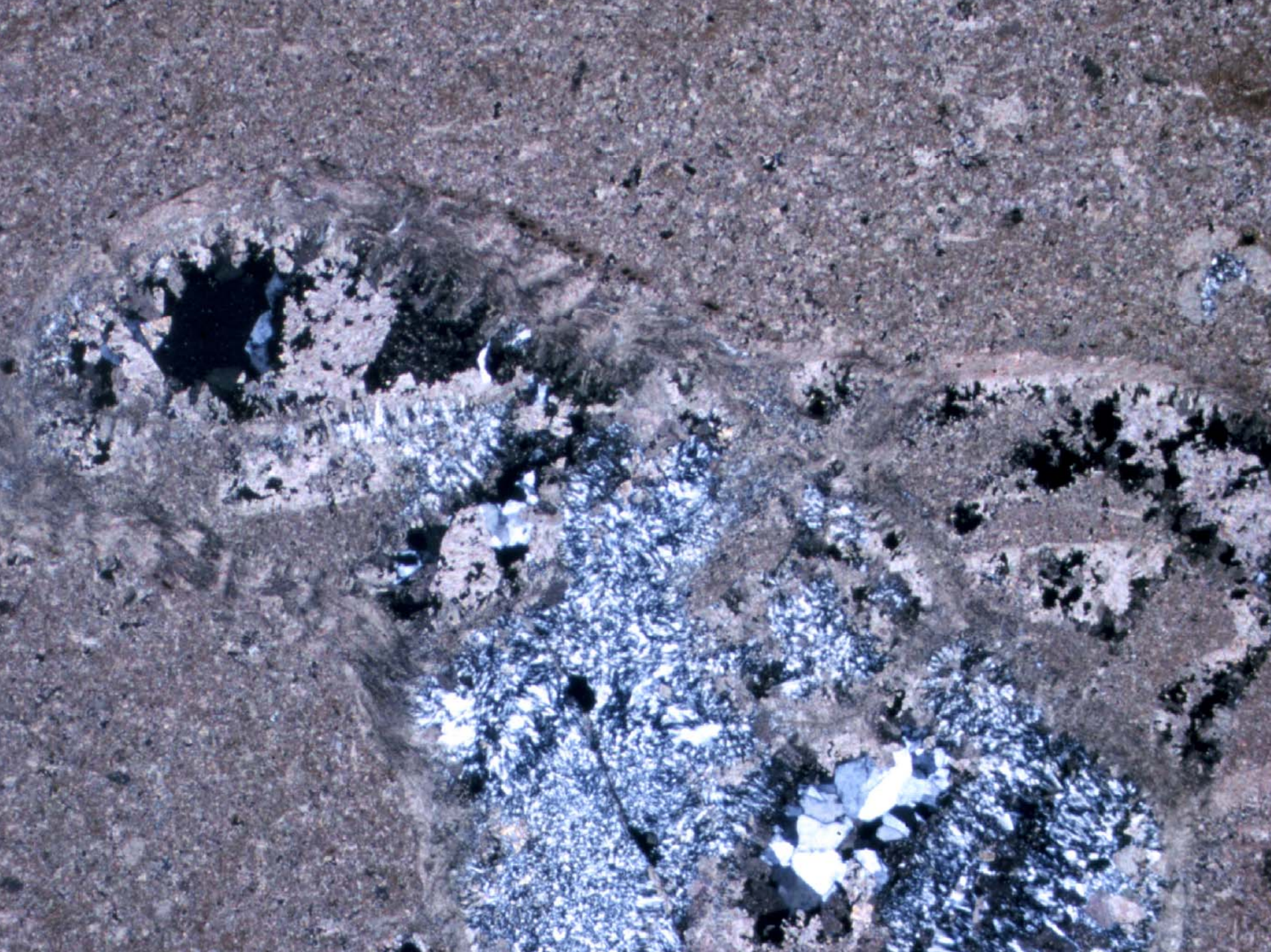

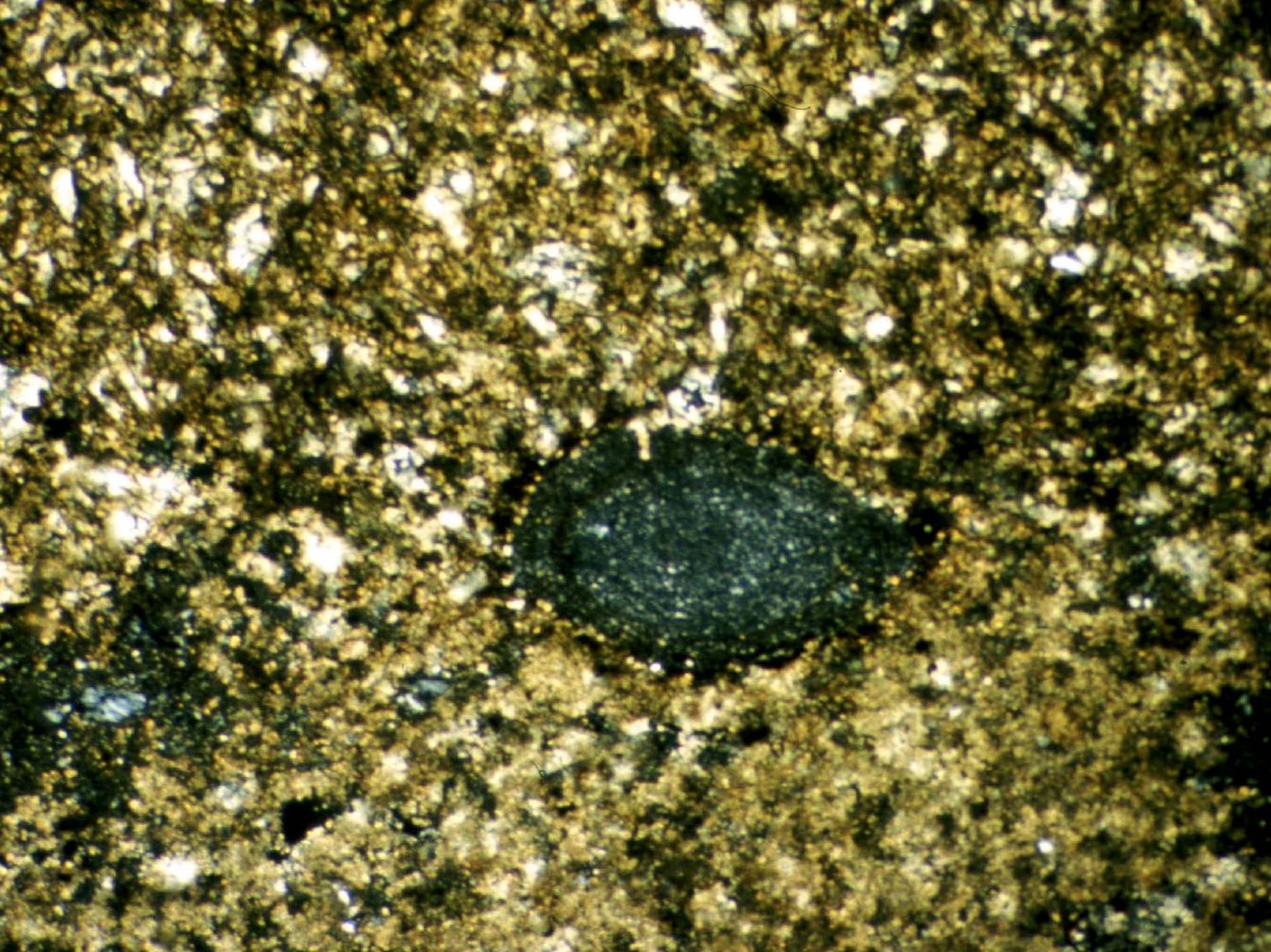

čtení:

M.E.Tucker: Sedimentary petrology. 3rd ed. Blackwell, 2001.
M.E.Tucker&V.P.Wright: Carbonate Sedimentology. Blackwell, 1994.
C.H.Moore (1989): Carbonate diagenesis and Porosity. Developments in sedimentology 46, Elsevier.
G.Harwood (1988): Principles of sedimentary petrography. In: M.Tucker ed.: Techniques in sedimnetology, Blackwell.